PHYSICO-MATHEMATICAL DETAILS OF ELECTRICAL METHODS OF GEOPHYSICAL PROSPECTING AND SOME APPLICATIONS ON THE ANALYSIS AND INTERPRETATION OF DATA FROM SELECTED SITES IN ETHIOPIA

by

GEBRECHRISTOS KASSA

A THESIS PRESENTED TO THE SCHOOL

OF GRADUATE STUDIES

and

FACULTY OF SCIENCE

ADDIS ABABA UNIVERSITY

IN PARTIAL FULFILLMENT OF THE REQUIREMENT FOR

THE DEGREE OF MASTER OF SCIENCE

IN PHYSICS

June, 1983

ADDIS ABABA UNIVERSITY

School of Graduate Studies

PHYSICO-MATHEMATICAL DETAILS OF ELECTRICAL METHODS OF GEOPHYSICAL PROSPECTING AND SOME APPLICATIONS ON THE ANALYSIS AND INTERPRETATION OF DATA FROM SELECTED SITES IN ETHIOPIA

by

Gebrechristos Kassa

Faculty of Science

Approved by the Examining Board:

Dr. Elaine Girgis Tadros	E. G. Tadros
External Examiner	
Dr. B. Zhakupov	
Advisor	
Mr. Wahi Ashok Kumar	
Member	
Dr. G. Guzzetta	
Member	
Dr. V. Davydov	
Chairman	

ACKNOWLEDGEMENT

I am deeply grateful to my Advisor Dr. Paiken F. Zhakupov for his untiring assistance in organizing this project.

Our thanks also go to the Geophysics Department, Ministry of Mines and Energy for supplying us with data; and to the petroleum searching unit in Dire Dawa, especially to Mrs. A.B. Selezneva, for their cooperation in making available to us their computer facilities.

TABLE OF CONTENTS

LIST OF FIGURES AND TABLES

ABSTRACT

Basic theoretical foundations are discussed as a preliminary, followed by a description of the various electrode spreads together with the relevant mathematical and physical considerations.

Interpretation techniques, old and recent are presented.

In the second part, practical work of analysis and interpretation of VES data from Dire Dawa and Tendaho are discussed, followed by remarks and conclusion.

I INTRODUCTION

Among the various techniques of Geophysical Prospecting, the electrical methods have branched out from a broader and more basic discipline: Geolectricity.

Geolectricity deals with the electrical state of the earth including aspects related to the electrical properties of rocks and minerals under different geological environments. It also discusses the influences of such electrical properties upon various geophysical phenomena.

The ultimate goal in electrical exploration is to make use of principles of geolectricity and obtain geological maps of concealed structures, prospect for ores, minerals and oil, and solve many hydrogeological and engineering geology problems.

In the pioneering days of electrical methods insufficient advances in technology had restricted their applicability only to very shallow depths. Today, however recent developments and refined techniques of interpretation have increased the depth of investigation to the order of 8-10 kms.

The electrical methods of exploration consist of various principles and techniques and make use of stationary as well as variable currents produced artificially by natural ways.

Among these diverse techniques, the one most commonly used and the one with which this paper is mainly concerned is known as the resistivity method. In this, a direct or low frequency alternating current is introduced into the ground by two or more electrodes and the potential difference between two suitably chosen points measured. The potential difference per unit current sent through the ground is a measure of the electrical resistance of the ground between the points or probes, and the resistance in turn depends on the geometrical configuration of the electrodes and the electrical parameters of the ground.

Resistivity measurements are classified into two categories. In the first, known as geolectric profiling or mapping, the electrodes and probes are shifted without changing their relative configuration. This gives an idea of the surface variation of the resistance /more preciscely resistivity/ within a given depth. In the second, known as geolectric sounding, the positions of the electrodes are changed with respect to a fixed point. In this manner the measured resistance values at the surface reflect the vertical distribution of the resistivities in geological section.

II BASIC FOUNDATIONS

A. CURRENT FLOW IN HOMOGENECUS EARTH

The physical principle of conservation of charge is the basis for the flow of current in a medium, mathematically this principle is expressed as

$$\text{div } \vec{J} = - \frac{\partial q}{\partial t} \qquad (1)$$

where $\vec{J}$ is current density

q is the charge density

Ohm's law relates the current density J and the electric field intensity $\vec{E}$

$$\text{by } \vec{J} = \frac{1}{\rho} \vec{E} = - \frac{1}{\rho} \text{ grad } V$$

Where ρ is the resistivity of the medium and V is the electric potential. Since for an isotropic medium ρ is a scalar function of the point of observation, the above ohmic relation renders $\vec{J}$ to be in the same direction as $\vec{E}$ but this is not true for an anisotropic medium, for then $\vec{J}$ will assume a directive property and it is not always in the direction of $\vec{E}$.

For the anisotropic case Ohm's law is modified, and for a rectangular coordinate system it becomes:

$$J_x = \sigma_{xx} E_x + \sigma_{xy} E_y + \sigma_{xz} E_z$$

$$J_y = \sigma_{yx} E_x + \sigma_{yy} E_y + \sigma_{yz} E_z \qquad (2)$$

$$J_z = \sigma_{zx} E_x + \sigma_{zy} E_y + \sigma_{zz} E_z$$

The six - component tensor σ_{ik} /conductivity/ is here defined as the current density in the direction of i per unit electric field in the direction of k, the conservation principle dictates that $\sigma_{ik} = \sigma_{ki}$, hence in an anisotropic medium conductivity is a symmetric tensor.

Now, the equation expressing the principle of charge conservation, also known as the equation of continuity, reduces to the form div. $\vec{J} = 0$ for a stationary current (ie. $\frac{\partial q}{\partial t} = 0$).

Replacing $\vec{J}$ by its equivalent from Ohm's law we obtain:

$$\text{div } (\frac{1}{\rho} \text{ grad } V) = 0 \qquad (3)$$

or expanding, we have

$$\text{grad } (\frac{1}{\rho}) \cdot \text{grad } V + \frac{1}{\rho} \text{ div grad } V = 0 \qquad (4)$$

This is the basic relation of direct-current electrical prospecting.

For a homogeneous medium ρ does not depend on the coordinates, and the above equation reduces to

$$\text{div grad } V = 0 \tag{5}$$

or

$\nabla^2 V = 0$ which is Laplace's eq. saying that the electric potential distribution for a direct current flow in a homegeneous isotropic medium satisfies Laplace's equation.

Next we shall consider how the resistivity is related to practically measured potential (or potential difference to be exact) when current I is introduced into the ground.

Case (i) Infinite Homogeneous Medium

Because of summetry for this case the potential at a distance r from the point of introduction of the current, P, will be only a function of r, and Laplace's equation reduces to

$$\frac{d^2 v}{dr^2} + 2/r \left(\frac{dv}{dr}\right) = 0 \tag{6}$$

whose solution is

$$V = C_1 + C_{2/r} \tag{6'}$$

From the boundary condition that the potential at infinite distance is zero we will have $C_1 = 0$.

For this case, the equipotential surfaces given by

$$V = C_2/r = \text{constant} \qquad (7)$$

or r = constnat, are clearly seen to be spherical; and the electric field lines and current lines as well being the gradient of the potential, point in the radial direction.

The current density J at a distance r is given by

$$J = -\frac{1}{\rho}\frac{\partial v}{\partial r} = -\frac{1}{\rho}\frac{d}{dr}\left(\frac{C_2}{r}\right) = \frac{1}{\rho}\frac{C_2}{r^2} \qquad (8)$$

The total current flowing out of a spherical surface of radius r (of surface area $4\pi r^2$) is given by

$$\text{J. surface area} = 4\pi r^2 J = 4\pi r^2\left(\frac{1}{\rho}\frac{C_2}{r^2}\right) = 4\frac{\pi}{\rho}C_2 \qquad (9)$$

But this total current is equal to the original current, I, introduced at point P.

Hence $$\frac{4\pi}{\rho}C_2 = I \quad \therefore \quad C_2 = \frac{I\rho}{4\pi} \qquad (10)$$

Case (ii)

For a semi-infinite medium (all other conditions in case (i) remaining unchanged).

Total current flowing out of a hemispherical surface of radius r(of surface area $2\pi r^2$) is given by

J. surface area $= 2\pi r^2 J$

$$= 2\pi r^2 \left(\frac{1}{\rho}\frac{C_2}{r^2}\right) = \left(\frac{2\pi}{\rho}\right) C_2$$

where $C_2 = I\rho/2\pi$ (11)

Hence the potential at any point due to a current source at the surface of a homogeneous earth becomes

$$V = C_1 + C_2/r = 0 + \frac{I\rho}{2\pi/r} = \frac{I\rho}{2\pi} \cdot \frac{1}{r} \quad (12)$$

In practice, however, current is introduced into the ground by two electordes, not by one: the source and the sink. Conventionally the source gives rise to a positive potential and the sink gives rise to a negative potential.

Hence we will have the potential at a point:

$$V_1 = I\rho/2\pi(1/r_1) \text{ ---- due to source}$$
$$V_2 = I\rho/2\pi(1/r_2) \text{ ---- due to sink} \quad (13)$$

Where r_1 and r_2 are the distances from point of observation, O, of V_1 and V_2 respectively.

We have for the resultant potential

$$V = V_1 + V_2 = \frac{I\rho}{2\pi}\left(\frac{1}{r_1} - \frac{1}{r_2}\right) \quad (14)$$

III FIELD PRACTICE

A. Idealised case (Homogeneous and Isotropic Earth) a direct current I is introduced into the earth through two point electrodes A and B

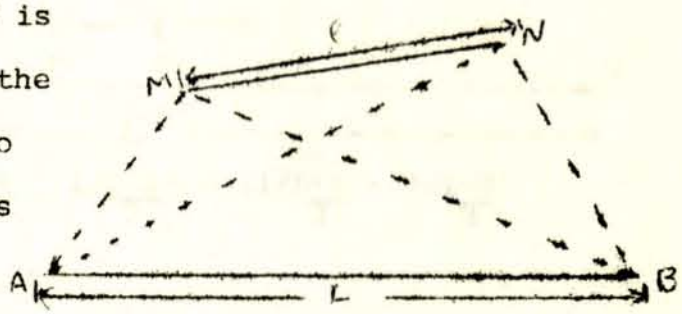

the potential difference between any two points M and N

$$\Delta V = V_M - V_N = I\rho/2\pi \left(\frac{1}{AM} - \frac{1}{BM}\right) - \left(\frac{1}{AN} - \frac{1}{BN}\right) \qquad (15)$$

Thus, it can be seen that the resistivity is determined from measurements of the potential at the surface and the geometry of the electrode layout which is also measured at the surface.

Various ways of arranging A,B,M and M have been used but the most common arrangements are

1. Symmetrical arrangement
2. Dipole arrangement.

In the symmetrical arrangement, the points A,M,N,B are aligned on a straight line and the points M and N are

symmetrically place about the center of the straight line formed by A and B, for this symmetrical array we have

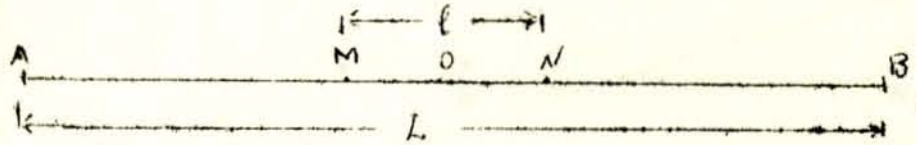

$$\Delta V = \frac{I\rho}{2\pi} \left(1/\frac{L-\ell}{2} - 1/\frac{L+\ell}{2}\right) - \left(1/\frac{L+\ell}{2} - 1/\frac{L-\ell}{2}\right) \qquad (16)$$

and from here

$$\rho = \frac{\pi}{4} \left(\frac{L^2 - \ell^2}{\ell}\right) \frac{\Delta V}{I} \qquad (17)$$

The Schlumberger array, one of the two symmetrical arrangements, has its ℓ much less than L(L> 5ℓ) and so we can approximate $L^2 - \ell^2$ by L^2 with an error less than 4% ; and in this case the resistivity becomes

$$\rho = \frac{\pi L}{4L} \frac{\Delta V}{I} = \frac{\pi L^2}{4} \frac{\Delta V}{\ell} \frac{1}{I} = \frac{\pi L^2}{4} \frac{E}{I} \qquad (18)$$

Because of this (ie. $E = \frac{\Delta V}{\ell}$) this arrangement is called a gradient arrangment. For Wenner array, the second of the symmetrical ones, where $L = 3\ell$ and here ℓ is conventionally taken as "a" (and L = 3 a) the resistivity is

$$\rho = 2\pi a \frac{\Delta V}{I} \qquad (19)$$

and this configuration is known as a potential vonfiguration (because of the presence of $\frac{\Delta V}{I}$ in the expression).

The possible dipole configurations are indicated below:

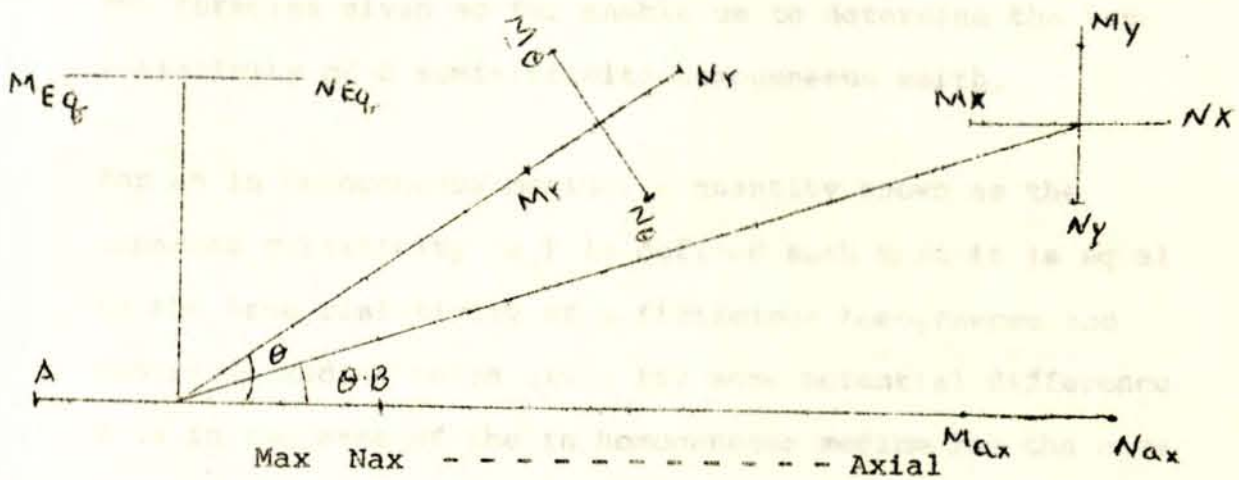

Max	Nax	- - - - - - - - - - - - - Axial
Mx	Nx	- - - - - - - - - - - - - Parallel
My	Ny	- - - - - - - - - - - - - Perpendicular
Mr	Nr	- - - - - - - - - - - - - radial
Mo	No	- - - - - - - - - - - - - azimuthal
Meq	Neq	- - - - - - - - - - - - - equatorial

The relations for the gradient of the potential given above indicate that the resistivity ρ can be determined if one only knows how to measure the electric field intensity E; and this can be accomplished by noting that $E \approx \frac{\Delta V}{I}$ if the separation between M and N is small enough.

It is to be noted that the equatorial arrangement ($\theta=90°$) is a special case of the parallel arrangement and it simplifies to $E_{eq}=\frac{I\rho L}{2\pi}\cdot\frac{3\cos^2 90-1}{r^3}=\frac{I\rho L}{2\pi}\left(\frac{-1}{r^3}\right)-\frac{I\rho L}{2\pi r^3}$ (20)

and for $\theta = 0$, we obtain the electric field for the axial arrangment

$$Eax = \frac{I\rho L}{\pi r^3} \qquad (21)$$

IV THE CONCEPT OF APPARENT RESISTIVITY

The formulas given so far enable us to determine the true resistivity of a semi-infinite homogeneous earth.

For an in homogeneous medium, a quantity known as the apparent resistivity (ρ_a) is defined such that it is equal to the true resistivity of a ficticious homogeneous and isotropic medium which gives the same potential difference V as in the case of the in homogeneous medium for the same current I and the same electrode arrangement.

So the apparent resistivity of a geologic medium depends upon the geometry and the resistivities of the various elements constituting the given formation.

We can write $$\rho_a = K \left(\frac{\Delta V}{I}\right) \qquad (22)$$

Where K is the geometrical coefficient with the dimention of length.

From the relations for the resistivities in the different arrays, one can see that

$$K_w = 6.28\ a \quad \text{- - - - - - - - - - - (Wenner)}$$

$$K_s = 0.785\ \left(\frac{L^2-\ell^2}{\ell}\right) \quad \text{- - - - - - - - (Schlumberger)}$$

$$K_r = \frac{\pi r^3}{L\ell \cos\theta} \quad \text{- - - - - - - - Dipole, radial}$$

$$K_\theta = \frac{2\pi r^3}{L\ell \sin\theta} \quad \text{- - - - - - - - dipole, animuthal}$$

$$K_x = \frac{2\pi r^3}{L\ell}\ \frac{1}{3\cos^2\theta - 1} \quad \text{- - - - dipole, parallel} \qquad (23)$$

$$K_y = \frac{2\pi r^3}{3\ell L}\ \frac{1}{\sin\theta \cos\theta} \quad \text{- - - - dipole, perpend.}$$

$$K_{eq} = \frac{2\pi r}{L\ell} \quad \text{- - - - - - - - dipole, equatorial}$$

$$K_{ax} = \frac{\pi r^3}{L\ell} \quad \text{- - - - - - - - dipole, axial}$$

V FIELD PRACTICES FOR RESISTIVITY SURVEYS

The main components in carrying out resistivity measurements include a power source, meters for measuring current and voltage (or alternatively a combined system to measure the resistance), electrodes, cables and reels. The power supply can either be DC or a low frequency (less than 60HZ) Ac. In cases where portability is given precedence a set of B batteries may be connected in series to give several hundred volts; otherwise, a motor generator having a capacity of several hundred watts is preferable for large scale work. It is customary to periodically reverse the polarity of the direct current in order to avoid effects of electrolytic polarization caused by the flow of current in only one direction.

The dc source, in addition to enabling measurement of dc resistivity, produces undesirable effects due to spontaneous potentials. This requires that porous pots be used as potential electrodes, and the spontaneous potential effect must be noted before the source is turned on, and then subtracted from the potential measured when current is flowing.

In addition to the use of a.c. or rapidly interrupted d.c. to eliminate the spontaneous potential effect, narrow-band

amplifiers tuned to the source frequency are employed to increase the signal-to noise ratio; however, this will give a resistivity lower than the true resistivity value.

Other serious problems that may be encountered are inductive coupling between current and potential cables, current leakage especially on the ground; and these effects increase with frequency.

VI SURVEYING PROCEDURES

a. Electric Drilling

We have seen earlier that the depth of current penetration varies with the current - electrode separation; so the procedure in the field is to use a fixed center with an expanding spread. This technique is particularly suited to detect the presence of horizontal or gently sloping beds of different resistivities; and in this respect it is often used to determine.

i) depth of overburden

ii) depth, structure and resistivity of flat sedimentary beds

iii) depth, structure and resistivity of basement

Even when the main interest may be in lateral exploration, it is often necessary to carry out, electric drilling at several locations in order to establish proper electrode spacings for the lateral search.

b. Electric Mapping

This method is mainly used in mineral exploration in order to detect isolated bodies of varying resistivities.

In all arrays that may be used except in those where one of the electrodes is located at infinity, the apparent resistivity is plotted at the mid-point of the potential electrodes.

If the potential electrodes are closely spaced (as in the schlumberger), the measurement becomes of potential gradient at the midpoint as can be seen from the following considerations:

Putting $2\ell = \Delta r$ in the relation

$$\rho_a = \frac{\pi L^2}{2\ell} \left(\frac{\Delta V}{I}\right) \text{, we will have}$$

$$\rho_a = \frac{\pi L^2}{I} \left(\frac{\Delta V}{\Delta r}\right) \tag{24}$$

Next we shall show that when the current electrodes are close together and remote from the potential electrodes, the measurement is that of the second derivative (or the curvature) of the potential field. For the double dipole:

$$\frac{\Delta V}{\Delta r} = \frac{\Delta V_1 - \Delta V_2}{\Delta r} = \frac{\Delta V_1}{\Delta r} - \frac{\Delta V_2}{\Delta r} \tag{25}$$

where $\Delta V_1 = V_{c_1}$ at $p_2 - V_{c_1}$ at p_1

and $\Delta V_2 = V_{c_2}$ at $p_2 - V_{c_2}$ at p_1

in the limit as $r \to 0$

$$\frac{\Delta V}{\Delta r} = \left(\frac{\partial V}{\partial r}\right)_{c_1} - \left(\frac{\partial V}{\partial r}\right)_{c_2} \tag{25'}$$

$$= \Delta \left(\frac{\partial V}{\partial r}\right) = \frac{\partial}{r} \left(\frac{\partial V}{\partial r}\right) \Delta r = \Delta r \left(\frac{\partial^2 V}{\partial r^2}\right)$$

or

$$\Delta V = (\Delta r)^2 \frac{\partial^2 V}{\partial r^2} \tag{26}$$

But, from the usual expression for the potential.

$$\Delta V = \frac{I\rho a}{2\pi} \frac{1}{r_1} - \frac{1}{r_2} - \frac{1}{r_3} \frac{1}{r_4} \tag{27}$$

and in the following notation

$$r_1 = r_4 = r$$

$$r_2 = r - \Delta r$$

$$r_3 = r + \Delta r$$

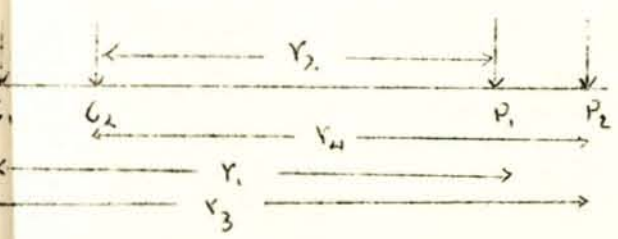

Then,

$$\Delta V = \frac{I\rho a}{2\pi} \left(\frac{1}{r} - \frac{1}{r-\Delta r} - \frac{1}{r+\Delta rR} + \frac{1}{r}\right)$$

$$= \frac{I\rho a}{2\pi} \frac{(r^2-(\Delta r)^2-r^2-r\Delta r-r^2+r\Delta r+r^2-(\Delta r)^2}{r(r-\Delta r)(r+\Delta r)}$$

$$= \frac{I\rho a}{2\pi} \frac{2(\Delta r)^2}{r^3-r(\Delta r)} = \frac{I\rho a}{2\pi} \frac{2(\Delta r)^2}{r^3} \simeq -\frac{I\rho a}{\pi} \frac{(\Delta r)^2}{r^3} \quad (28)$$

The two expressions for V must then be equal and we will have:

$$(\Delta r)^2 \frac{\partial^2 V}{\partial r^2} \simeq - \frac{I\rho a}{\pi} \left(\frac{\Delta r}{r^3}\right)^2$$

which gives

$$\rho_a = \frac{-\pi r^3}{(\Delta r)^2 I} (\Delta r)^2 \frac{\partial^2 V}{\partial r^2} = - \frac{\pi r^3}{I} \frac{(\partial^2 V)}{\partial r^2} \quad (29)$$

The lateral exploration is best suited to detect dipping contacts and dykes of contrasting resistivity.

VII INTERPRETATION TECHNIQUES OF RESISTIVITY SURVEYS

a. Schlumberger

We have seen earlier that master curves prepared with a computer on the basis of the relation:

$$\rho = \rho_1 (1+2 \sum_{n=1}^{\infty} \frac{\delta^3 K^n 12}{[\delta^2+(2n)^2]^{3/2}} \qquad (30)$$

are available as an aid to interpretation the details of which will be discussed in this section. The above formula generates master curves for a two layer earth. Two sets of theoretical two-layer master curves are available for (ρ_2/ρ_1) greater than unity, ie. ascending type and for (ρ_2/ρ_1) less than unity. For the first set the values of (ρ_2/ρ_1) for which curves have been plotted are:

ρ_2/ρ_1 = 11/9, 3/2, 13/7, 2, 7/3, 3, 4, 5, 17/3, 7, 9, 19, 39, 99.

and for the second set

(ρ_2/ρ_1)= 9/11, 2/3, 7/13, 1/2, 3/7, 1/3, 1/4, 1/5, 3/17, 1/7, 1/9, 1/19, 1/39, 1/99, 0.

Apart from the possibility that three layer, four-layer or in general multilayer master curves could be drawn with a computer using their corresponding formulae, the

available two-layer curves could be used to plot three layer or four layer curves for certain special cases, as we shall see below in a selected example:

$$\rho_1 = 100\ \Omega m \quad \rho_2 = 5\ \Omega m \quad \rho_3 = \infty$$

$$h_1 = 10\ m \quad h_2 = 10\ m \quad h_3 = \infty$$

Then in the three-layer formula for the coeficient $A_1(m)$

$$A_1(m) = q\,\frac{K_{12}g^{p1} + K_{23}g^{p2}}{1-K_{12}g^{p1}-K_{23}g^{p2}+K_{12}K_{23}g^{(p2-p1)}} = q\sum_{n=1}^{\infty} b_n g_n \tag{31}$$

where

$$q = \frac{I\rho_1}{2\pi}\ ,\ g = e^{-2mH_O}\ ,\ p_1 = \frac{H_1}{H_O} \tag{32}$$

$$p_2 = \frac{H_2}{H_O} \tag{33}$$

$$K_{12} = \frac{\rho_2 - \rho_1}{\rho_2 + \rho_1}\ ,\ K_{23} = \frac{\rho_3 - \rho_2}{\rho_3 + \rho_2} \tag{34}$$

$$H_1 = h_1\ ,\ H_2 = 2h_1$$

$$P_1 = 1 \qquad P_2 = 2$$

For the special values selected:

$$A_1(m) = q\,\frac{K_{12}q + q^2}{1-q^2} = q \sum_{n=1}^{\infty} b_n q^n \qquad (35)$$

This gives $$\frac{K_{12}q + q^2}{1-q^2} = \sum_{n=1}^{\infty} b_n q^n \qquad (36)$$

$$\frac{(1+k)q(1+q) + (1-k)(-q)(1-q)}{2(1-q^2)} = \sum_{n=1}^{\infty} b_n q^n$$

denote $\frac{1 + K_{12}}{2} = a$ and $\frac{1 - K_{12}}{2} = C$

and we will have

$$a\,\frac{q}{1-q} + c\,\frac{-q}{1+q} = \sum_{n=1}^{\infty} b_n q^n$$

and on expansion into a series

$$a(q+q^2 + q^3 + \ldots\ldots) + c(-q - q^2 - q^3 \ldots) = \sum_{n=1}^{\infty} b_n q^n$$

This gives

$$b_1 = b_2 = b_3 \ldots\ldots = \underline{\underline{a - c}} \qquad (37)$$

with these values for b_n the expression for $\bar{\rho}/\rho_1$ becomes:

$$\bar{\rho}/\rho_1 = 1+2 \sum_{n=1}^{\infty} \frac{bn\delta^3}{(\delta^2 + 4n^2)^{3/2}}$$

$$= \frac{1+1+K_{12}}{2} \cdot 2 \sum_{n=1}^{\infty} \frac{\delta^3}{[\delta^2 + (2n)^2]^{3/2}} \qquad (38)$$

$$+ \frac{1-K_{12}}{2} \cdot 2 \sum_{n=1}^{\infty} \frac{\delta^3 (-1)^n}{[\delta^2 + (2n)^2]^{3/2}}$$

The value of $\bar{\rho}/\rho_1$ can be computed from the above expression for certain value of $K_{12}(\rho_2/\rho_1)$ for different values of $\delta = r/h_1 = AB/2h_1$

For a highly convergent series five to ten terms can give sufficient accuracy; however for some unfavourable conditions it may be necessary to consider a much larger number of terms (50 or more).

The above expression can further be simplified (ie. expressed in terms of ρ_∞: $\bar{\rho}$ of two layer earth with $\rho_2 = \infty$ and $\bar{\rho}_o$: $\bar{\rho}$ of two layer earth with $\rho_2 = 0$, enabling one to use the two layer curve for plotting the three - layer curve.

To see this, let us write the familiar relation for a two layer earth:

$$\bar{\rho} = \rho_1 (1+2 \sum_{n=1}^{\infty} \frac{\delta^3 K_{12}^n}{[\delta^2 + 4n^2]^{3/2}}$$

for $\rho_2 = \infty$, $K_{12} = \frac{\rho_2 - \rho_1}{\rho_1 + \rho_2} = 1$

$$\bar{\rho}_\infty = \rho_1 (1+2 \sum_{n=1}^{\infty} \frac{\delta^3}{[\delta^2 + (2n)^2]^{3/2}} \tag{39}$$

for $\rho_2 = 0$, $K_{12} = \frac{\rho_2 - \rho_1}{\rho_1 + \rho_2} = -1$

$$\bar{\rho}_o = \rho_1 (1+2 \sum_{n=1}^{\infty} \frac{\delta^3 (-1)^n}{[\delta^2 + (2n)^2]^{3/2}} \tag{40}$$

In terms of these $\bar{\rho}_\infty$ and $\bar{\rho}_o$ the expression for $\bar{\rho}/\rho_1$ becomes:

$$\bar{\rho} = \frac{1 - K_{12}}{2} \bar{\rho}_o + \frac{1 + K_{12}}{2} \bar{\rho}_\infty \tag{41}$$

This means if two-layer master curves for $\rho_2 = 0$ and $\rho_2 = \infty$ are available, with the help of the above formula we can plot the three layer master curves for the given case.

The whole set of three-layer sounding curves are divided into four groups, depending on the relative values of ρ_1 , ρ_2 , ρ_3

1. Minimum type or H type: $\rho_1 > \rho_2 < \rho_3$

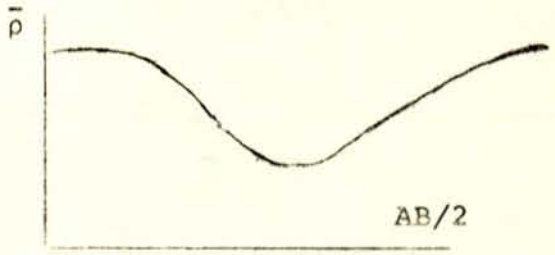

2. Double ascending type (A-type): $\rho_1 < \rho_2 < \rho_3$

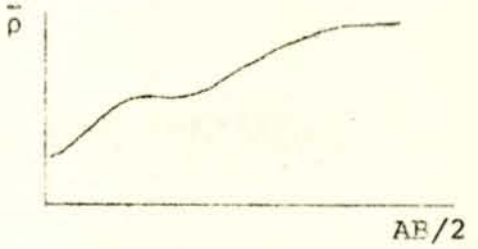

3. Maximum type (K-type): $\rho_1 < \rho_2 > \rho_3$

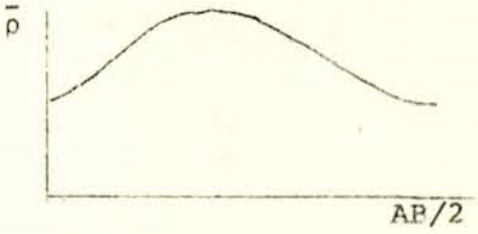

4. Double descending type (O-type): $\rho_1 > \rho_2 > \rho_3$

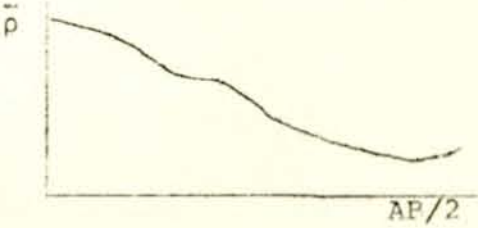

From a combination of the types H,A,K and Q there can be only eight types of four-layer covers:

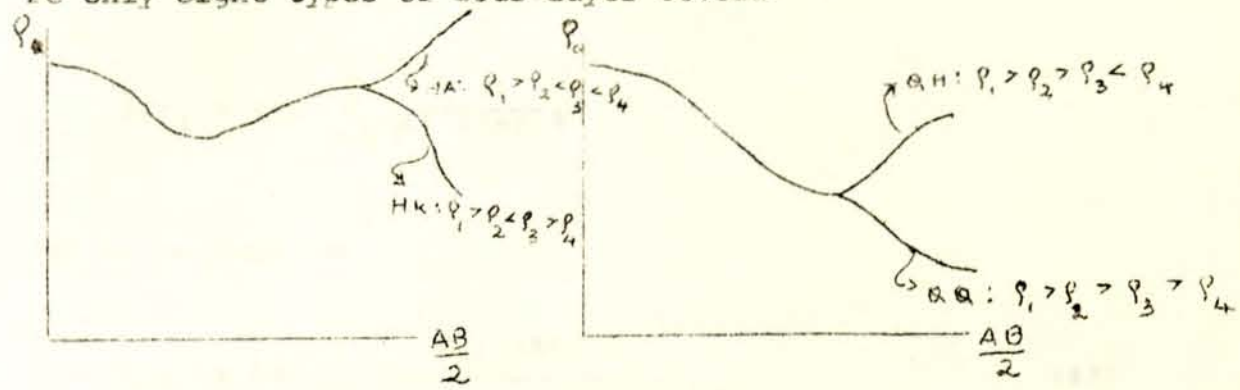

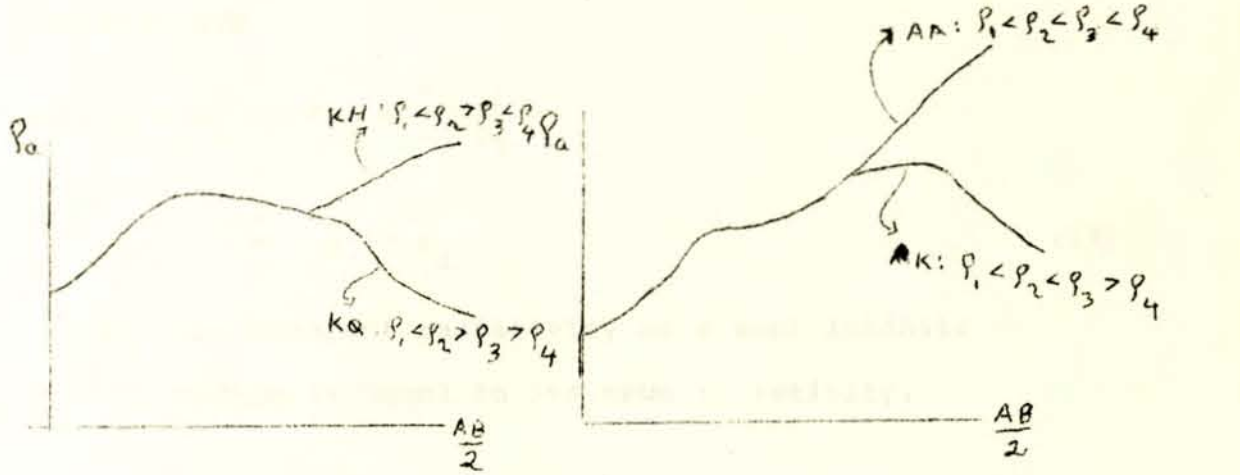

Asymptotic Values

The apparent resistivity for a two-layer earth:

$$\bar{\rho}/\rho_1 = 1+2 \sum_{n=1}^{\infty} \frac{\delta^2 K_{12}^n}{(\delta^2 + 4n^2)^{3/2}}$$

can be written as:

$$\bar{\rho}/\rho_1 = 1+2 \sum_{n=1}^{\infty} \frac{K_{12}^n (AB/2h_1)^3}{[(AB/2h_1)^2 + (2n)^2]^{3/2}} \qquad (42)$$

Several limiting cases which can be derived from this equation are:

a) $\rho_2 = \rho_1 \rightarrow K_{12} = \frac{\rho_2 - \rho_1}{\rho_2 + \rho_1} = 0$

$$\rightarrow \bar{\rho} = \rho_1 \qquad (43)$$

ie. The apparent resistivity of a semi intinite medium is equal to its true resistivity.

b) Small values of electrode separation

$$(\frac{AB}{2} \rightarrow 0) \rightarrow \bar{\rho} = \rho_1 \qquad (44)$$

ie. For small electrode separation the apparent resistivity of a two layer earth is equal to the true resistiviting of the first layer.

c) $\frac{AB}{2} \rightarrow \infty$, $\bar{\rho} = \rho_2$, (45)

ie. The apparent resistivity is equal to the true resistivity of the second layer for large values of electrode separation.

If we assume K_{12} = constant (or ρ_2/ρ_1 is constant), the expression for $\bar{\rho}/\rho_1$ can be written in the form:

$$\bar{\rho} = \rho_1 \, f \, (AB/2h_1) \tag{46}$$

If $\bar{\rho}$ is plotted against $AB/2h_1$ from this equation on an arithmatic scale, different curves are obtained for different values of ρ_1 even for a fixed value of h_1 and similarly for each value of h_1 with ρ_1 fixed.

To avoid the influence of ρ_1 and h_1 on the form of the curve plotted we take the logarithm of the relation:

$$\bar{\rho}/\rho_1 = f \, (AB/2h_1) \tag{47}$$

$$\log \bar{\rho} - \log \rho_1 = f' \, (\log AB/2 - \log h_1) \tag{48}$$

Where f' is the new function into which f has evolved after taking logarithms

$$\text{or} \qquad \log (\bar{\rho}/\rho_1) = \log F (\log \frac{AB}{2h_1}) \qquad (49)$$

where $\log F = f'$

The equation in the box shows that a plotting of $\bar{\rho}$ as ordinate and $\frac{AB}{2}$ as abasica will generate curves of exactly the same form for any ρ_1 and h_1.

The only effect of varying ρ_1 and h_1 would be the vertical and lateral shifting of the curve respectively.

The conclusion is thus that the form of the VES curves, plotted on a double logarithmic scale is independent of the resistivity and thickness of the first layer in a two layer section if ρ_2/ρ_1 is constant. It can be shown that this is also valid for a multi-layer geolectric section.

Correlation of Field Curves with Master Curves

We have seen that field measurements give us the apparent resistivity as a function of the electrode separation:

$\bar{\rho} = f\ (AB/2)$; and using logarithmic scale we obtain:

$$\log \bar{\rho} = F\ (\log AB/2) \qquad (50)$$

This equation and the master curve equation

$$\log \bar{\rho} - \log \rho_1 = F\ (\log \frac{AB}{2} - \log h_1)$$

are of the form $y - b = f\ (x - a)$

and $y = f\ (x)$, which are similar to each other except that the first curve $(y - b) = f\ (x - a)$ is shifted parallel to the coordinates with respect to the second curve plotted on logarithmic scale. This shows that the use of logarithmic scale enables the interpretation of field curves by matching with the theoretical curves. Furthermore, we need not have different curves for each value of ρ_1 and h_1 as single master curve can be used for any value of ρ_1 and h_1 as long as ρ_2/ρ_1 is constant.

The method of finding ρ_1 and h_1 is described with reference to the figure below:

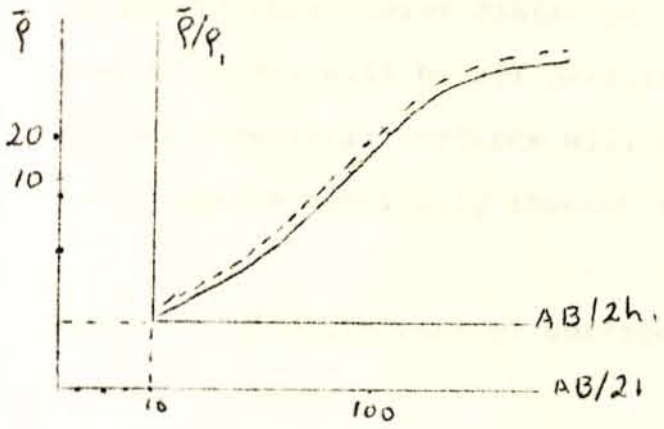

The field curve is plotted on a transparent double logarithm graph paper with a medulus the same as that for the theoretical master curve. It is then super imposed on the master curve and moved parallel to the coordinates until a match is obtained as indicated in the figure. The point on the transparent sheet coinciding with the origin of the master curve

$$(\bar{\rho}/\rho_1 = 1,\ \frac{AB}{2h_1} = 1)$$

gives along the abscisa, $\log AB/2 = \log h_1$ ie. $h_1 = \frac{AB}{2}$ and along the ordinate it gives $\log \bar{\rho} = \log \rho_1$ or $\bar{\rho}=\rho_1$

Next we shall show that the assymptotic nature of the schlumberger curves are still retained; and we will find the asymptotic value of the apparent resistivity, when

the second layer is of infinite resistivity.

At sufficiently large distances from the source, the current lines will be all parallel to the surface, and the equipotential surfaces will be cylindrical, with axis passing vertically through the source.

Consider an equipotential surface at a large distance r then,

$$I = 2\pi r^{h_1} J \tag{51}$$

since $J = E/\rho_1$, $E = \rho_1 I/2\pi r h_1$

for schlumberger:

$$\bar{\rho} = 2\pi r \quad (E/I) = (\rho_1/h_1)r \tag{52}$$

on taking logarithms we obtain

$$\log \bar{\rho} = \log r + \log (\rho_1/h_1)$$

$$= \log r - \log (h_1/\rho_1) \tag{53}$$

This is the equation of a straight line inclined at an angle of 45° to the obscisa, cutting it at a distance (h_1/ρ_1) from the origin.

Thus, the assymptotic value of the apparent resistivity when the second layer is of infinite resistivity is a straight line inclined at an angle of 45°.

Reduction of Two-layers

In a unit-cross sectional prism of resistivity ρ and thickness h.

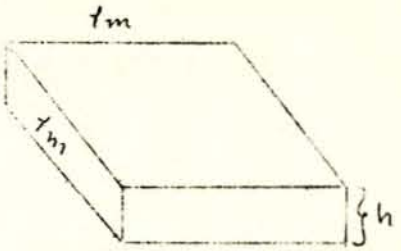

The resistance normal to the face of the prism is:

$T = h\rho$ and the conductance parallel to the face is:

$S = h/\rho$ from which we obtain:

$$h = \sqrt{ST} \tag{54}$$

$$\rho = \sqrt{T/S} \tag{55}$$

Thus, each value of S and T is associated with a section which has definite values of h and ρ given by the above equations for h and ρ

from the equations $T = h\rho$ or $\rho = T/h$

we have $\log \rho = -\log h + \log T$, and this equation defines a straight line inclined at an angle of 135° to the h-axis and cutting the h-axis at a distance T from the origin if ρ is plotted against h on a double logarithmic scale.

Similarly the equation $S = h/\rho$ gives $\log \rho = \log h - \log S$ which defines a straight line inclined at an angle of 45° with the h-axis and intercepting it at a distance of S from the origin.

Thus, the point of intersection of the two straight lines defined by the equations:

$$\log. \quad \rho = -\log_h + \log_T \tag{56}$$

$$\log. \quad \rho = \log_h - \log_S \tag{57}$$

then uniquely defines the resistivity and thickness for a particular combination of T and S.

If now we consider the prism to consist of n parallel homogeneous and isotropic layers of resistivities ρ_1 ρ_2 ... ρ_n and thicknesses h_1 h_2.... h_n respectively as indicated below:

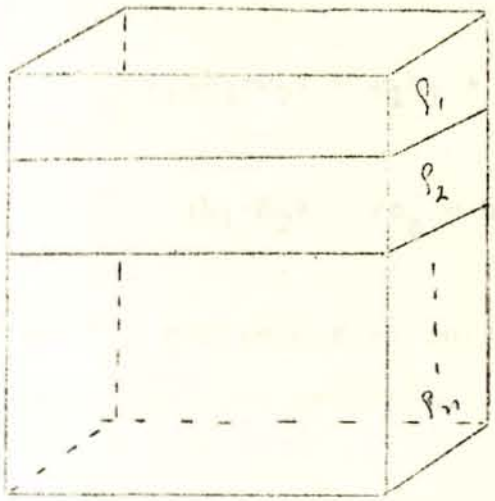

When the current is flowing normal to the base, the total resistance of the prism is:

$$T=T_1+T_2 + \ldots T_n = \sum_{i=1}^{n} T_i$$

$$= \rho_1 h_1+\rho_2 h_2 + \ldots {}_n h_n$$

$$= \sum_{i=1}^{n} \rho_i h_i \qquad (58)$$

When the current is flowing parallel to the base, the total conductance is:

$$S = S_1+S_2 + \ldots\ldots\ldots + S_n = \sum_{i=1}^{n} S_i$$

$$= h_1/\rho_1+h_2/\rho_2+\ldots. h_n/\rho_n = \sum_{i=1}^{n} h_i/\rho_i \qquad (59)$$

T and S are known as the transverse resistance and longitudinal conductance. If ρ_s and ρ_t are respectively, the longitudinal and transverse resistivities of the block,

$$\rho_t(h_1+h_2) = \rho_1 h_1 + \rho_2 h_2 \tag{60}$$

$$(h_1+h_2) \quad /\rho_s = h_1/\rho_1 + h_2/\rho_2$$

Thus, the coeficient of anisotropy (λ) and the mean resistivity (ρm) as defined earlier become:

$$\lambda = \sqrt{(\rho_t/\rho_s)} = \frac{1}{h_1+h_2}\{(\rho_1 h_1 + \rho_2 h_2)(h_1/\rho_1 + h_2/\rho_2)\}^{\frac{1}{2}} \tag{61}$$

$$\text{and} \quad \rho_m = \lambda\rho_s = \frac{1}{\lambda}\rho_t \frac{h_1\rho_1 + h_2\rho_2}{h_1/\rho_1 + h_2/\rho_2} \tag{62}$$

If we now assume that the two-layer anisotropic prism is replaced by a homogeneous and isotropic prism of thickness he and resistivity ρ_e: effective thickness and effective resistivity.

$$\text{Then} \quad \rho_e h_e = T = \rho_1 h_1 + \rho_2 h_2 \tag{63}$$

$$h_e/\rho_e = S = h_1/\rho_1 + h_2/\rho_2 \tag{64}$$

from which we obtain:

$$h_e = \left(\frac{h_1\rho_1 + h_2\rho_2}{h_1 + h_2}\right)(h_1/\rho_1 + h_2/\rho_2)^{\frac{1}{2}} = H \qquad (65)$$

$$\rho_e = \left(\frac{h_1\rho_1 + h_2\rho_2}{h_1/\rho_1 + h_2/\rho_2}\right)^{\frac{1}{2}} = \rho_m = \lambda\rho_s \qquad (66)$$

Thus, it is possible to reduce an isolated two-layer block into a single homogeneous and isotropic medium.

An example of a complete isolation of this kind is an A-type curve with the third layer highly resistive and the second layer more resistive than the first; and for this case we can write:

$$h_e = \lambda H \qquad (67)$$

$$\rho_e = \rho_m \qquad (68)$$

Since λ is always greater, the effective thickness of the composite layer is greater than the total thickness of the two layers.

Next we shall consider the case of a three-layer earth.

Case I: H Type:

In this case the resistivity of the intermediate layer is lower than that of the top and the bottom layers. If the resistivity of the bottom layer is large enough, for large values of AB, the flow of current in the upper layers will be approximately parallel to the horizontal strata. Hence, for this case the transverse resistance (T) can be neglected and the longitudinal conductance is the sum of the two layers.

If we replace the two upper layers by a single homogeneous layer with effective thickness h_H and effective resistivity ρ_H, we can write

$$h_H = h_1 + h_2$$

$$\rho_H \overset{=}{=} \frac{h_1 + h_2}{S_1 + S_2} = (h_1+h_2)/(h_1/\rho_1+h_2/\rho_2) = \rho_s \qquad (69)$$

These are known as Hummel's parameters; plotted on double-logarithm paper the equation $h_H = h_1 + h_2$ is a straight line parallel to the ordinate and the equation

$$\rho_H = \frac{h_1 + h_2}{S_1 + S_2} \qquad (70)$$

is a straight line inclined at an angle of 45° to the x-axis cutting it at $S_1 + S_2$.

The point of intersection of the two curves is called the Hummel point H, whose coordinates give ρ_H and h_H.

In practice the two equations are used to plot what are known as auxiliary H-point charts for a large number of values of $\mu_2 = \rho_2/\rho_1$ and different values of $\nu_2 = h_2/h_1$

$$\text{with abscisa} = x_H/h_1 = \frac{h_1+h_2}{h_1} = 1 + \frac{h_2}{h_1} = 1 + \nu_2 \qquad (71)$$

$$\text{and ordinate} \quad y_H/\rho_1 = \frac{1+\nu_2}{1 + \nu_2/\mu_2} \qquad (72)$$

These auxiliary point charts are directly used to find the H point (ie. ρ_H and h_H). Although these charts are strictly valid only for $\rho_3 = \infty$, they can be used even for any ρ_3 sufficiently greater than ρ_2, and this is the basis of a simple method of construction of empirical H-type curves.

Case II: A-Type:

In this case the intermediate layer is more resistive than the first ($\rho_2 > \rho_1$), and hence the transverse resistance cannot be neglected.

In addition, since $\rho_3 > \rho_2$, the longitudinal conductance is considered.

For the homogeneous layer reduced from the top two layers.

$$T = T_1+T_2 = h_1\rho_1+h_2+\rho_2 \tag{73}$$

$$S = S_1+S_2 = h_1/\rho_1+h_2/\rho_2 \tag{74}$$

We have seen earlier that for this case

$$h_A = \sqrt{TS} = \lambda(h_1+h_2) = \lambda H \tag{75}$$

$$\rho_A = \sqrt{T/S} = \rho_m = \lambda\rho_S \tag{76}$$

These points are the coordinates of the intersection of the T and S lines. This point is called the "anisotropy point".

As in the case of the H-type, the equations

$$h_A = \sqrt{TS} = \lambda(h_1+h_2) = \lambda H \text{ and } \rho_a = \sqrt{T/S} = \rho_m = \rho_S$$

are used to plot the auxiliary point charts (A) for

various values of μ and ν_2. But before plotting the equations are rewritten as

$$x_A/h_1 = (1 + \nu_2/\mu_2)\ (1 + \nu_2/\mu_2)^{\frac{1}{2}} \tag{77}$$

$$y_A/\rho_1 = \left(\frac{1 + \nu_2\mu_2}{1+(\nu_2)/\mu_2}\right)^{\frac{1}{2}} \tag{78}$$

The coordinates of the point A(h_A and ρ_A) can the directly be read off these auxiliary point charts.

Case III: K-Type

In this, the resistivity of the intermediate layer is higher than that of the top and bottom layers. The current in the upper two layers will be similar to case II, especially at smaller AB. Therefore, both T and S should be considered. In this case however, since the intermediate layer is underlain by a less resistive layer the current flow lines within the second layer should have a large vertical component than that of A-type. Hence, we expect the conditions to be different.

An examination of the theoretical curves shows in this case that the resistivity of the reduced layer remains

the same as in the A-type section whereas its thickness is found to be greater: $h_k = \varepsilon(h_1 + h_2)$ where ε is a function of λ always greater than unit.

The relationship between λ and ε is plotted empirically as shown below:

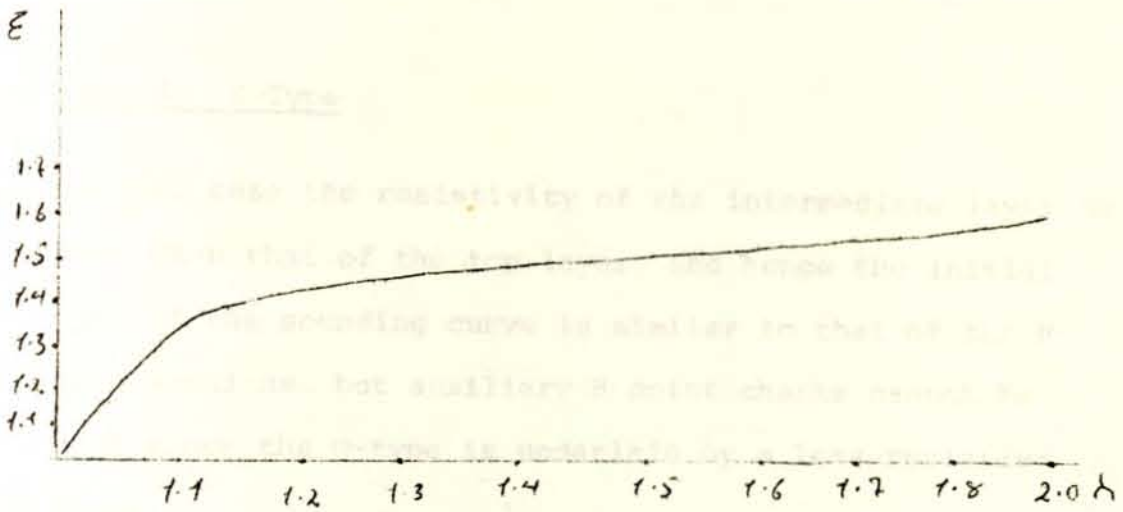

The values of λ and the corresponding values of ε may be tabulated as shown below:

λ	1.10	1.20	1.30	1.40	1.50	1.7	2.00	2.50	3.00
ε	1.17	1.17	1.29	1.32	1.33	1.36	1.381	.40	1.42

Thus, the parameter of the reduced layer is determined by the coordinates of the point K, given by

$$x_k = \sqrt{TS} \tag{79}$$

$$y_k = \sqrt{T/S} \tag{80}$$

point k is known as the "displaced anisotropy" point.

The equation for plotting the auxiliary point chart (k) can be shown to be

$$\frac{x_k}{h_1} = \varepsilon\,(1+\nu_2/\mu_2)\;(1+\nu_2/\mu_2)^{\frac{1}{2}} \qquad (81)$$

$$y_k/\rho_1 = \left(\frac{1+\nu_2\,\mu_2}{1+\nu_2/\mu_2}\right)^{\frac{1}{2}} \qquad (82)$$

Case IV: Q-Type

In this case the resistivity of the intermediate layer is less than that of the top layer, and hence the initial part of the sounding curve is similar to that of the H-type sections, but auxiliary H-point charts cannot be used since the Q-type is underlain by a less-resistive layer.

It is empirically found in this case that the total thickness of the reduced layer is less than (h_1+h_2) by a factor η, depending on the values of μ_2 and ν_2 of the electrical section. The value of η can be read from the curves shown below for various values of μ_2 and ν_2.

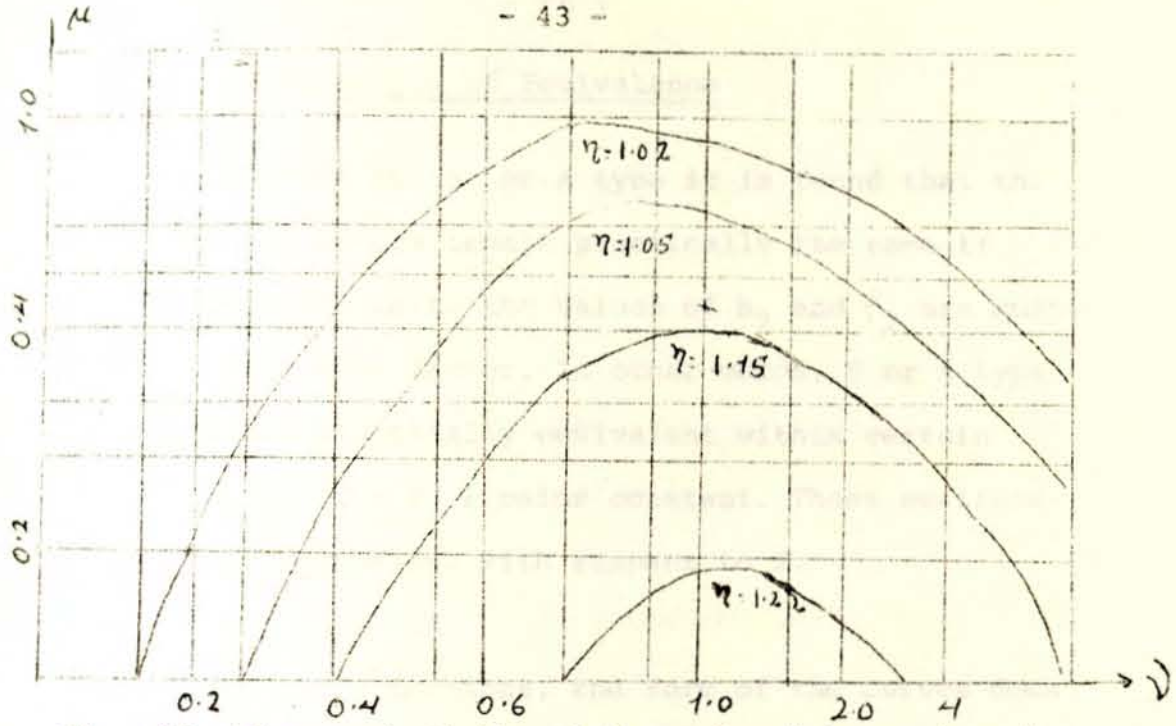

The effective resistivity of the reduced layer is also taken as less than the mean longitudinal resistivity by the same factor η. Then the coordinates of O are given by

$$x_O = H/\eta \tag{83}$$

$$y_O = 1/\eta \frac{H}{S} \tag{84}$$

and these equations can be rewritten for the purpose of plotting the auxiliary point charts (O) for various values of μ_2 and ν_2 as

$$x_O/h_1 = \frac{1}{\eta}(1+\nu_2) \tag{85}$$

$$y_O/\rho_1 = \frac{1}{\eta} \frac{1+\nu_2}{1+(\nu_2/\mu_2)} \tag{86}$$

Use of the Principle of Equivalence

For sections of the H or A-type it is found that the forms of the curves temain practically the same if, within certain limits the values of h_2 and ρ_2 are multiplied by the same factor. In other words, H or A-type sections are practically equivalent within certain limits if $h_2/\rho_2 = S_2$ remains constant. These sections are called equivalent with respect to S.

Also for K and Q sections, the form of the curves does not change appreciably if h_2 is increased or decreased by a certain factor and ρ_2 is correspondingly decreased or increased by the same factor. Thus, if $h_2\ \rho_2 = T_2$ remains constant, any change of h_2 and ρ_2 separately does not produce any noticeable change in the form of the curve. Such sections may be called equivalent with respect to T.

The principle of equivalence applies only for small values of $\nu_2 = h_2/h_1$ which may be different for different values of $\mu_2 = \rho_2/\rho_1$ and $\mu_3 = \rho_3/\rho_1$. For interpretation of sounding data, it is therefore important to know the maximum values of h_2/h_1 beyond which the principle of equivalence does not apply; and it is also

important to know the limits within which h_2 and ρ_2 may be varied, satisfying the equivalence of the curves. The limits ν_2 or μ_2 are usually obtained by "Pylayev's nomograms".

The principle of equivalence plays an important role in the graphical construction of field curves as well as in their interpretation.

Suppose, for example, it is necessary to find an H-type curve with parameters $\mu_2 = 1/30$, $\nu_2 = 4$ and $\rho_3 = \infty$. A theoretical curve with such parameters does not exist in the sets of master curves published. The closest theoretical curve has the value $\mu_2 = 1/39$, Pylaev's nomogram shows that for the given parameters μ_2 may be changed within the limits of equivalence. Thus, the corresponding value of ν_2 is given by $\nu_2/\mu_2 = 120 = \nu_2^1/\mu_2^1$ ie. $\nu_2^1 = 120/39 = 3.1$. Thus, we can use the curve $\mu_2 = 1/39$, $\nu_2 = 3, \rho_3 = \infty$ which is equivalent to the given section within an error of 5% Q, To get a K-type curve, equivalent with respect to T for the values $\mu_2 = 30\nu_2 = 4$ and $\rho_3 = 0$ we can use the relation $\nu_2^1 = \mu_2\nu_2/\mu_2^1$ and $\mu_2^1 - \mu_2\nu_2/\nu_2$ then the parameters of the new curve equivalent to the given section are $\mu_2 = 39$, $\nu_2 = 3$ and $\rho_3 = 0$. For Q and A-type sections the procedure is exactly the same as for those of K and H-types.

Qualitative Interpretation

It is sometimes useful to make a rapid qualitative study of the field curves before a detailed quantitative interpretation is under-taken. Of the several methods available we shall discuss below a common method. This method depends on the determination of the total longitudinal conductance (s) of the geoelectric section from the right-hand asymptotic part of the sounding curve.

We have seen earlier that the asymptotic part of the sounding curve is a straight line, inclined at an angle of 45°, when the basement is of infinite resistivity, and that the intersection of this straight line with the abscissa (ie. AB/2 at $\bar{\rho} = 1$ gives the value of the total longitudinal conductance of the section:

$$S = s_1 + s_2 + \ldots \frac{h_1 + h_2}{\rho_s} + + \ldots \frac{H}{\rho_s} \qquad (87)$$

where ρ_s is the longitudinal resistivity of the whole section.

In the case of a two-layer earth with a basement complex of a high resistivity ($\rho_2 = \infty$), the value of $\bar{\rho}$ for small AB (ie. AB → 0) gives ρ_1, and the value of S read

from the assymptotic part gives: $h_1 = \rho_1 S$. If the section underlain by the basement is a finely layered thick sedimentary section, the depth obtained from the S value and the resistivity of the surface layers may not give the true depth of the basement because of the anisotropy. In this case the depth is given by $h = \rho_s S$, and it is necessary here to find ρ_s from some independent measurements of the true depth (by actual well lagging or geophysical well logging) at a few places where sounding curves are available.

It is found that ρ_s does not change much in an area with lateral variations of the resistivity and thickness of the sedimentary section.

Hence, if ρ_s is known at a few control points, it is possible to map the basement from the S-part of the sounding curves only. This procedure may be extended for basement mapping in a multi-layer section if the assumption of a small variation in ρ_s is approximately valid.

Thus, if conditions are favourable it is possible to obtain a rapid qualitative idea of the depth of basement in an area through an investigation of the S-part of the curve.

In the interpretation of three-layer H and A-type field curves ($\rho_3 = \infty$) the following procedure that requires only two-layer master curves is used for qualitative interpretation:

a) ρ_1 and h_1 are obtained by matching the left hand part of the field curve with the two layer master curves.

b) S is read from the intersection of the tangent to the assymptotic part of the field curve with the abscissa at $\bar{\rho} = 1$, and from this step

$$S = S_1 + S_2 \tag{88}$$

$$= h_1/\rho_1 + h_2/\rho_2$$

$$S_2 = S - S_1 = S - (h_1/\rho_1) = h_2/\rho_2) \tag{89}$$

c) If ρ_2 is known from some independent measurements at certain parts of the area, then

$h_2 = s_2\rho_2$, and finally, we have for the total depth of the basement

$$H = h_1 + h_2$$

Using the same procedure for other points, the basement can be mapped from a knowledge of ρ_2 and the use of two layer master curves only.

This semi-quantitative method can be extended to a multi-layer sedimentary section underlain by a basement.

Quantitative Interpretation

In electrical sounding, the basic problem of quantitative interpretation is to determine the thickness of the different formations having different resistivities from the field sounding curves. The commonest interpretation method is based on comparing the field curve with curves obtained theoretically or constructed graphically, having suitably chosen parameters.

In the case of perfect coincidence of the theoretical with the field curve (complete matching), the values of the field parameters are the same as those of the geoelectrical section for which the theoretical curves have been constructed.

But in practice a complete set of theoretical curves representing all geological conditions met in the field is not available; which makes it necessary to devise means of interpreting observed field curves with the help of a limited number of theoretical curves available in published form.

To interpret two-layer VES (vertical electrical sounding) field curves by this method, the field curve is first plotted on a double-logarithm transparent graph sheet with $\bar{\rho}$ on the ordinate and AB/2 along the abscissa; and then it is superposed on the set of two layer master curves to obtain a good match by shifting the curve, keeping the axes parallel to the coordinate system.

The coordinates of the origin of the master curves as read on the field curve give the values of ρ_1 and h_1; the value of $\mu_2 = \rho_2/\rho_1$ read from the matching theoretical curve and ρ_2 calculated.

For a finely layered sedimentary section, ρ_1 and ρ_2 represent the mean resistivities of the top and botom layers. If no exact match is obtained interpolation is necessary.

Interpretation of three-layer sounding curves are similarly achieved with the help of available two - and three layer master curves and complementary curves known as auxiliary point charts.

Step-wise reduction of multi-layer curves to equivalent two or three-layer cases renders possible their interpretation using the same methods as the two and three-layer ones.

Effect of Dip on Interpretation

The discussion so far was only in connection with a horizontally stratified earth.

But often, electrical sounding is carried out in regious where the boundaries between different layers are inclined.

It is therefore necessary to examine the effect of this inclination of beds on vertical electrical sounding curves.

Various workers have investigated this problem and among them AL' pin (1940) has published a set of 16 two-layer master curves for schlumberger configuration parallel to the strike direction, an example of which is shown below:

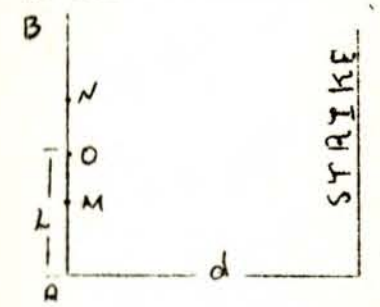

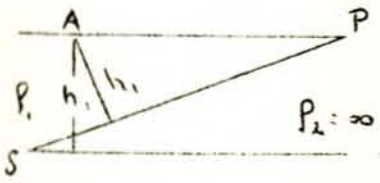

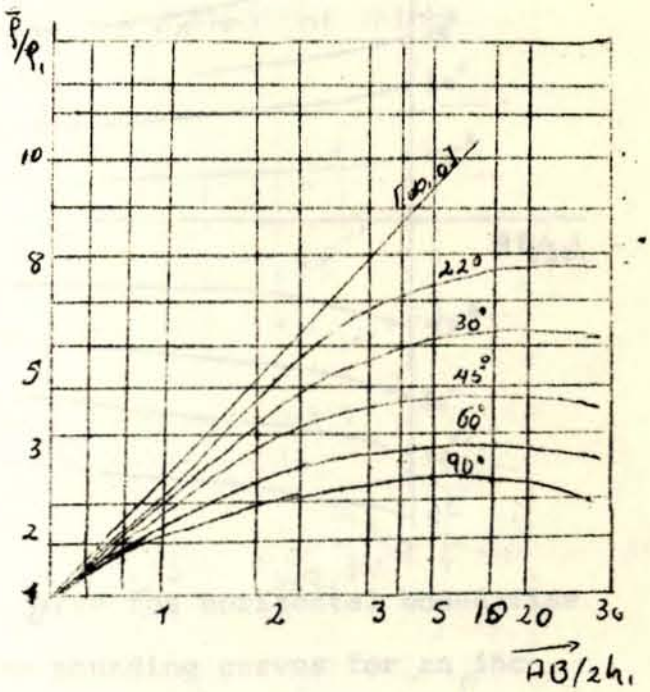

In this curve the apparent resistivity is plotted against $AB/2h_1$ where h_1 is the depth perpendicular (not the vertical depth h) to the boundary. The curves are plotted for different values of the angle of inclination $\alpha = 0°, 22°, 30°, 45°, 60°, 90°$ corresponding to $\rho_2/\rho_1 = \infty$

Similar curves are availlable for different values of resistivity contrast.

Another variant of master curves for a similar situation have also been recently published. One such set of curves is shown ebelow:

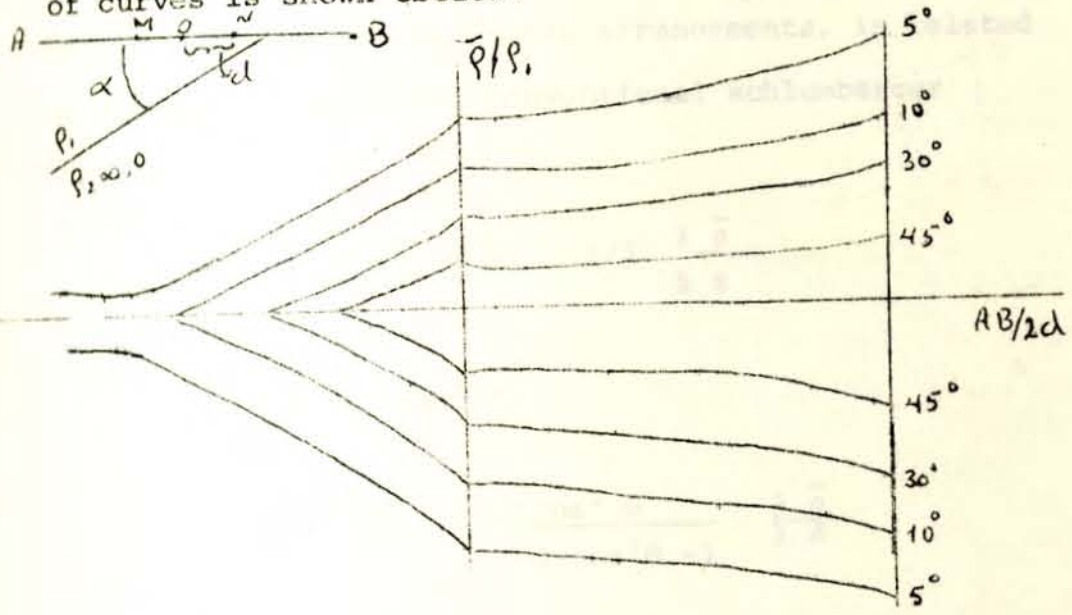

If the two-layer master curve for horizontal boundaries are used to interpret the sounding curves for an inclined two layer contact, considerable error is involved particularly when α is large. But if the angle of inclination (α) is not more than 20 , the ordinary two layer master curves may be used without significant error.

In practice if it is known before hand that the boundary is inclined, quantitative interpretation can be carried out if one of the parameters (α or ρ_2/ρ_1) is known. Using the master curves for inclined contact, the other Parameter and depth of bottom layer can be determined.

Interpretation of Dipole Sounding

We have seen earlier that the apparent resistivity measured by any of the dipole arrangements, is related to that obtained by the conventional schlumberger arrangement:

$$\bar{\bar{\rho}}_r = \bar{\bar{\rho}}_{ax} = \bar{\rho} - \delta/2 \frac{\partial \bar{\rho}}{\partial s}$$

$$\bar{\bar{\rho}}_\theta = \bar{\bar{\rho}}_{eq} = \bar{\rho}$$

$$\bar{\bar{\rho}}_x = \bar{\rho} - \frac{\delta \cos^2 \theta}{3 \cos^2 \theta - 1} \frac{\partial \bar{\rho}}{\partial \delta}$$

$$\bar{\bar{\rho}}_y = \bar{\rho} - \delta/3 \frac{\partial \bar{\rho}}{\partial \delta}$$

This entails the possibility of construction of dipole electric sounding curves from conventional sounding curves; and particularly for $\bar{\bar{\rho}}_\theta$, since it is equal to the schlumberger apparent resistivity $\bar{\rho}$ for the same spacing, the master curves available for conventional sounding may be used directly for azimuthal dipole sounding; and the method of interpretation is the same.

In general, dipole electric sounding differs from the conventional sounding in its possibility for bilateral and multilateral measurements. This is explained with the help of illustration below:

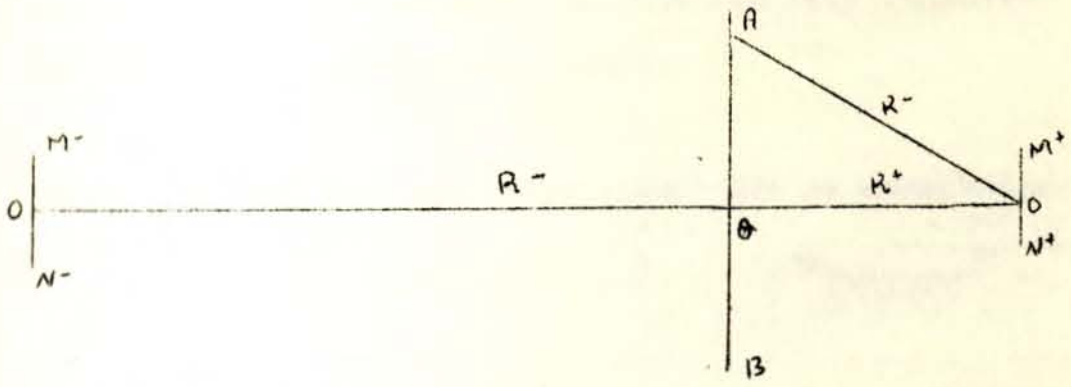

For a certain position of the current dipole AB two potential dipoles M^+ N^+ and M- N- can be placed on either side at distances R + and R -, enabling two values of resistivity ρ^+ and ρ^- corresponding to the mid points of QO^+ and QO^-

This arrangement is called a bilateral sounding with the symbols + and - indicating whether the moving electrodes are mvoing towards the contact or away from it.

For a horizontally stratified earth, the values of both resistivity ρ^+ and ρ^- will be the same, for an

inclined horizon the values of ρ^+ and ρ^- will be different and the difference will be a measure of the inclination of the horizontal. The average of ρ^+ and ρ^- will be the resistivity corresponding to the conventional sounding. This means, for dipole sounding one can construct three curves: the positive, the negative and the average resistivity curves.

Let us consider the case of a dipping bed as shown below:

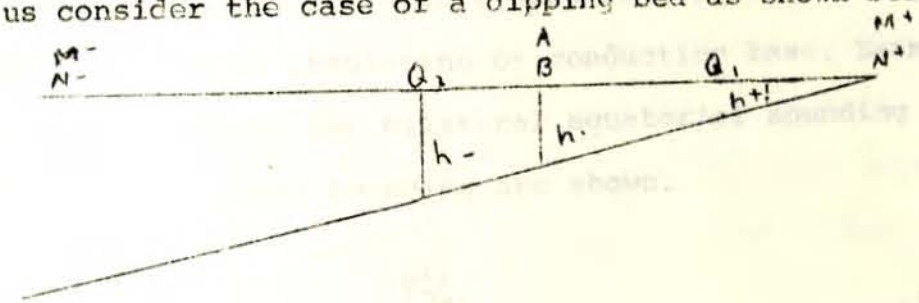

The conventional sounding gives the depth of the horizon only at its center; but if the current dipole of the bilateral sounding set-up is placed at the center, it is possible to get three depths from the three constructed curves:

h + (up-dip), h - (down-dip) and

h (center) thus,

the location of the horizon is more reliable with the bilateral dipole sounding than the conventional method.

The large number of master curves available for conventional sounding can be used directly for azimuthal (or equatorial) dipole sounding. In addition special theoretical curves have been constructed for the radial (or axial) dipole sounding of a three-layer earth along with two sets of two-layer curves.

Theoretical curves are also available for an inclined layer lying on an insulating or conducting base. Examples of such curves for bilateral equatorial sounding and bilateral axial sounding are shown.

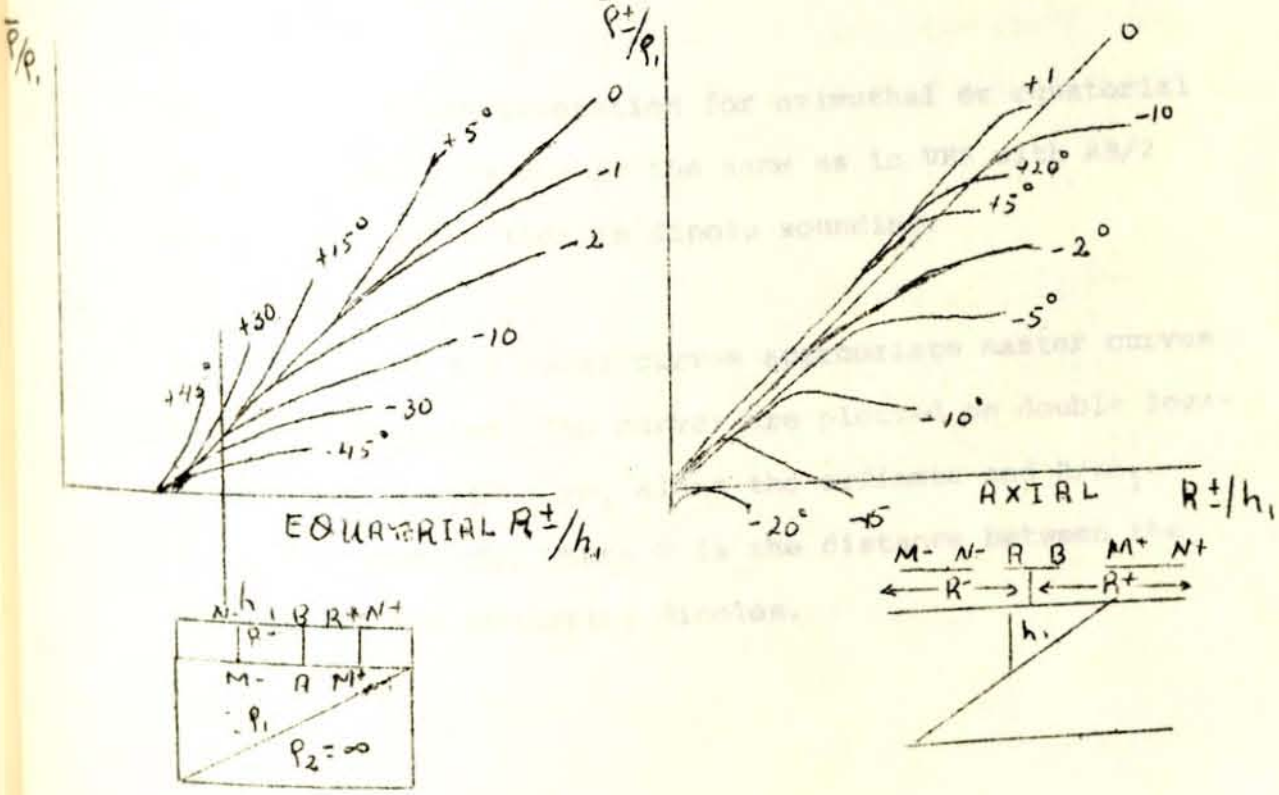

It is seen from the first figure that even for an inclination of 2° the separation between the positive and negative resistivity curves is quite noticeable, and for the axial it is seen that an inclination of as little as 1° can be detected by the separation of the positive and negative curves.

Since the dipole sounding is very sensitive to lateral variations, the inhomogenieties of the surface layers can distort the resistivity values for the deeper layers. This is avoided by using the conventional method for sounding up to a depth of 200 - 300; beyond that depth the sounding may be undertaken by the dipole method.

The method of interpretation for azimuthal or equatorial dipole sounding curves is the same as in VES with AB/2 equivalent to $\bar{R}$ - (AO) in dipole sounding.

For the radial and axial curves appropriate master curves have been prepared. The curves are plotted on double logarithmic scale with $\ddot{\rho}/\rho_1$ along the ordinate and $R/2h_1$ along the abscissa. Where R is the distance between the current and the measuring dipoles.

As an illustration we present below the procedure followed in interpreting three layer radial dipole sounding curves with the help of published curves.

a) The left hand part of the field curve is superposed over the two layer radial master curve set, keeping axes parallel until a good match is obtained. This step gives ρ_1 , h_1 and $\mu = \rho_2/\rho_1$

b) From the asymptotic part of the curve ρ_3 is guessed and ρ_3/ρ_1 determined.

c) With the obtained ρ_3/ρ_1 as a guide to chose the proper set of three-layer master curves, the field curve as a whole is matched over the selected set of three layer curves.

The final step of matching gives $\mu = \rho_2/\rho_1$, $\nu = h_2/h_1$ and ρ_3

VIII LATEST ACHIEVEMENTS

In the following section we shall outline recent innovations in resistivity work advanced by several workers:

1. The Method of Field Differences

In the discussion of bihole - dipole field difference by U.C. Das and R.D. Singh. The differential apparent resistivity ($\rho_w^D(a)$)

obtained by the technique of differential resistivity sounding for the wenner array was defined as:

$$\rho_w^D(a) = \delta a \frac{d\rho_w(a)}{da} \tag{90}$$

Where $\rho_w(a)$ is the wenner apparent resistivity at electrode separation a, δ is the spacing increment; and similarly for the schlumberger array:

$$\rho_s^D(s) = \frac{ds}{d\left[s/\rho_s(s)\right]} \tag{91}$$

Where $\rho_s(s)$ refers to the Schlumberger apparent resistivity at the half current electrode separation S.

The transverse and longitudinal differential resistivities for the schlumberger case were also defined as

$$\rho^{D}_{s,T}(S) = \frac{d(s.\rho_s(s))}{ds} \tag{92}$$

and

$$\rho^{D}_{s,2}(S) = \frac{ds}{d[s/\rho_s(s)]} \tag{93}$$

respectively.

The bibole potential V_B (s) being defined as:

$$V_B(s) = \frac{I}{2\pi} \int_{SA}^{SB} \frac{\rho_s(s)}{s}\, ds \tag{94}$$

Where $\rho_s(s)$ is the schlumberger apparent resisitivity,

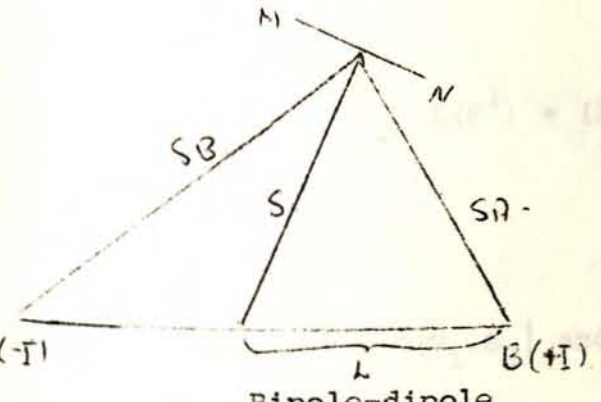

Bipole-dipole

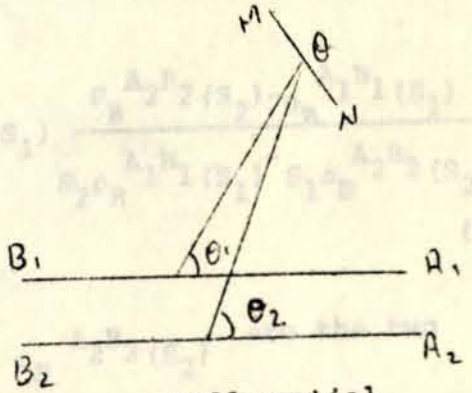

Differential bibole-dipole

Das and Singh defined the differential resistivities for such a system as

$$\rho^{D}_{B,T}\ (S^{1}) = \frac{d(s.\rho_{B}(s)}{ds} \tag{95}$$

$$\rho^{D}_{B,L}\ (S^{1}) = \frac{ds}{d[s/\rho_{B}(S)]}\ , \tag{96}$$

where $\rho_{B}(S)$ is the bibole-dipole apparent resistivity at distance S = OQ.

relation to the given figure the above two equations can be expanded as

$$\rho^{T}_{B,\ T}(S^{1}) = \frac{S_2\rho_B{}^{A_2B_2}(s_2) - S_1\rho_B{}^{A_1B_1}(S_1)}{S_2 - S_1} \tag{97}$$

and

$$\rho^{D}_{B_1,\ L}(S^{1}) = (S_2 - S_1)\ \frac{\rho_B{}^{A_2B_2}(S_2) - \rho_B{}^{A_1B_1}(S_1)}{S_2\rho_B{}^{A_1B_1}(S_1) - S_1\rho_B{}^{A_2B_2}(S_2)} \tag{98}$$

Where $S^{1} = \sqrt{(S_1.S_2)}$ and $\rho_B{}^{A_2B_2}(S_2)$ are the two apparent resistivities at the point of measurement due to two bibole sources A_2B_2 and A_1B_1 placed parallel to each other at distances S_2 and S_1 from the point of measurement, as shown in the figure. S_2/S_1 <1.2

The apparent resistivity field equations for the two bibole sources are:

$$\rho_B^{A_2B_2}(S_2) = K_2 \frac{\Delta V_2}{I_2} \tag{99}$$

$$\rho_B^{A}(S_1) = K_1 \frac{\Delta V_1}{I_1} \tag{100}$$

Where K is the geometric factor, V is the potential difference and I is the current. Combining these two equations with the equation:

$$\rho_{B_1}^{D} T(S^1) = \frac{S_2 \rho_B^{A_2B_2}(S_2) - S_I \rho_B^{A_1B_1}(S_1)}{S_2 - S_1}$$

we obtain

$$\rho_{B,1}^{D} T(S^1) = \frac{\frac{K_2 S_2 \Delta V_2}{I_2} - K_1 S_1 \frac{\Delta V_1}{I_1}}{S_2 - S_1} \tag{101}$$

$$= \frac{K_2 S_2}{I_2(S_2-S_1)} \frac{\Delta V_2 - K_1 S_1}{K_2 S_2} \cdot \frac{I_2}{I_1} \Delta V_1$$

$$\text{or} \quad \rho_{B_1}^{D} T(S^1) = K_T^D , \frac{\Delta(\Delta V)}{I_2} \tag{102}$$

$$\text{Where} \quad K_T^D = \frac{K_2 S_2}{S_2 - S_1} \tag{103}$$

$$\Delta(\Delta V) = \Delta V_2 - \Delta V_1 \tag{104}$$

and $$I_2 = \frac{K_2 S_2}{K_1 S_1} I_1 \tag{105}$$

The last two equations suggest that when the current in $A,B,$ and A_2B_2 is sent simultaneously in opposite directions satisfying the last equation, then we can directly measure $\Delta(\Delta V)$ at the measuring point and obtain ρ_B^D , $T(S^1)$ through the equations

$$\rho_B^D \, , \, T(S^1) = K_T^D \, \frac{\Delta(\Delta V)}{I_2}$$

and $$K_T^D = \frac{K_2 S_2}{S_2 - S_1}$$

Similarly combining appropriate equations, we obtain

$$\rho_{B,\,L}^D(S) = (S_2 - S_1) \frac{K_2 \frac{\Delta V_2}{I_2} \cdot K_1 \frac{\Delta V_1}{I_1}}{S_2 K_1 \frac{\Delta V_1}{I_1} - S_1 K_2 \frac{\Delta V_2}{I_2}} \tag{106}$$

$$= \frac{K_2}{I_2} \cdot \frac{S_2 - S_1}{S_2} \cdot \frac{\Delta V_2 \cdot \Delta V_1}{\left(\Delta V_1 - \frac{K_2 S_1}{K_1 S_2} \cdot \frac{I_1}{I_2} \Delta V_2\right)}$$

or $$\rho_{B\,,\,L}^D(S^1) = \frac{K_1 D}{I_2} \, \frac{\Delta V_1 \Delta V_2}{\Delta(\Delta V)} \tag{107}$$

Where

$$K_L^D = K_2 \frac{S_2 - S_1}{S_2} \tag{108}$$

$$\Delta(\Delta V) = \Delta V_1 - \Delta V_2 \tag{109}$$

and $$I_2 = \frac{K_2 S_1}{K_1 S_2} I_1 \tag{110}$$

Thus, to measure ρ_B^D , $L(S^1)$ one has to separately send currents in A_2B_2 and A_1B_1 to measure ΔV_2 and ΔV_1 respectively, and then $\Delta(\Delta V)$ is measured by passing currents through both biboles simultaneously but in opposite direction satisfying the equation.

$$I_2 = \frac{K_2 S_1}{K_1 S_2} I_1$$

We obtain the required ρ_B^D , $L(S^1)$ through the equations

$$\rho_B^D , L(S^1) = K_L^D / I_2 \frac{\Delta V_1 - \Delta V_2}{\Delta(\Delta V)}$$

and $$K_L^D = K_2 \frac{S_2 - S_1}{S_2}$$

2. The Resistivity Transform

Slichter's (1933) method of direct interpretation of resistivity sounding data with the help of the Kernel function has been the subject of continued interest since its proposition. The first step of Slichter's method is to determine the Kernel function from the field measurements and in the second step the layer parameters are detected from the Kernel function.

Santini and Zambrano (1981) presented a numerical method of calculating the Kernel function which is based on a decomposition method. The observed apparent resistivity data are approximated by utilizing a linear combination of simple fitting functions chosen in such a way that they allow the determination of the Kernel analytically. The fitting operation is carried out by the least squares method.

This numerical method was developed for Schlumberger curves.

As an illustration we shall discuss below the numerical method developped by Rakesh Kumar and MV Ramanaiah

chowdary to calculate the Kernel function for wenner resistivity curves.

On the surface of horizontally n-layered earth the wenner apparent resistivity ρ_{aw} is given by

$$\rho_{aw} = \rho_1\left[1+4a\int_0^\infty k(\lambda)\ \{\ J_o(\lambda a)-J_o(2\lambda a)\ d\lambda\ \}\right] \qquad (111)$$

Where a is the wenner spacing ρ_1 is the resistivity of the top layer, J_o is the bessel function of the first kind and zero order, $K(\lambda)$ is the Kernel function which depends on depth and reflection coefficients of the interfaces involved and can take values between - 0.5 and $+\infty$ and λ is the integration variable.

Putting $Y = \dfrac{\rho_{aw} - \rho_1}{2\rho_1}$ and (112)

multiplying the equation for apparent resistivity by $J_o(ax)$ and integrating, we obtain,

$$\int_0^\infty yJo\ (ax)da = \int_0^\infty\int_0^\infty ak(\lambda)\left\{\ Jo(\lambda a)-J_o(2\lambda a)\right\}J_o(ax)\,da\,d\lambda \qquad (113)$$

On applying the fourier-Bessel integral of the form

$$\int_0^\infty\int_0^\infty r\lambda F(\lambda)\ J_o(r\lambda)\ J_o(rx)\ dr\,d\lambda = F(x) \qquad (114)$$

to the right hand side, we get

$$\int_0^\infty y\, J_o(ax)\, da = \frac{2k(x)}{x} - \frac{k(k/2)}{x} \qquad (115)$$

If y is approximated by a linear combination of suitable functions $f(a, \varepsilon_i)$ chosen in such a way that they allow the Kernel to be determined analytically:

$$Y^* = \sum_{i-1}^{m} bi\, f(a, \varepsilon_i) \qquad (116)$$

Kumar and chowdary found that the best fitting such function was

$$f(a, \varepsilon_i) = \frac{a}{\sqrt{a^2 + \varepsilon_i^2}} - \frac{a}{\sqrt{4a^2 + \varepsilon_i^2}} \qquad (117)$$

with these substitutions the equation

$$\int_0^\infty yJo\ (ax)\ da = \frac{2k(x)}{x} - \frac{k(x/2)}{x}$$

becomes:

$$\sum_{i=1}^{m} b_i \int_0^\infty \frac{a}{\sqrt{a^2 + \varepsilon_i^2}} - \frac{a}{\sqrt{4a^2 + \varepsilon_i^2}}\, J_o(ax)\, da$$

$$= \frac{2k^*(x)}{x} - \frac{K^*(x/2)}{x} \qquad (118)$$

It is known from the theory of bessel functions that

$$\exp(-\varepsilon x)\, J_o(ax)\, dx = \frac{1}{\sqrt{\varepsilon^2 + a^2}} \tag{119}$$

and application of Hankel transformation gives

$$\int_o^\infty \frac{a}{\sqrt{(a^2+\varepsilon^2)}} J_o(ax)\, da = \frac{\exp(-x)}{x} \tag{120}$$

and with the help of the last relation the equation

$$\sum_{i=1}^{m} \int_o^\infty bi \left[\frac{a}{\sqrt{a^2+\varepsilon_i^2}} - \frac{a}{(4a^2+\varepsilon_i^2)} \right] J_o(ax)\, da = \frac{2k^*(x) - k^*(x/2)}{x}$$

becomes

$$\sum_{i=1}^{m} bi \left[(\exp(-\varepsilon_i x) - \frac{\exp(-\varepsilon_i x/2)}{2} \right] = 2k^*(x) - k^*(x/2) \tag{121}$$

Substituting in the last equation we have for $k^*(\lambda)$

$$k^*(\lambda) = \sum_{i=1}^{m} bi \exp(\varepsilon_i \lambda) \tag{122}$$

This means that the Kernel can be expressed by means of a linear combination of functions $g(\lambda, \varepsilon_i)$

$$k^*(\lambda) = \sum_{i=1}^{m} bi\, g(\lambda, \varepsilon_i) \tag{123}$$

Where $g(\lambda, \varepsilon_i) = \dfrac{\exp(-\varepsilon_i \lambda)}{2}$ (124)

The actual determination of y^* and consequently $k^*(\lambda)$ depends on the number m, on the constants ε_i and on the coeficients bi.

Next we intend to determine y^* such that it approximates y according to the principle of least squares. Therefore

$$\sum_{j=1}^{K+1} \left\{ \sum_{i=1}^{m} bi \left[\frac{a_j}{\sqrt{a_j^2+\varepsilon_i^2}} - \frac{a_j}{\sqrt{(a_j^2+\varepsilon_i^2)}} \right] - y_j \right\}^2 = \min \tag{125}$$

Where Y_j is the value of y at $a = a_j$

after the number m is fixed, the above equation is solved for the unknown coeficients b_1 establishing the m values of ε_i which are chosen by first taking them in a geometric progression, the desired quality of fitting of y being dependent on the ratio of the progression. It is suggested that one uses three or four fitting functions for each logarithmic cycle of the resistivity curve; and the extrem values of i can be fixed by choosing $\varepsilon_1 \approx a_1$ and $\varepsilon_m \; 0.5^{a_k}$

where a_1 and a_k are the first and last abscissae values of the observed (or extrapolated) resistivity curve.

Continuation of the least squares operation then leads to a symmetric normal linear system of equations for m unknowns, the m^{th} normal equation being

$$b_1 \sigma_{1\ m} + b_2 \sigma_{2\ m} \ldots + b_m \sigma_{m\ m} = \eta_m \tag{126}$$

Where

$$\sigma_{x,\ y} = \sum_{j=1}^{k+1} f(a_j;\ \varepsilon_x)\ f(a_j;\ \varepsilon_y) \tag{127}$$

$$\eta_x = \sum_{j=1}^{k+1} f(a_j;\ \varepsilon_x)\ y_j \tag{128}$$

Once the b_i are known as solutions of the normal equations y^* and $k^*(\lambda)$ can be determined using

$$y^* = \sum_{i=1}^{m} bi\ \ f(a,\ \varepsilon_i)$$

$$f(a,\ \varepsilon_i = \frac{a}{\sqrt{(a^2+\varepsilon_1{}^2)}} - \frac{a}{\sqrt{(4a^2-\varepsilon_i{}^2)}}$$

and $$K^*(\lambda) = \sum_{i=1}^{m} bi\ \frac{\exp(-\varepsilon_i \lambda)}{2}$$

after $K(\lambda)$ is determined, a related function, the resistivity transform $T(\lambda)$ which is a useful version of $K(\lambda)$ used in the second step of interpretation may be computed

$$T(\lambda) = \rho_1 \left[1+2k(\lambda)\right] \tag{129}$$

IX PART II. PRACTICAL WORK

As outlined in the title of this project the second part of the work consists of analysis and interpretation of data from selected sites.

Accordingly two regions were selected: one around Dire Dawa in the Eastern part of Ethiopia and another around Tendaho in the Northern part. Refer to location maps for precise location.

We acknowledge the Geophysics Department, Ministry of Mines and Energy for supplying a greater portion of the resistivity data.

The procedures of investigation, methods of analysis and results are reported in this paper.

A. DIRE DAWA

Geology of Dire Dawa Area

Bedrocks are mainly composed of acidic magnetite precambrian overlain by Triassic Adigrat sandstone, Jurassic Antalo limestone and cretaceous upper sandstone. These formations are overlain by the lower Tertiary Trap series lavas. After being tilted by

block faulting, they were covered by stratoid flood basalt which errupted after these major block faulting in Mid Tertiary.

The thickness of the lower sandstone is less than 100 meters. It passes upwards into sandy limestone through a series of alternating calcareous siltstone, marl, limestone and dolomite.

The antalo limestone which is about 175 m thick, has as its lower part alternating shale and chalk. Brown limestone layers are common and druses of quartz occur towards the top. The lower levels contain thin beds of dolomite. The upper part consists of grey limestone with concretions of chert and drusses of quartz.

The cretaceous upper sandstone is about 200 m thick; thin lenses of marl with small lateral extent occur frequently. Intercalated limestone bed of 3-15 meters has been found in adjacent areas.

The down-thrown blocks NE of Dire Dawa consist of basaltic lavas interbedded with some ignibritic and tuff units. Rhyolitic lavas extruded after the main

block faulting followed by the erruption of stratoid flood basalts along a possible swarm of parallel fissures related to the ESE trend of faults in the northern part of the area.

The superficials are presumed to have been deposited in a lacustrine environment that existed before the extrucssion of the floor basalts; and they are classified as belonging to the alluvial plain and the escarpment zone.

Those of the alluvial plain comprise of alluvium, river gravels, fans and travertine; whereas those of the escarpment are mainly colluvials comprising of talus and fluviates.

Bore-Hole Information

As an aid to the Geophysical analysis to follow, the following bore-hole data from the region closest to the area under investigation is included.

ERER GOTA PROJECT EXPLORATORY BOREHOLE (AIR PORT)

Drilled,	October 1, to November 10, 1970
Total Depth,	120.4 m
Hole Diameter,	50.8 mm to 27 m and 12.7 mm to 93.7 m
Static Water Level,	16 m
Yield,	18 m^3/hr draw dawn: less than 1 m
Specific Capacity,	20 + m^3/hr/m
0-2.1 m	Upper sandy soil
2.1-8.4	Sandstone, well cemented, brown
30-32.5	Brown siltstone, shales, limonitic stained
32.5-70.0	Silicious tuff, with some concretions of calcite
70-84.0	Hard, quartizitic snadstone grey and greenish
84.0-87.0	Brown, brittle limonite stained shales
87-95.5	Brownish, very hard, fine-medium, quartizitic snadstone
95.5-101.0	Sandy clay and silt, brown, slightly calcareous with brown shales
101.0-105.5	Greenish clay and silt calcareous
105.5-112.0	Loose uncemented sand, a lot of ferrugious gravels
112-116	Brownish, very hard, medium grained quartzitic purplish brown, hard shales.

An account of the rocks found in the area together with their physical properties (determined at the Geophysical Observatory from samples given by the Ministry of Mines) is stated below as a preliminary.

a) Effusive Rocks:

Represented by trachytes, stratoid basalt, -trap series basalt. The trachytes displayed relatively low mean density (2.15 gm/cm^3) and high mean porosity (5.01%) with negligible density variation and considerable porosity variation (standard deviation of 2.46). The correlation coeficient between the two parameters ($R_{P/D}$ = 0.676) displayed a favourable relationship.

A deviation from the general trend in this formation was observed for the stratoid basalts and trap series basalts with density range for the stratoid basalt between 2.72 and 2.77 gm/cm^3 ($\bar{D}$ = 2.58) and for the trap series basalt $\bar{D}$ =2.86.

As for porosities the former has $\bar{P}_{STB}$ = 4.81% and the latter $\bar{P}_T$ = 1.36% .

The low porosity deviations may be accounted for by the fact that closed pores may be present; and these closed pores may have a far greater influence on the density than on the porosity.

Also the number of pores and their size was observed to vary with depth which is in conformity with the relatively low correlation coeficient for the stratoid basalts ($R_{P/D}$ = - 0.488). On the other hand, the correlation coeficient between porosity and density for the trap basalt was a bit higher (-0.501).

b) Sedimentary Rocks:

Represented by upper and lower sandstones, and limestones of Jurasic age.

(D_{LST} = 2.67 gm/cm^3; P_{LST} = 1.08%)

The limestones consist of shell, clay, sand, etc. and it contains a large number of cavities. This makes the average density of the massive formations lower than those determined from samples.

The upper and lower sandstones displayed lower values of density (D_{USS} = 2.5 g/cm³) $\bar{D}_{ASS}$ 2.29 cm³, and higher values of porosity ($\bar{P}_{USS}$ = 5.24% ; $\bar{P}_{ASS}$ = 12.06% with a high value of standard deviation for both parameters.

The correlation coeficient for ASS was found to be 6.778, and that for the limestone is high whereas that for the upper sandstone is low.

c) Intrusive Rocks:

Represented by diorite, granite and dyke basalt. The diorites displayed high density and porosity ($\bar{D}_d$ = 2.45 gm/km³).

($\bar{P}_a$ = 6.62%) with a high correlation coeficient of 0.788.

The values obtained for the granite are 2.59 gm/cm³ for density and 1.98% for porosity.

The dyke basalt displayed a high density and a low porosity characteristic of such formations.

Geophysical Data

The data supplied by the Geophysics Department, Ministry of Mines was VES data (vertical electrical sounding) carried out along seven profiles oriented as indicated in the location map. The sounding was done at intervals of 500 m, and the array employed was schlumberger with a maximum current separation of 1.5 km. The distance between the potential electrodes was 1/3-1/25 of the current electrode separation. The orientation was mainly along the profiles with only 3% perpendicular to the profiles.

It was communicated to us along with the data that the instrument used was a Russian Auto Compensator, A372.

Independent surveys along some of the same profiles was also conducted by this project in order to ascertain ambiguous cases and to collect more data. The instrumentation used for this part was an RAC-direct current resistivity meter.

Methods of Data Analysis

To obtain a preliminary idea of thicknesses & resistivities in the survey area, use was first made of the conventional procedure of matching the field curves plotted on double logarithm paper (ρ_a versus AB/2) with available standard master curves and auxilliary curves.

The main steps employed in the procedure of interpretation by curve matching were the following:

a) The left-hand part of the field curve plotted on a transparent double-logarithm graph sheet is superposed on the set of two-layer master curves and matched keeping axes parallel to the coordinates. The coordinates of the origin of the master curve, as read on the field curve, give ρ_1 and h_1. From the curve on which the match is obtained, and by interpolation if necessary, $\mu_2 = \rho_2/\rho_1$ can be read. Since ρ_1 is known ρ_2 can be calculated.

b) In accordance with the type of the first portion of the field curve (H, K, Q, or A) a corresponding auxilliary set of curves is chosen and its origin superposed on the mark placed, on the field curve in step (a).

Corresponding to the origin of the two-layer theoretical master curves. The line on the auxiliary curves corresponding to the value of μ obtained in step (a) is then traced on to the field curve (keeping axes parallel) up to the mark (+) mentioned above.

c) The field curve is then shifted back to the master curves and a best coincidence with one of the curves found, making sure that the auxiliary curve traced on the field curve passes through the origin.

The corresponding value of μ thus obtained gives $\rho = \rho_3/y$ where y is the ordinate of the position of the master-curve origin marked in this second matching.

d) The field curve is again superposed on the selected set of auxiliary curves ensuring that the point of origin of master curves (+) marked in step (c) coincides with the origin of the auxiliary curves, and the value of ν gives $\nu = \frac{h2}{x}$ where x is the abcisa of the point (+) marked in step (c).

e) If there are still more portions in the field curve corresponding to more types (H,K,A,Q) and hence to more layers, the steps a-d are repeated succesively giving rise to ρ_4 , ρ_5 ... etc. and h_3, h_4... etc.. The method is illustrated below in detail, taking profile 0 picket 50 as an example:

After the initial matching, the coordinates of the origin of the two-layer master curve give:

$$\rho_1 = 80\Omega\text{-m}$$

$$h_1 = 3.5 \text{ m}$$

with $$\mu_1 = \rho_2/\rho_1 = 3/2$$

and this gives $\rho_2 = 120\Omega\text{-m}$

Matching field curve and auxiliary curve gives

$$\nu_1 = h_2/h_1 = 5 \text{ , from which we obtain}$$

$h_2 = 17.5$ m

Matching the second part of the curve after finding the K-point we read the corresponding

$$\mu_2 = \rho_3/y_k = 1/5; \; y_k = 110$$

$$\Rightarrow \rho_3 = 1/5 \times y_k = 1/5 \times 110 = 22 \; \Omega\text{-m}$$

we also read $\nu_2 = h_3/x_k = 9$; $x_k = 18$

$$h_3 = 9x_k = 9x18 = 162 \text{ m}$$

From the final matching of the last part of the curve, we have $\mu_3 = \rho_4/y_H = 3$; $y_H = 30$

$$\rho_4 = 3y_H = 3x30 = 90 \ \Omega\text{-m}$$

The models constructed from these first approximations were then incorporated into a computer program which was written to directly calculate the theoretical curves corresponding to specified models. The availlable computer program was written on the basis of Gosh filter method (1971) a brief account of which is given below. The curve thus obtained is then compared with the field curve and modifications made on the model if a satisfactory match is not obtained. The procedure is repeated again and again until a reasonable match is attained.

The Gosh method uses a digital filter procedure to evaluate the Stefanesco integral. The apparent resistivity is calculated at a series of points separated by one third of a decade on the logarithmic scale. Also intermediate points spaced by one

third of a decade may be computed by choosing a different starting point.

The method consists of:

1. To obtain the resistivity transform function by means of a recurrence formula, which is then sampled at the above - mentioned interval.

2. To calculate the convolution of this resistivity transform with the resistivity filter. Digitally speaking this means calculating the convolution of the inverse digital filter coeficients with the sampled values of the resistivity transform function.

The program can handle horizontally - layered earth models up to ten layers including the substratum. The input consists of resistivities and thicknesses of the layers; and the output is a series of plotted points which form the apparent resistivity versus electrode separation curve when joined up.

Please refer to attached charts, tables, graphs and figures for the results obtained.

DISCUSSION AND CONC.USSION

The apparent resistivity in the investigated area ranges from 5 - 150 ohm - m and the values are low on the average vecause of the alluvial overburden. The interpretation of the VES curves indicates that there are on the average about four geoelectrical layers.

The thickness of the first layer (top soil) is not more than 2 meters with resistivity ranging from 25 - 350 ohm-meters. The relatively extreme variation of resistivity in this part may be accounted by the effect of percolating rain water.

The underlying second layer varies in thickness from several meters to about a hundred meters. Test boreholes need to be drilled to ascertain the exact geologic nature of this layer.

The third layer (presumed to be composed of alluvial sands) has resistivity variations from 10 to 40 - m and thickness ranges from 5 - 300 m; with minimum thickness on the center of the survey area and maximum on the edges. A test borehole is necessary for distinguishing which of the several factors (composition, grain size, degree of water saturation etc) causes the fluctuation in the resistivity of this layer.

The last layer (bed rock) presumed to be composed of sandstones, limestones and precambrian magnetite shows large variations in electrical properties, and hence resistivity survey alone is not sufficient to make desired differentiations among the various components.

Even for a finite bed rock resistivity (400 - 600 m) the portions of the curves that correspond to the bed rock show an infinite resistivity due to the low resistivity of the aluvium over burden.

The corresponding depth of the apparent resistivity range (70 - 150 m), is that of the bed rock in the central part of the survey area and of the alluvium deposits at the edges. The zone of high resistivity in the central part also corresponds to shallow depth to bed rock (not more than 100 m).

B. TENDAHO

General Geological Aspects of the Survey Area

The area surveyed lies on the aAfar, a vast triangular shaped depression of about 150,00 sq.km area, where the three units of the Ethiopian Rift; The Main Ethiopian Rift, The Guld of Aden Rift and The Red Sea Rift meet.

Much of this depression lies below sea-level. On the west it is bounded by the N-S scarp of the Ethiopian plateau, on the south by the E-N E - W-S W. scarp of the Somalian plateau, and on the north east by the Danakil Alps horst.

From the plains of Afar, the Awash river extends through several small lakes to the closed basin of Lake Abbe in the North.

The immense 8000 sq.km occupied by the salt plain with an average elevation of 70 m typifies the general lack of relief of internal Afar.

The rocks of Afar, as part of the whole rift system, have as their basement, the extremely folded and foliated precambrian, covered by mesozoic marine strata and tertiary flood basalt.

Among the dominant formations are to be found sand (present), lacustrine deposits, recently emerged area (upper Holocene), eolian sands (lower and middle pleistocene), Lacustrine limestones (lower to middle holocene Basaltic fissure flows of the upper part of the stratoid series (pliestocene); basaltic lava flows of transitional nature with alkaline tendencies and the Afar stratoid series (Pliopleistocene).

DISCUSSION AND CONCLUSION

The palletes of A.M. pylaev were used to interpret the field curves obtained.

Twenty curves of VES along the main profile were interpreted. The types obtained were HA, HKHA, HKHKH and others.

The pseudo cross-section of apparent resistivity (ρa) the graph of longitudinal conductance (s) in siemens and the geoelectrical cross - section were plotted.

The diagram of summarized longitudinal conductances (s) reflects the surface relief of the hard rocks of the basement. And the picture of the pseudo cross-section of apparent resistivity indicates the presence of some faults in the geoelectrical section.

In the geoelectrical section we can clearly distinguish the conducting stratum with resistivity which varies from 1 - 2 ohm meters up to 6 - 8 ohm-meters. In general one can realy observe three or four layers in this geoelectrical section.

An example of the semi-quantitative interpretation procedure employed is given below, taking VES 149 (HKH) as an example:

Matching the initial part of the curve with a two-layer master curve gives:

$$\rho_1 = 10\ \Omega\text{-m}$$

$$h_1 = 8\ \text{m}$$

The value of S (longitudinal conductance) is read from the intersection of the tangent to the assymptotic part of the field curve with the abscisa at $\rho_a = 1$. In the five-layer case at hand, $S = S_1+S_2+S_3+S_4$

where $S_1 = h_1/\ _1$

$S_2 = h_2/\ _2$

$S_3 = h_3/\ _3$

$S_4 = h_4/\ _4$

The value of S, thus read, for the given example gives S = 520 mhos.

The three-layer Pylayev master curves also contain so called m_2 lines ($m_2 = h_1+h_2$) which enable to determine the depth to the third layer. For the five-layer curve of our example we have $m_4 = h_1+h_2+h_3+h_4$.

For such multi-layer cases the three-layer master curve is used by the method of successive reduction of overlying layers into single equivalent layers and then proceeding as in the case of a three layer-earth to establish $m_3 = h_e+h_3$; $m_4 = h_{e'}+h_4$ where -1

$$h_e = h_1+h_2 \quad \text{and} \quad h_{e'} = h_e+h_3 = h_1+h_2+h_3$$

each succesively established with the three-layer Pylaev master curve.

Application of this operation for the example at hand gives:

$$m_4 = h_1+h_2+h_3+h_4 = H = 2094 \text{ m.}$$

REFERENCE

1. Telford W.M. et al (1976) Applied Geophysics. Cambridge University Press, Cambridge, pp 860.

2. Keller G.V. Frischknecht, F.C., (1966), Electrical Methods in Geophysical Prospecting, Perogamon Press, N.Y., pp. 519.

3. Grant, F.S. and West, (1965), G.F., Interpretation Theory in Applied Geophysics, (McGraw-Hill Book Company), N.Y., pp 584.

4. Parasnis D.S., (1973), Mining Geophysics, Elsevier, Amsterdam), pp 395.

5. Heilland, C.A., (1940) Geophysical Exploration, Prentice Hall, N.Y., pp 1013.

6. DAS, U.C. and Singh, R.D., (1982), Bipole-Dipole Field Difference - A New Resistivity Sounding Technique Geoph[illegible] Prospecting 30, 323-330.

7. Kumar, R. and Chowdary, R., (1982), A Numerical Method to Compute the Resistivity Transform from Wenner Sounding Data, Geoph[illegible] Prospecting 30, 898-909.

8. Szaraniec, F., (1982), Use of the Seismic Dynamic Deconvolution Algorithm in Direct Resistivity Interpretation, Geoph· , Prospecting 30, 850-854.

9. Emilia, D.A., et al, (1976) Geophysical Exploration for Ground Water in Ethiopia, Bull of Geophysical Observatory, No.16.

10. Tesfamichael Keleta, (1974), Hydrogeology of Dire Dawa A Statement of Present Knowledge, Unpublished Report, No.11, Geological Survey of Ethiopia, A.A.

11. Mohr, P.A., (1971), The Geology of Ethiopia, Addis Ababa University Press, pp 171-174.

The results of interpretation of vertical electrical sounding's curves along the main profile at Tendaho - Dubti area

Type of a curve	VES No.	ρ_1	ρ_2	ρ_3	ρ_4	ρ_5	ρ_6	ρ_7	h_1	h_2	h_3	h_4	h_5	h_{6m}	H(m)	S (mhos)
QHKH	1	320	17	2	6	2	∞		4	8	25	12	300		353	110
HKH	151	2	1	3	2	∞			6	13	114	550			684	380
QQH	2	18	4	3	1	∞			10	40	65	855			973	540
HKH	150	12	1	3	1	∞			5	74	173	420			672	450
KHKQH	147	65	585	30	238	6	2	∞	2	21	27	36	255	650	992	470
HKH	149	10	2	9	4	∞			8	26	150	1830			2094	520
HAKH	148	2	1	2	11	5	∞		5	6	126	145	1630		1912	440
KHKH	146	12	218	4	14	4	∞		8	26	360	73	1380		1847	480
HKHKH	145	3	2	5	2	10	4	∞	14	27	31	150	150	1030	1402	360
HKH	144	3	1	8	3	∞			17	51	225	1390			1683	500
HKH	134	8	1	4	3	∞			9	25	768	891			1193	400
KHKH	135	3	8	3	14	8	∞		5	5	48	390	2580		3028	330
HKHKH	136	16	7	22	7	18	6	∞	5	8	22	420	920	900	2275	450
KHKH	137	10	200	4	13	7	∞		7	27	133	500	890		1557	200
KQHKH	138	37	111	17	3	13	3	∞	8	12	78	92	520	800	1511	320
HKH	139	48	2	11	6	∞			21	42	210	1398			1671	270
HKHA	140	20	5	9	3	14	∞		12	12	260	180	1830		2292	220
HKHA	141	9	4	43	5	10	∞		12	49	15	145	1500		1720	190
HA	142	26	1	6	25	?			10	120	440				?	
HAA	143	8	3	7	58				12	20	1280	2280			3592	90

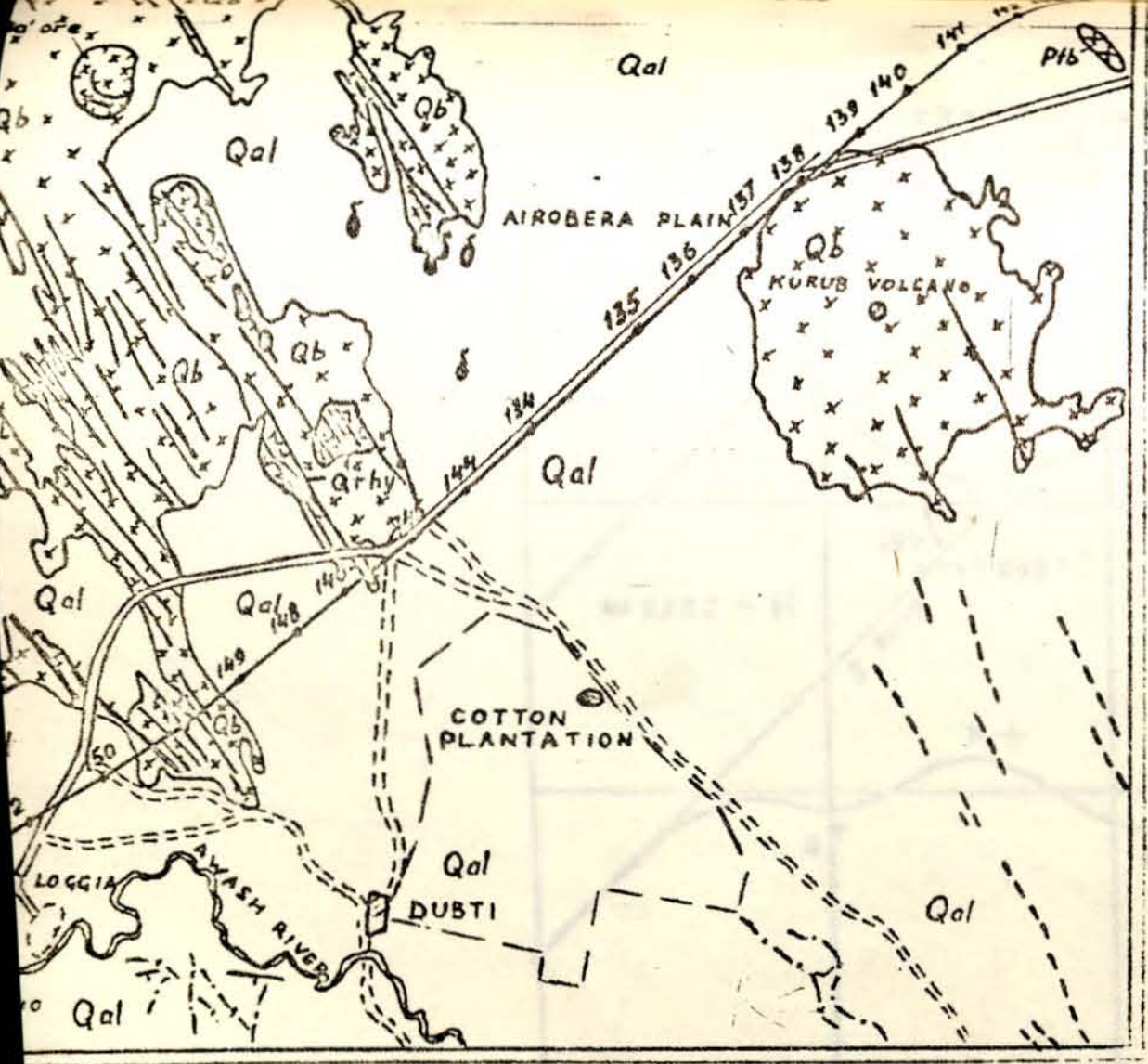

QUATERNARY ALLUVIAL DEPS...

QUATERNARY ACIDIC EXTRUSI...

QUATERNARY BASALT FLOWS

POST TRAP BASALT FLOWS

FAULTS WITH DOWN-THROWN SIDE INDICATED

TECTONIC LINES HIDDEN UNDE... ALLUVIUM

GEOLOGICAL CONTACT

ALL WEATHER ROAD

DRY WEATHER ROAD

TOWNS AND VILLAGES

MAJOR RIVERS

INTERMITTENT STREAMS

VOLCANIC CRATERS

HOT SPRINGS

FUMAROLES

MAIN PROFILE WITH POINTS OF VERTICAL ELECTRICAL SOUNDIN...

FIG 1 GEOLOGIC MAP OF TENDAHO GRABEN

BY GETAHUN DEMISSIE

1 0 1 2 3 4 5 10

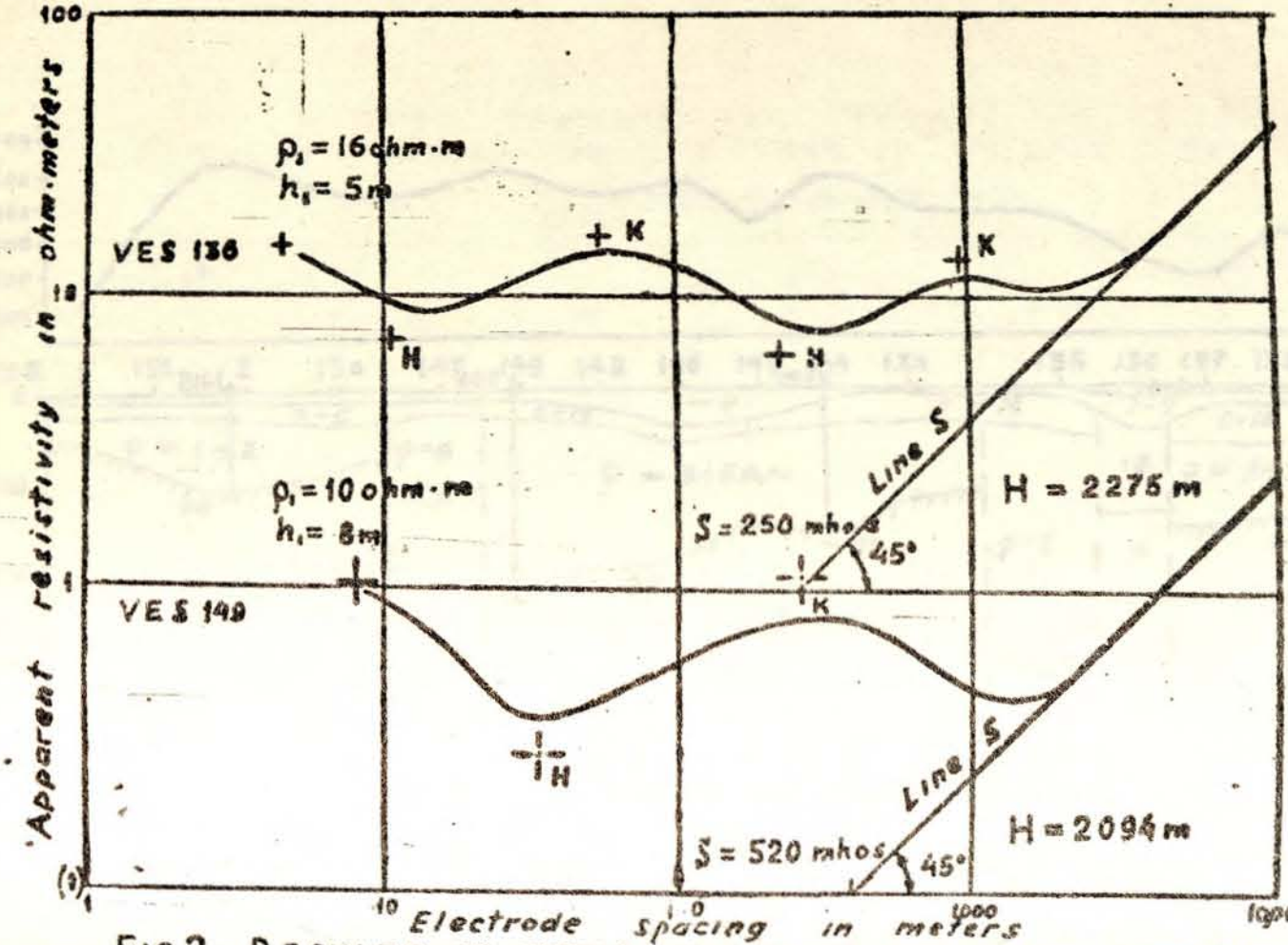

FIG.2 RESULTS OF INTERPRETATION OF THE FIELD VERTICAL ELECTRICAL SOUNDING CURVES.

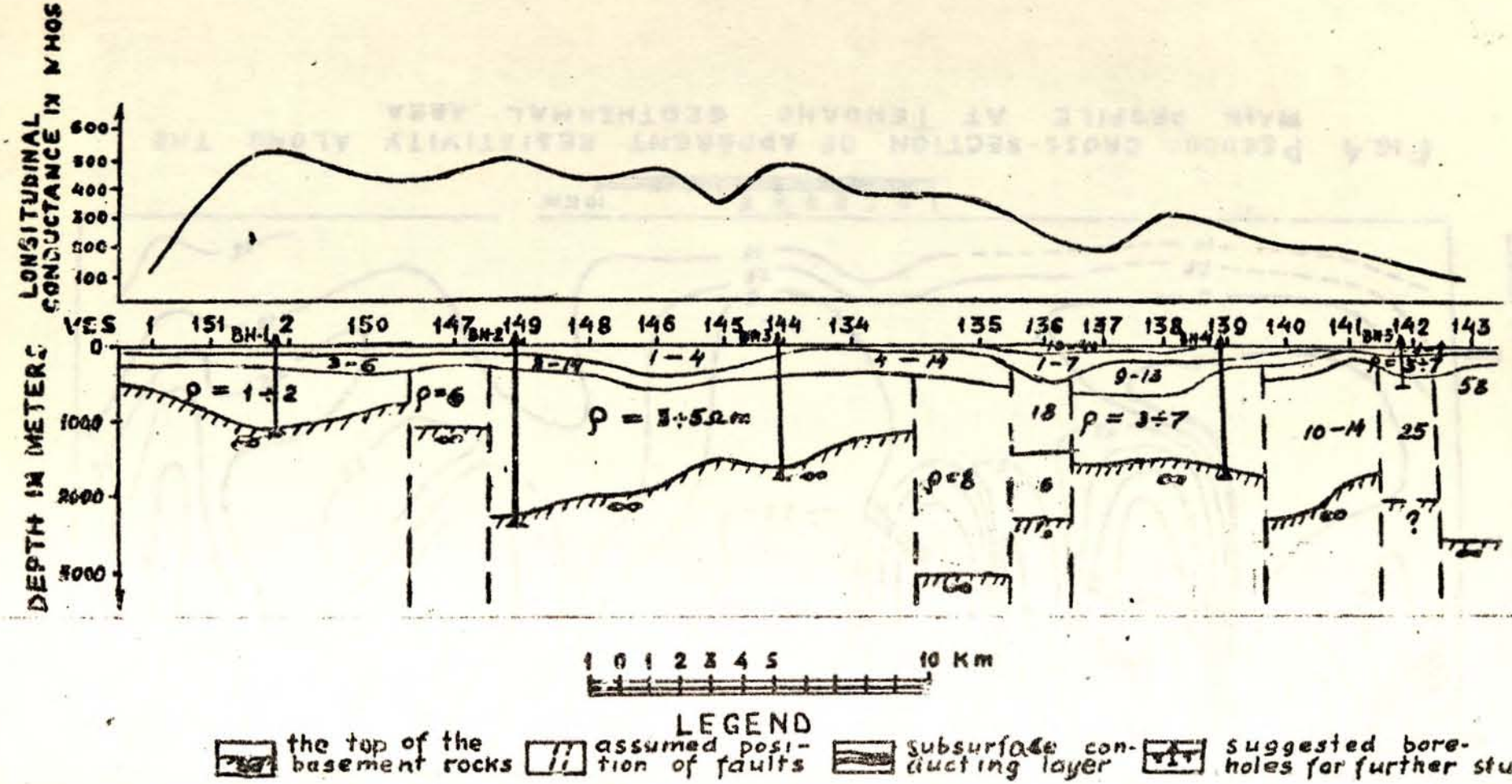

Fig·3. Geoelectrical cross-section along the main profile at Tendaho area with the diagram of summarized longitudinal conductance (S).

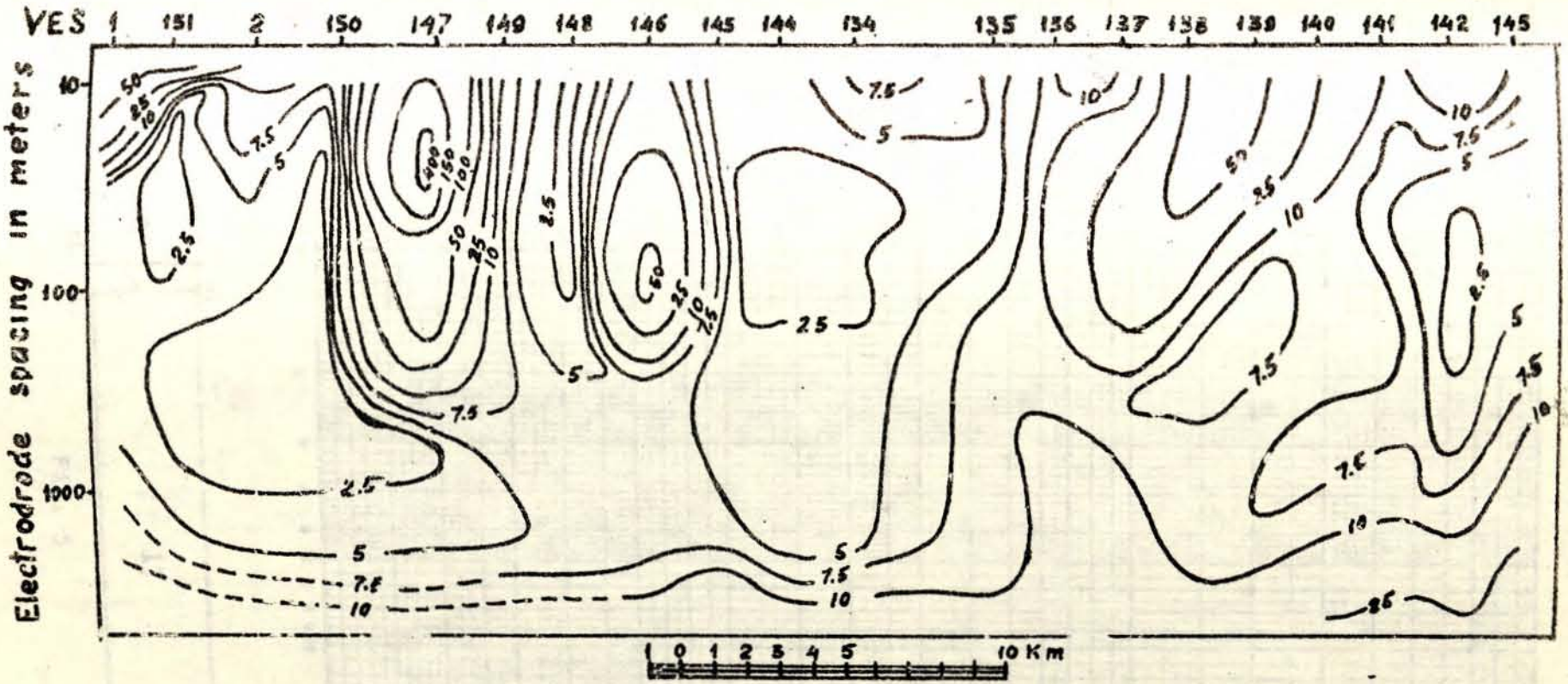

FIG.4 PSEUDO CROSS-SECTION OF APPARENT RESISTIVITY ALONG THE MAIN PROFILE AT TENDAHO GEOTHERMAL AREA.

PROFILE II - PICKET O: DIRE DAWA

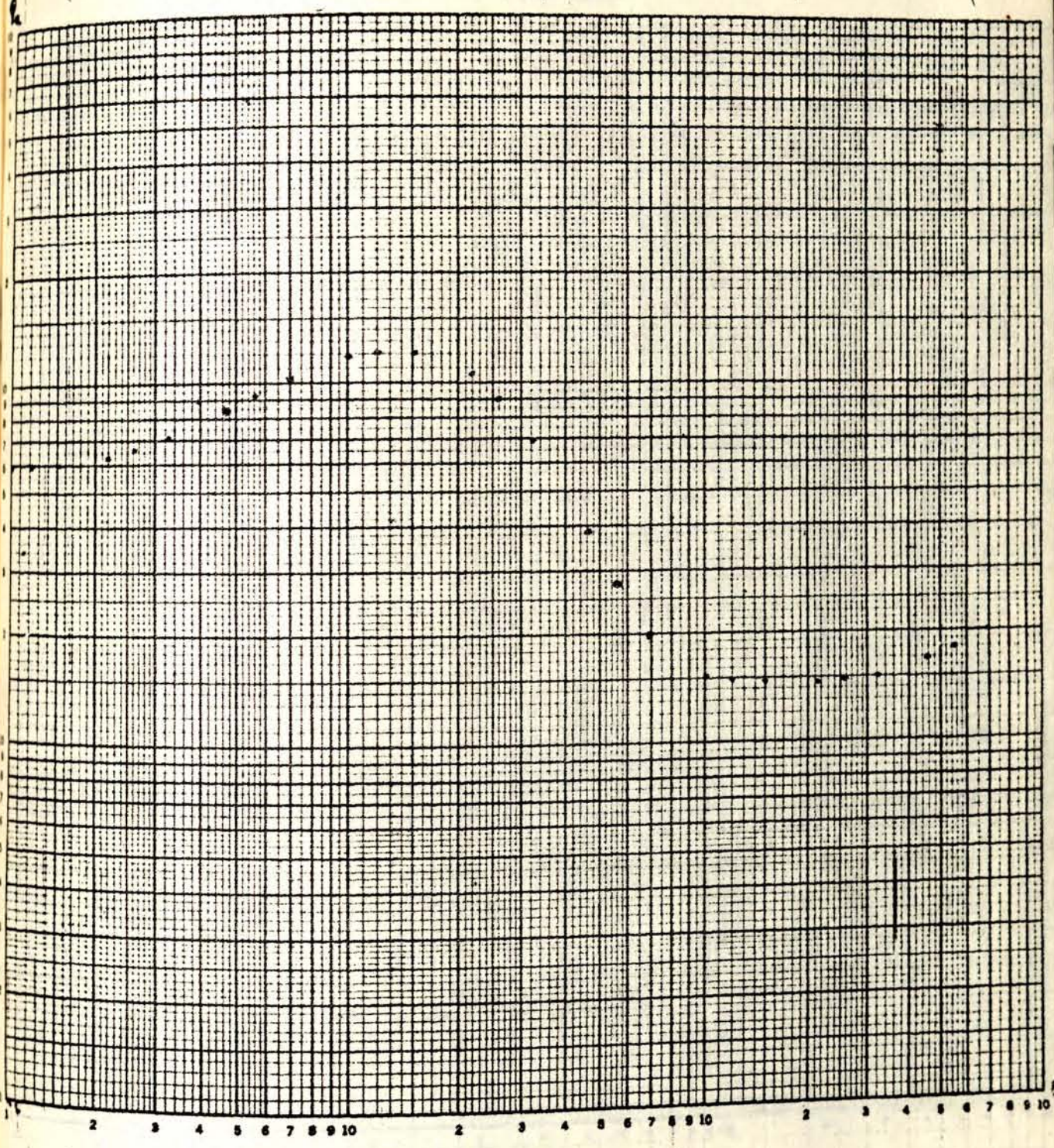

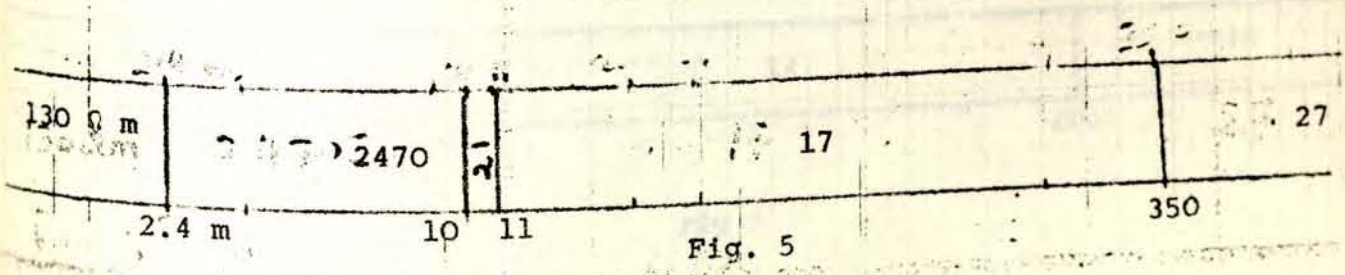

Fig. 5

PROFILE II - PICKET 5: DIRE DAWA

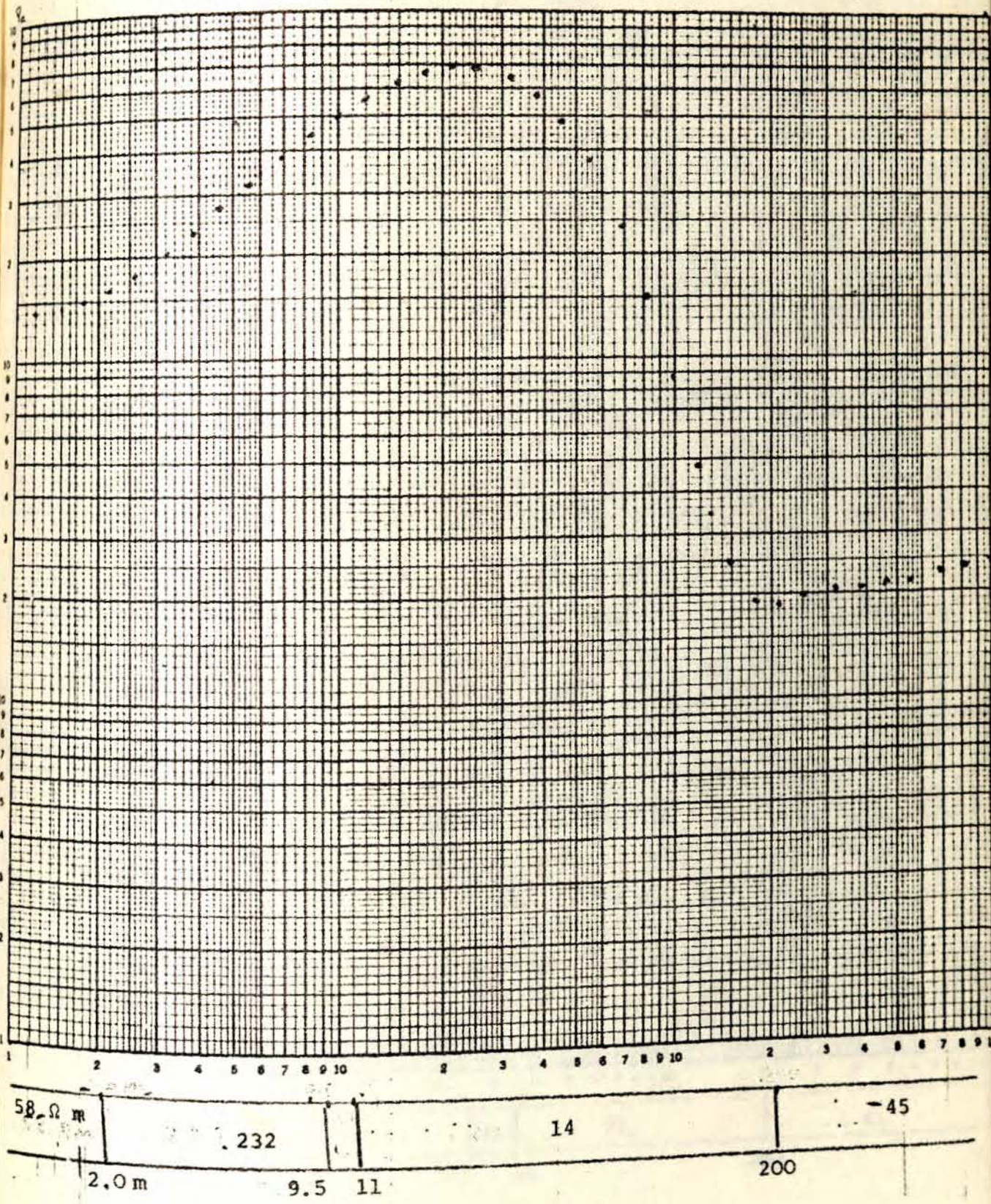

Fig.6

PROFILE II - PICKET 10: DIRE DAWA

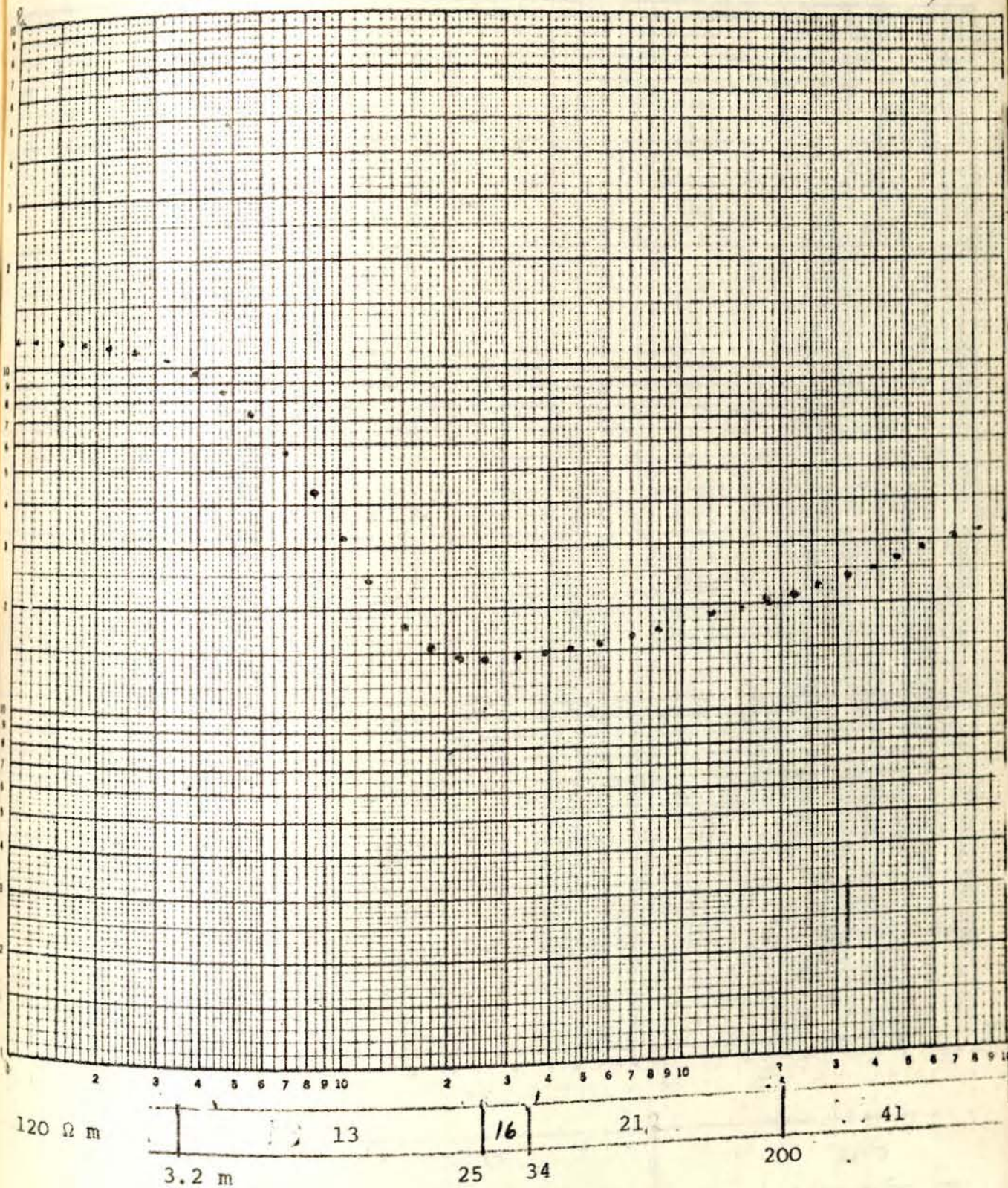

Fig. 7

PROFILE II - PICKET 15: DIRE DAWA

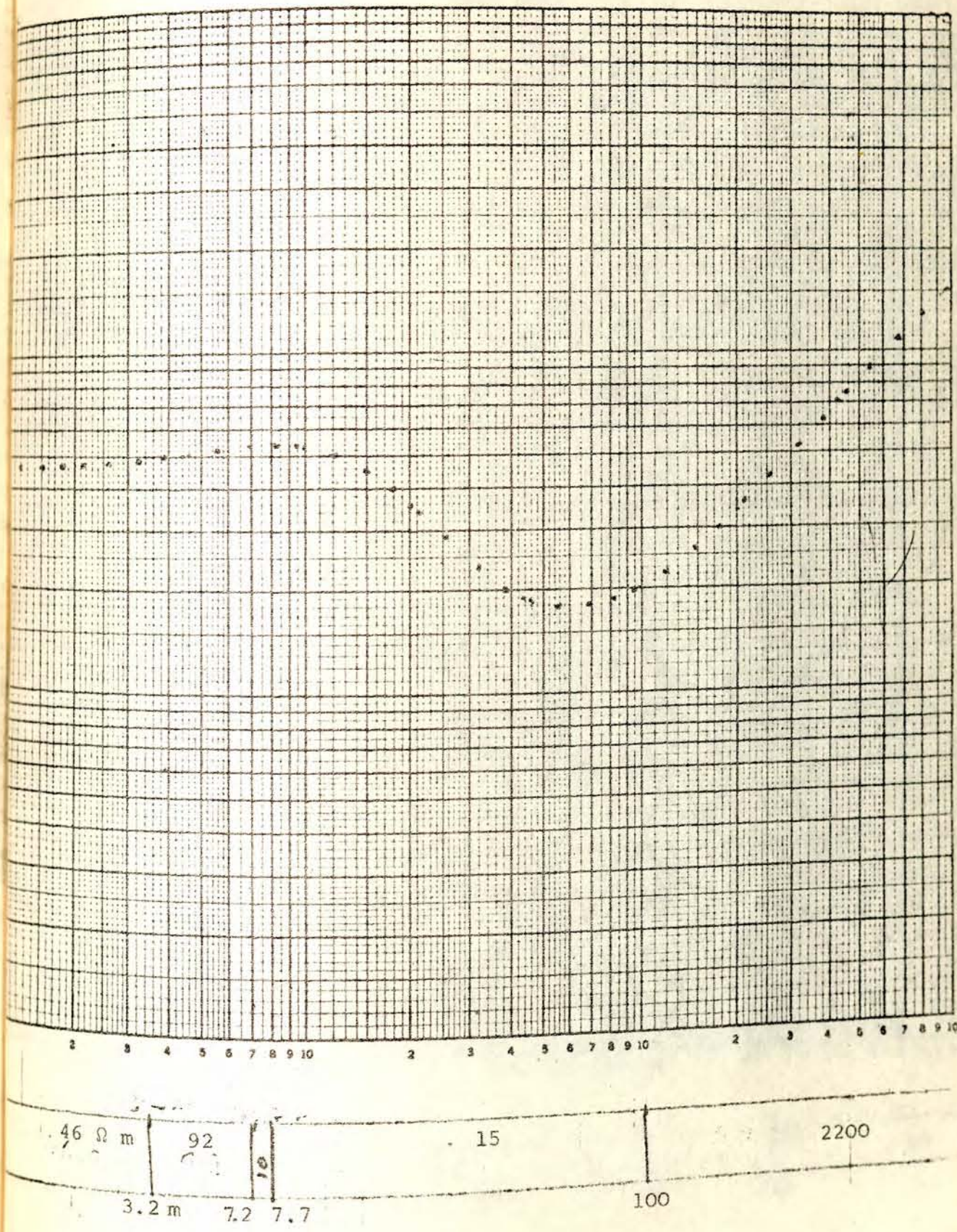

Fig. 8

PROFILE II PICKET 20: DIRE DAWA

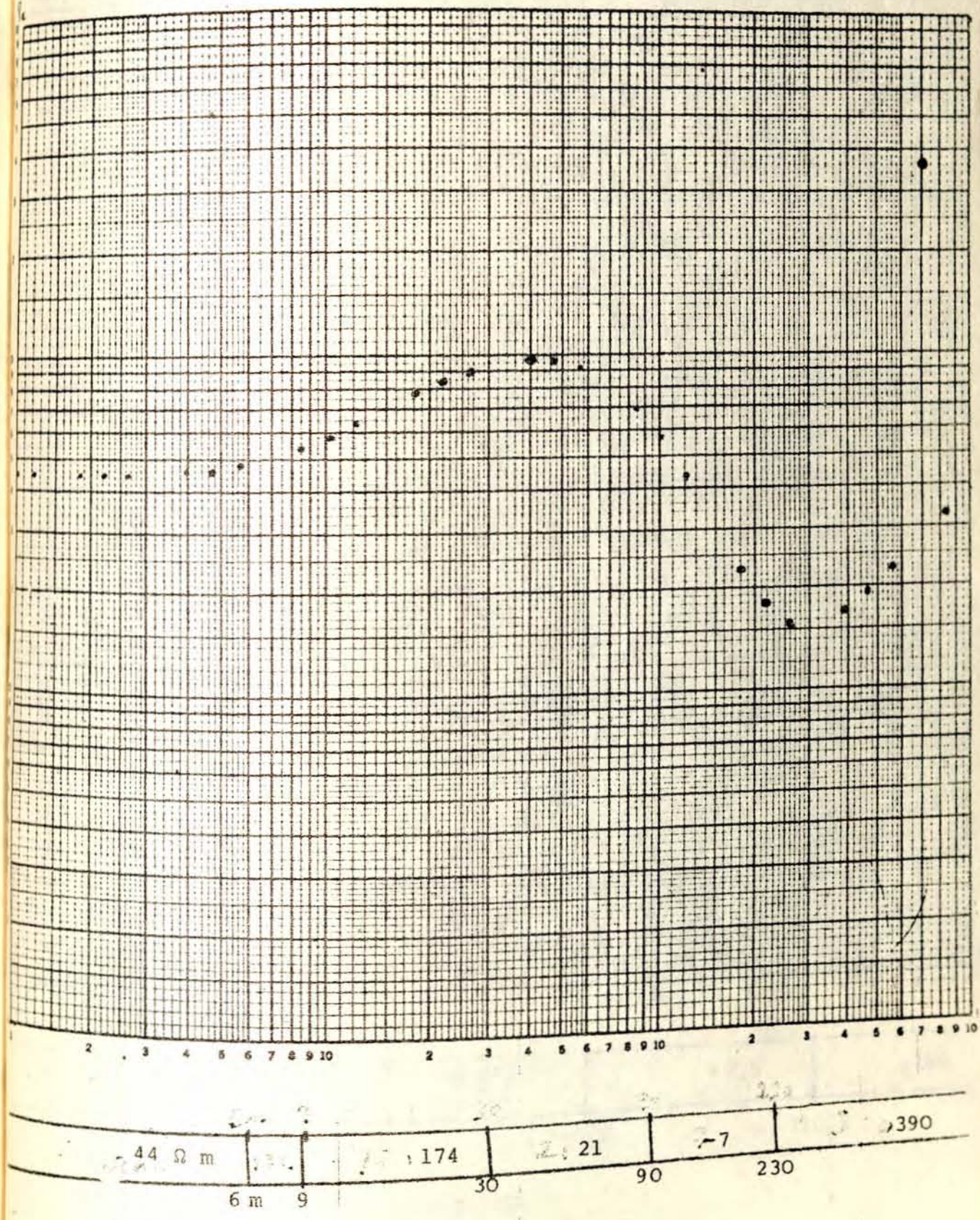

Fig. 9

PROFILE II PICKET 25: DIRE DAWA

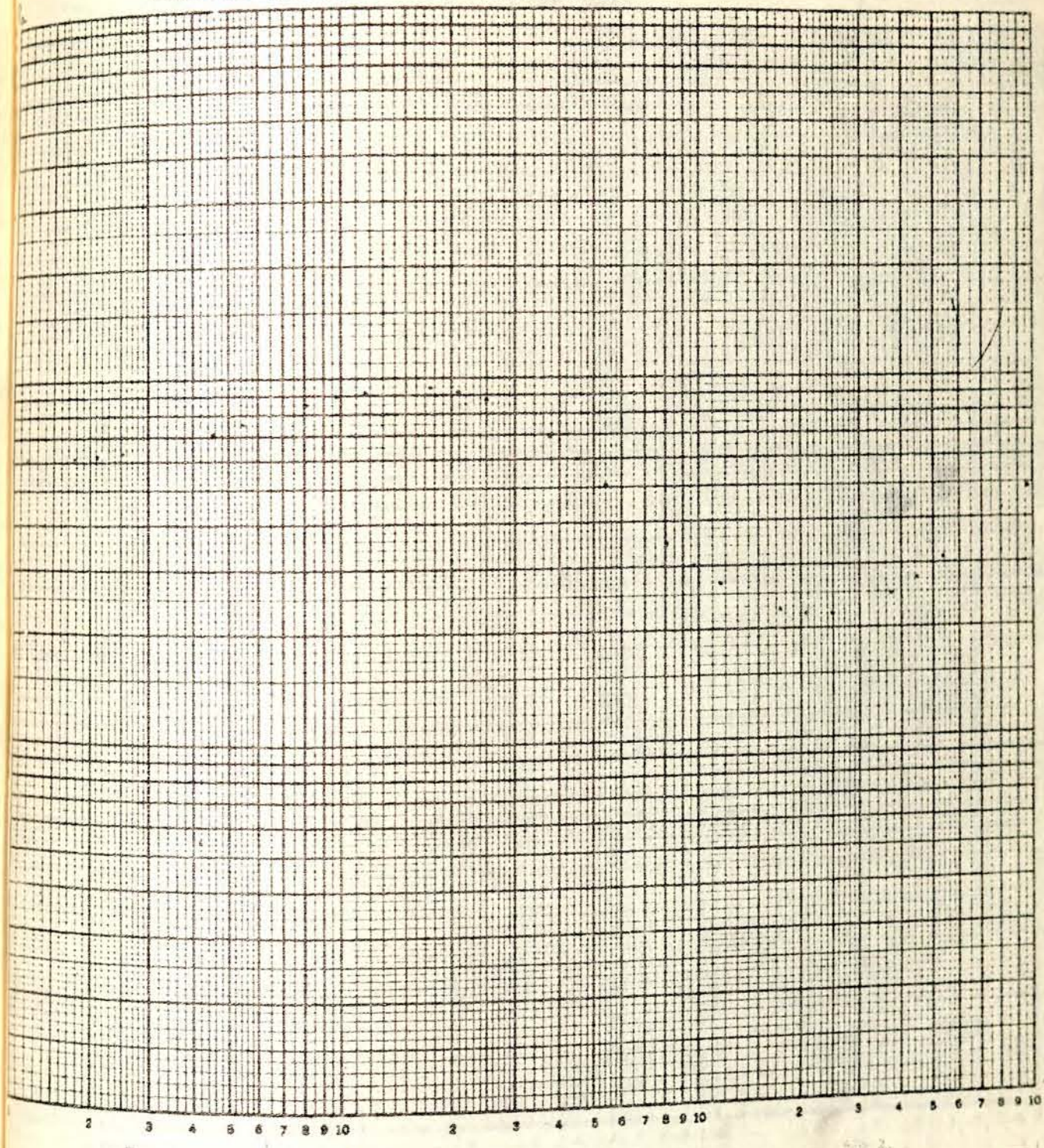

Fig. 10

PROFILE II PICKET 30: DIRE DAWA

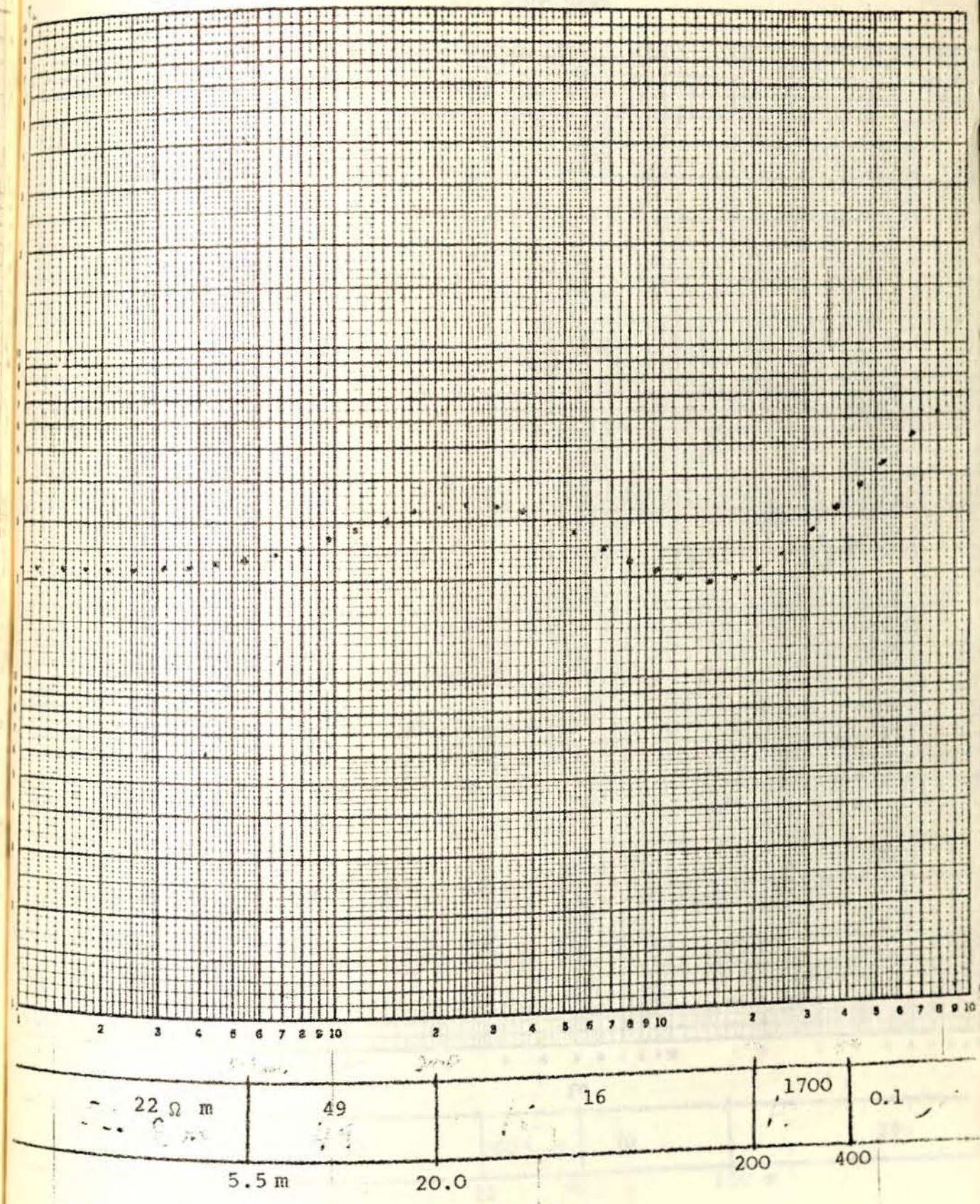

Fig. 11

PROFILE II PICKET 35: DIRE DAWA

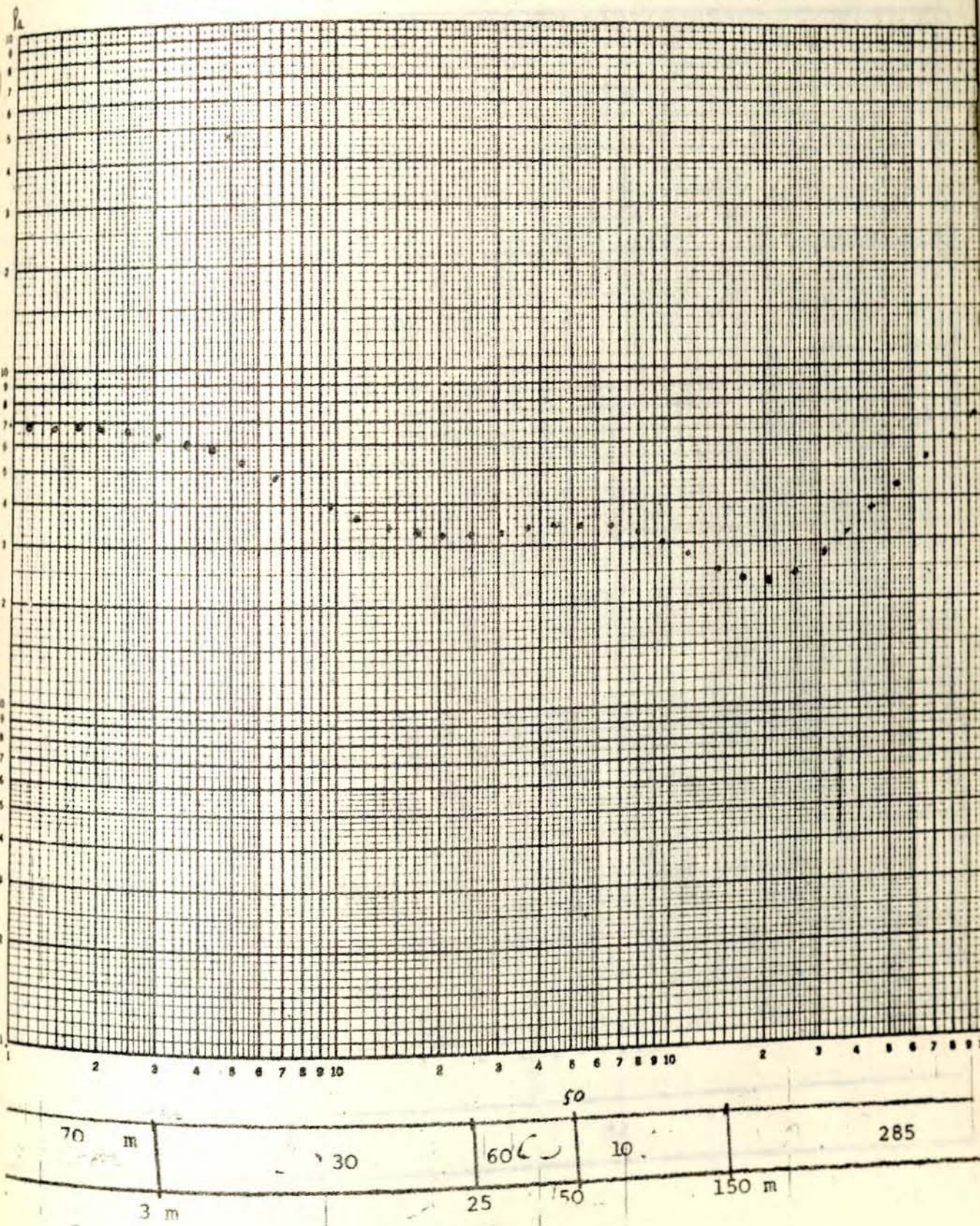

Fig. 12

PROFILE II PICKET 40: DIRE DAWA

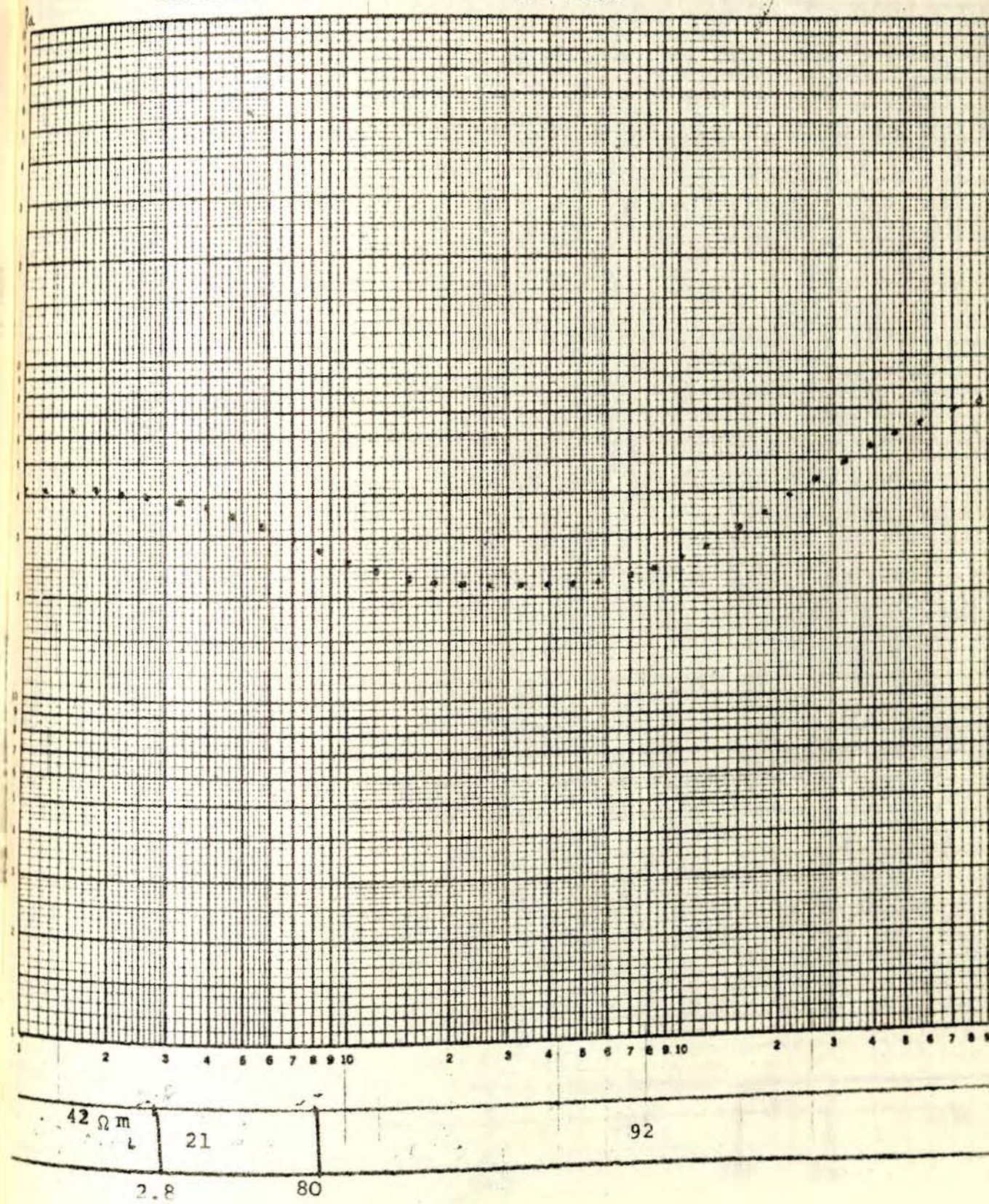

Fig. 13

PROFILE II PICKET 45: DIRE DAWA

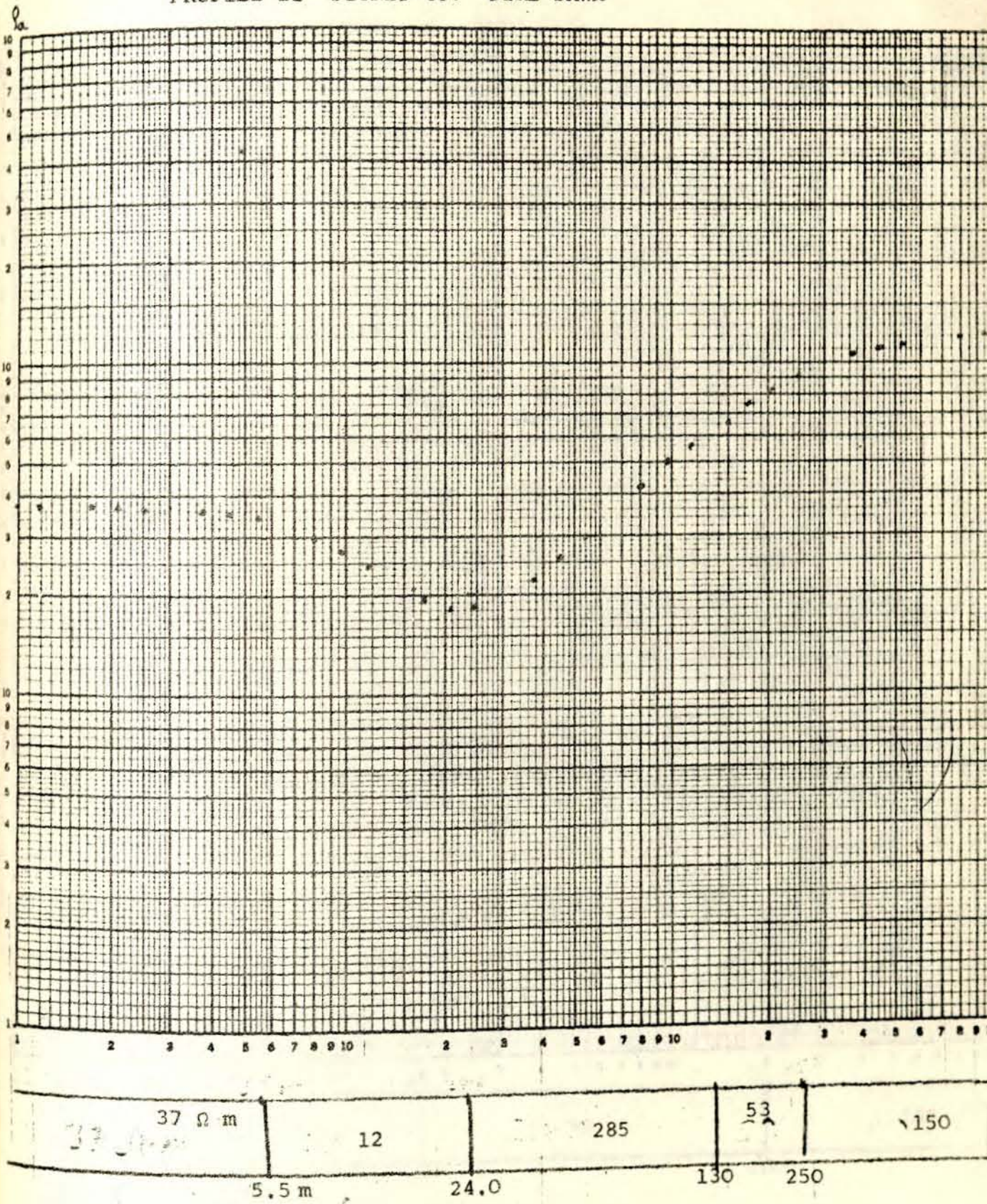

Fig. 14

PROFILE II PIKCET 50: DIRE DAWA

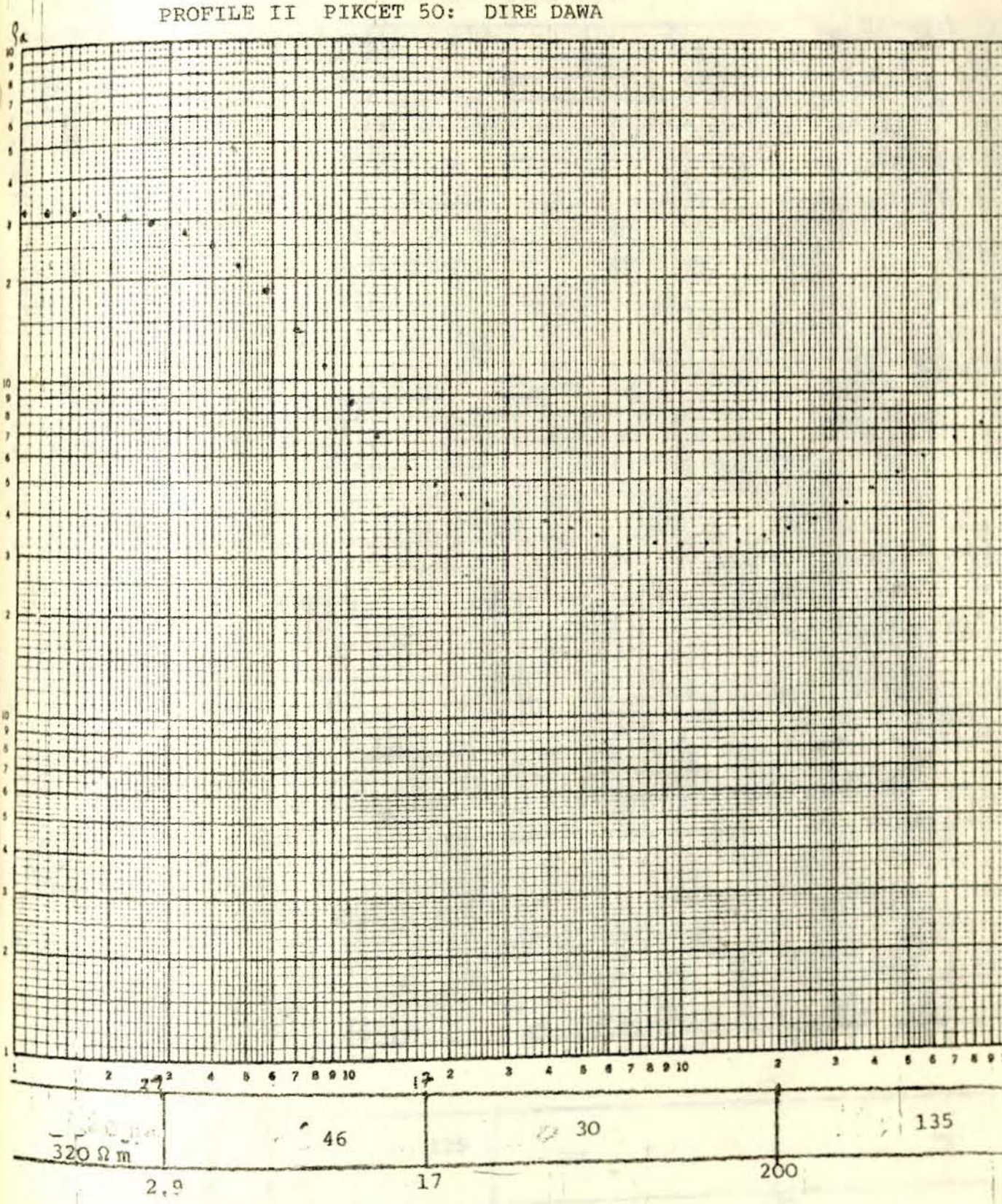

Fig. 15

PROFILE II PICKET 55: DIRE DAWA

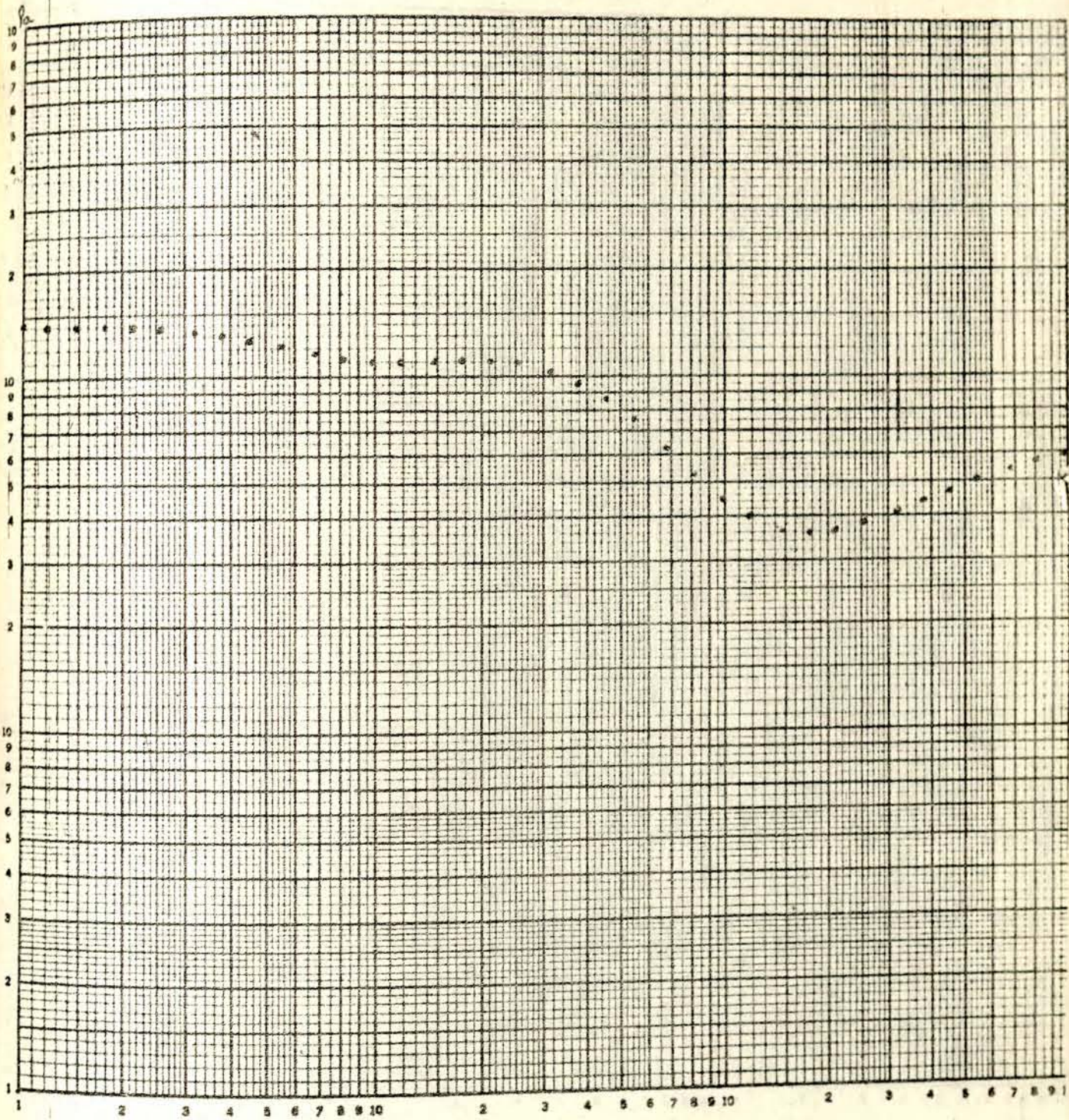

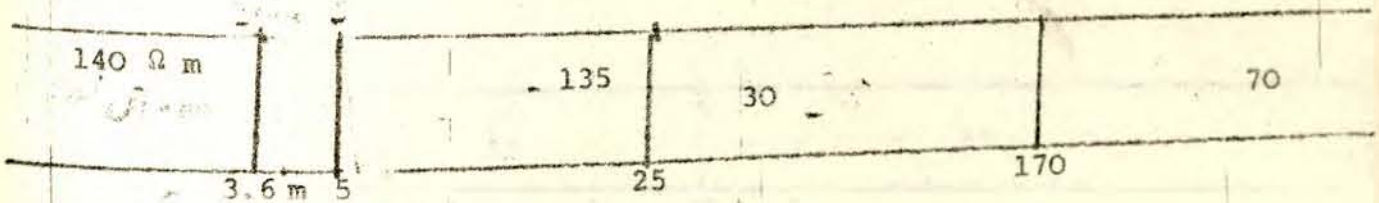

Fig. 16

PROFILE II PICKET 60: DIRE DAWA

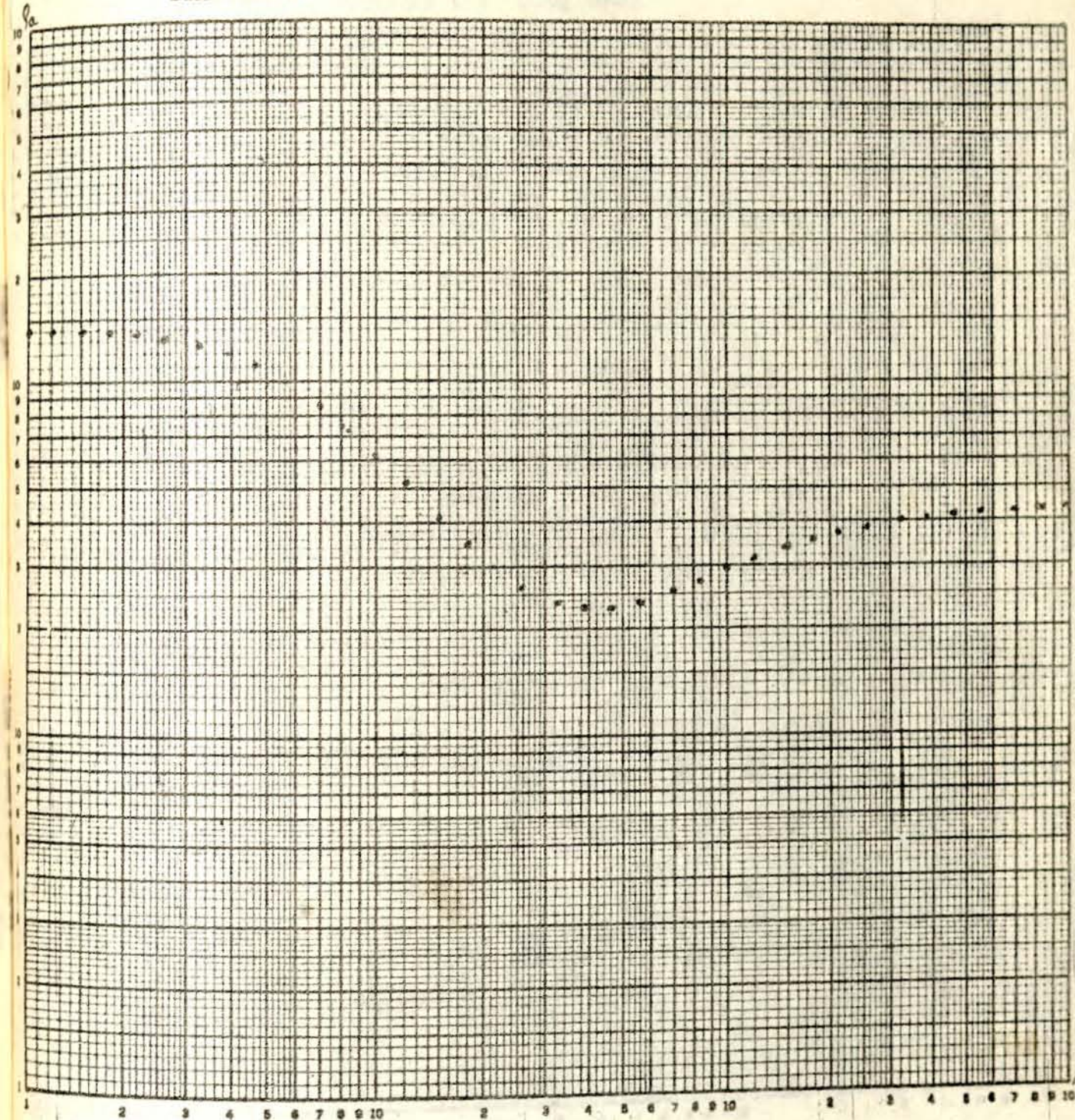

140 Ω m	47	18	44
3 m	9	38	

Fig. 17

PROFILE II PICKET 65: DIRE DAWA

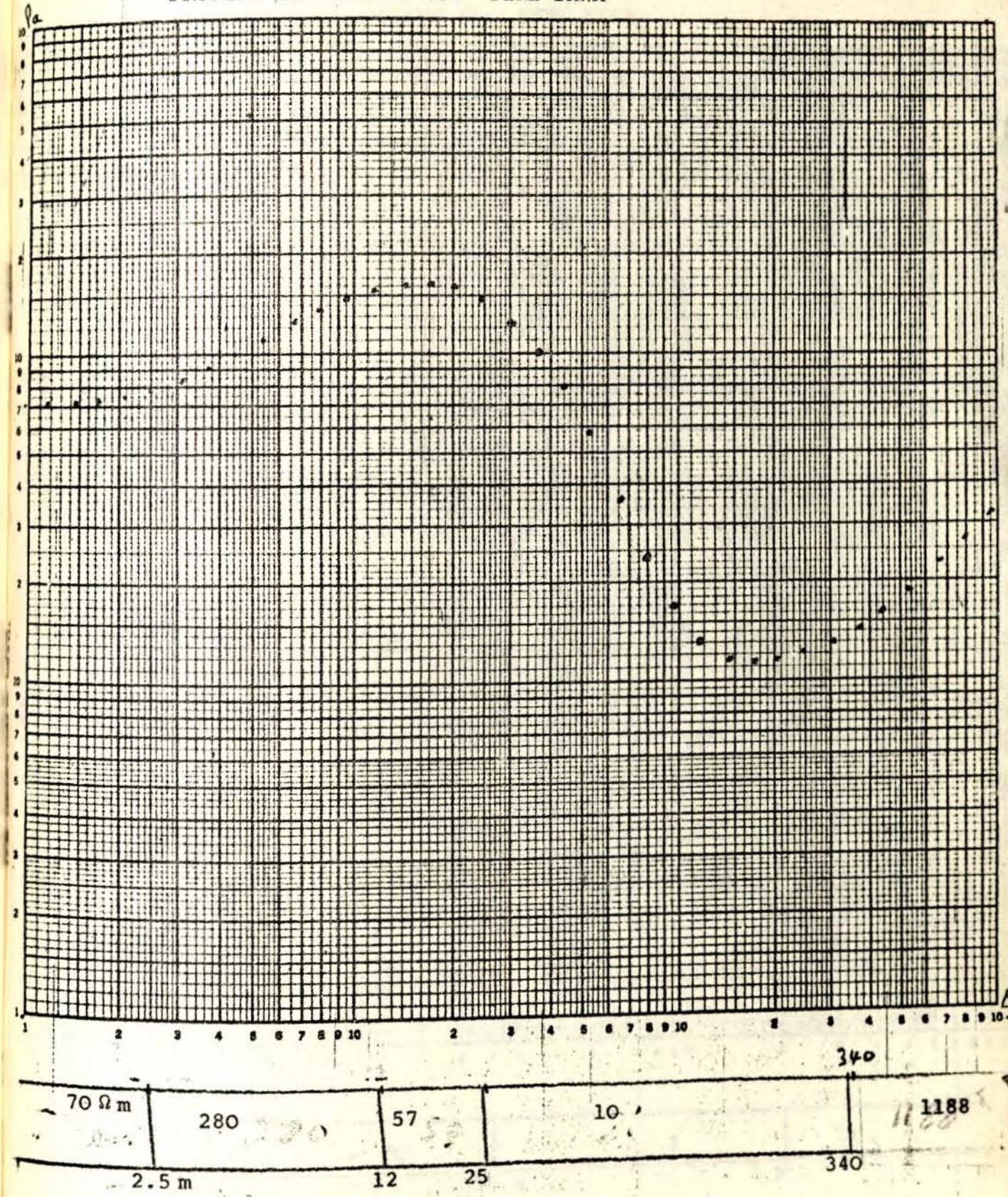

Fig. 18

PROFILE II PICKET 70: DIRE DAWA

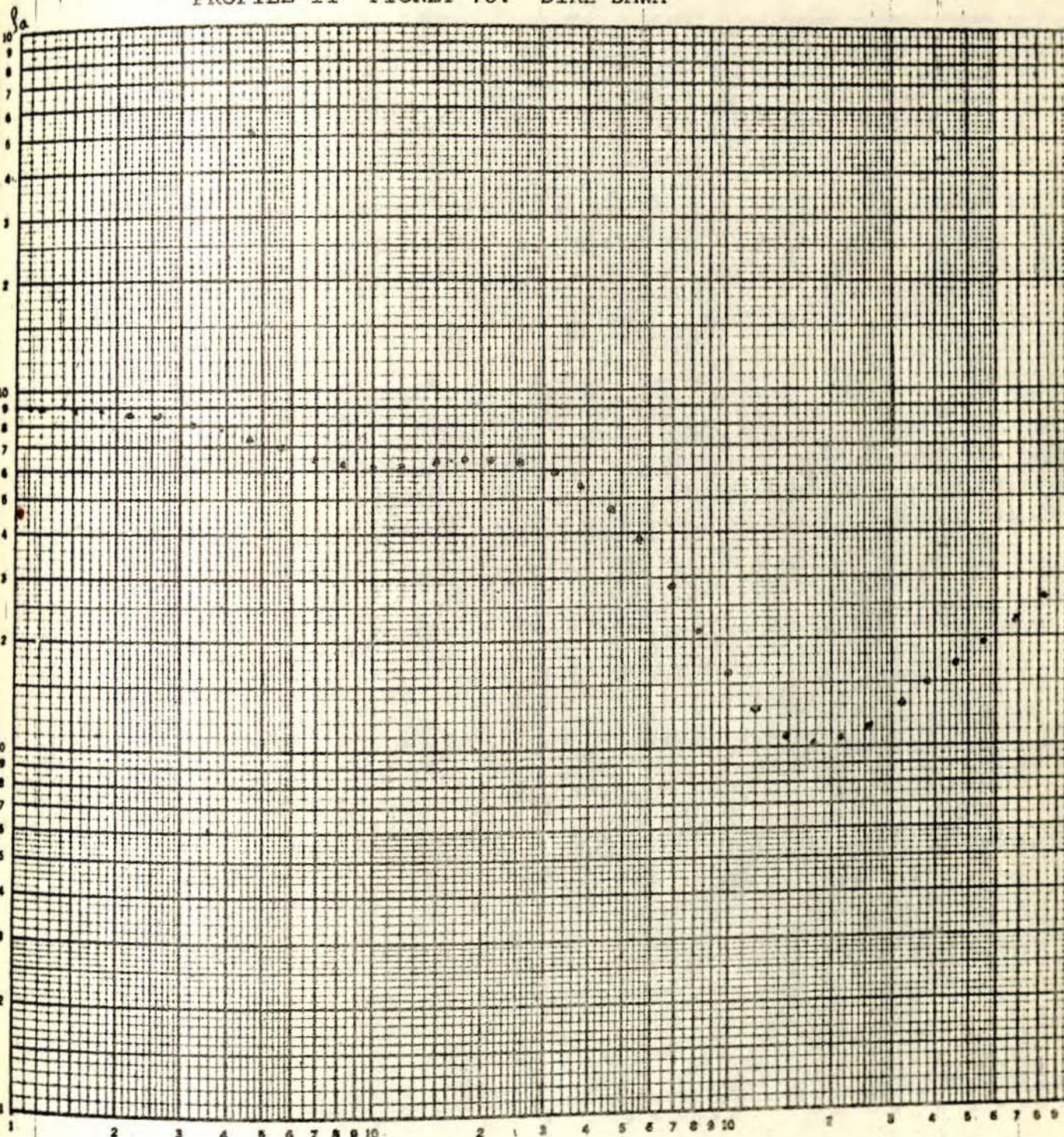

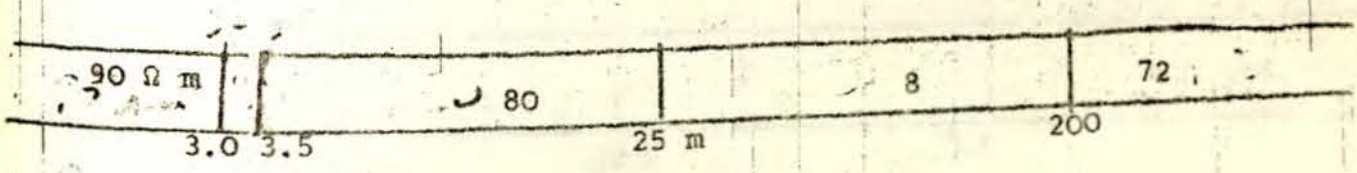

Fig. 19

PROFILE II PICKET 75: DIRE DAWA

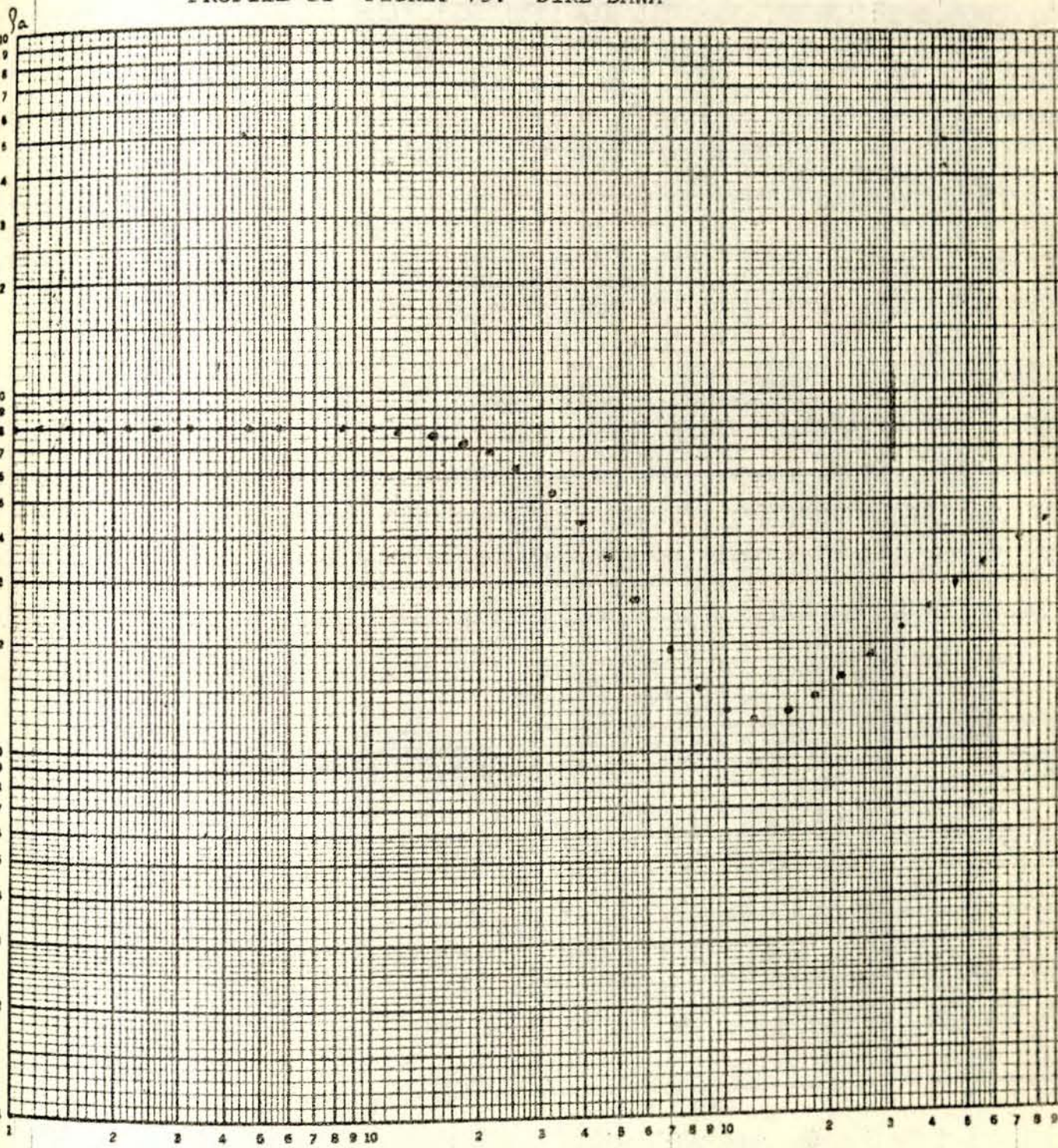

Fig. 20

PROFILE II PICKET 80: DIRE DAWA

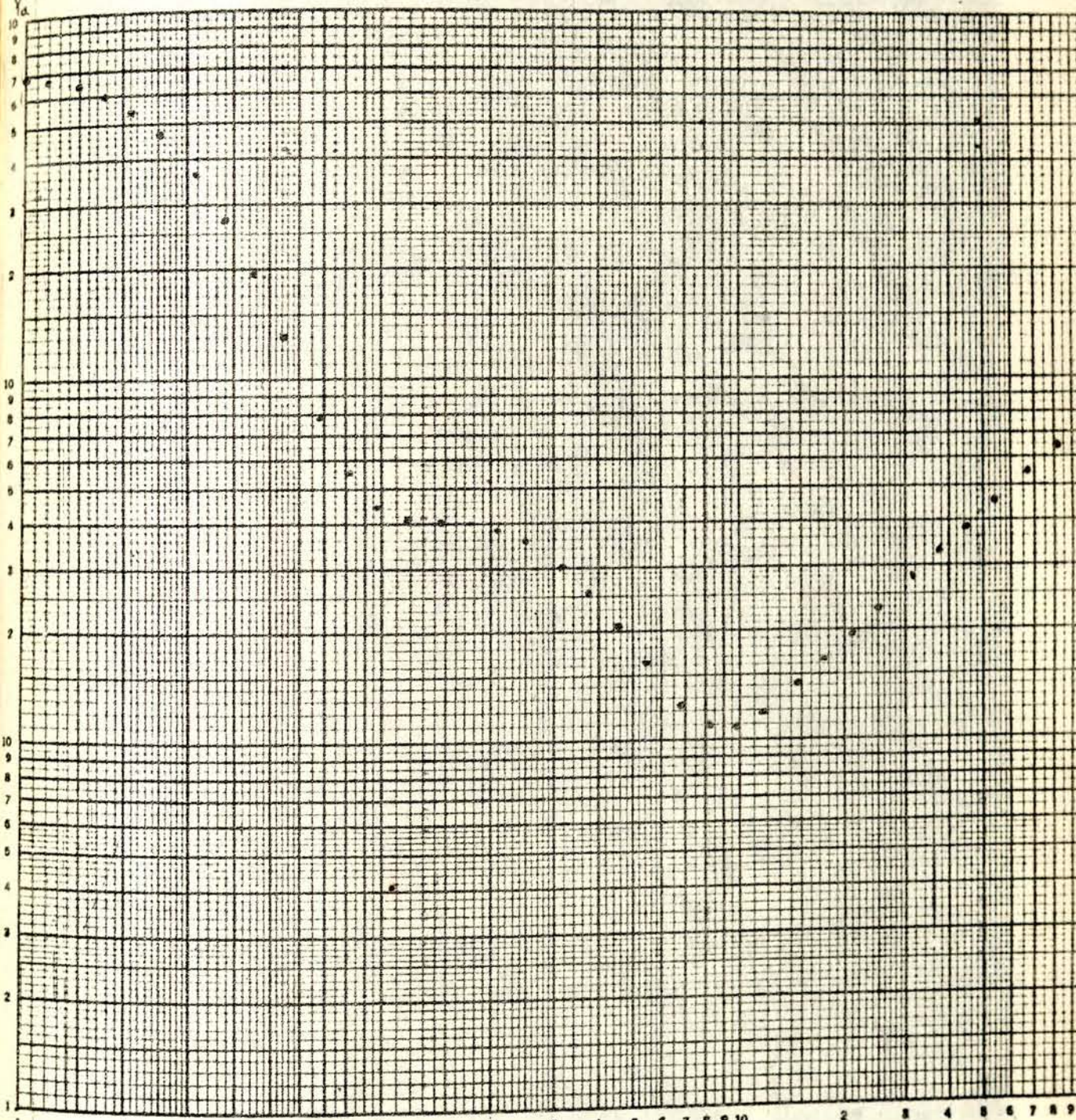

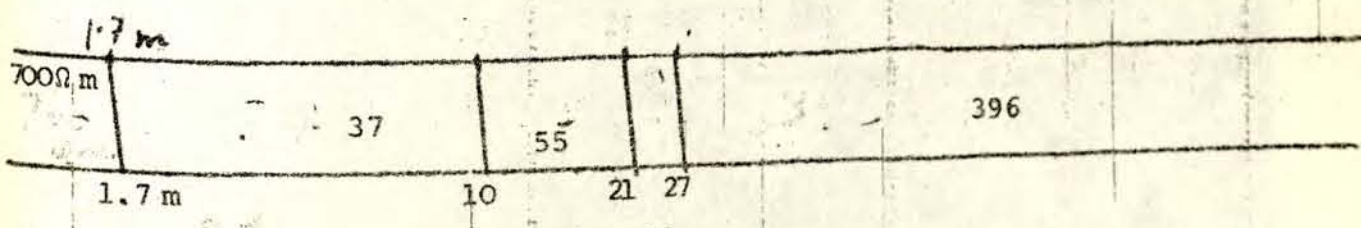

Fig. 21

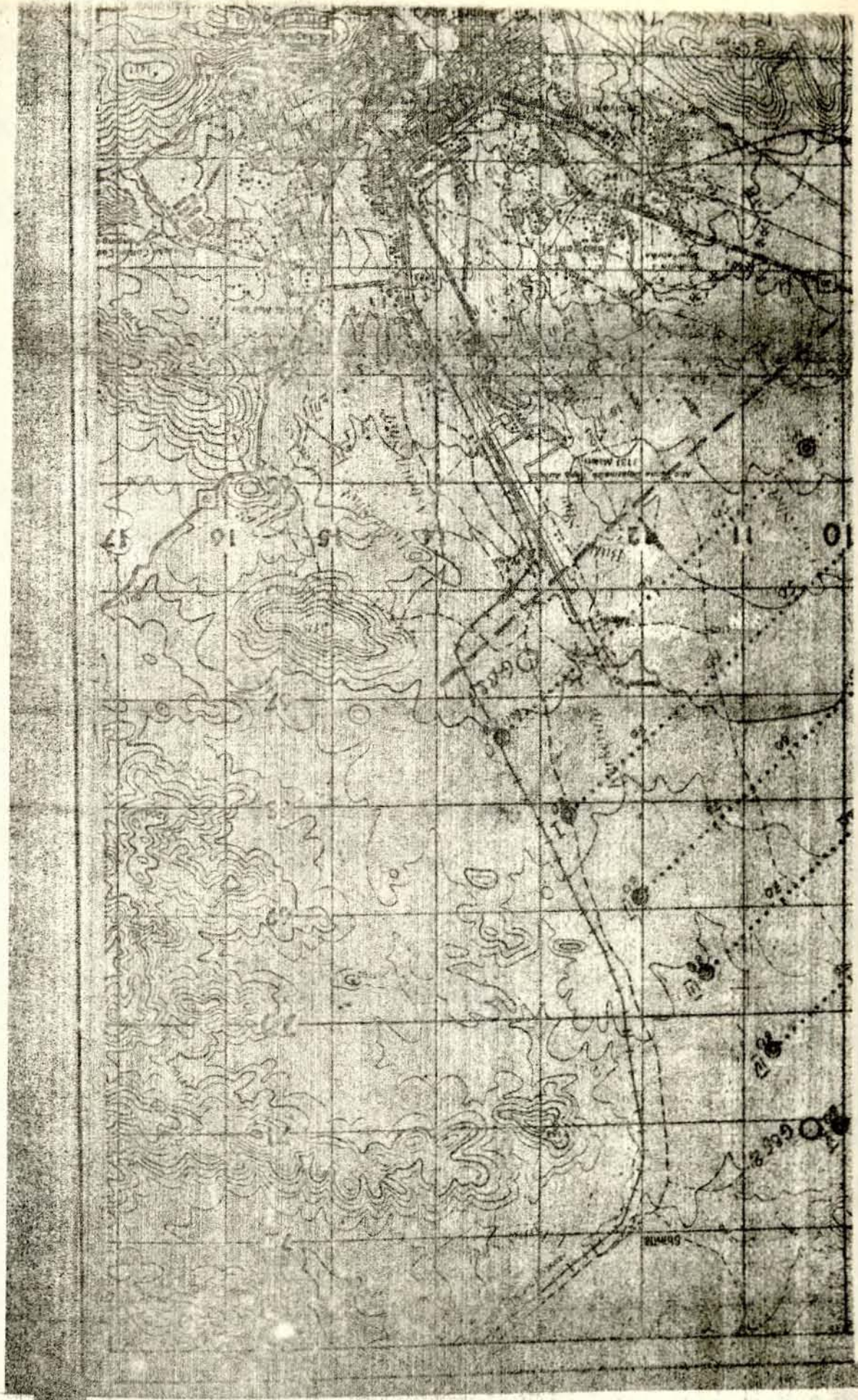

Fig. 22 Location Map of the Geophysical Profiles - Dire

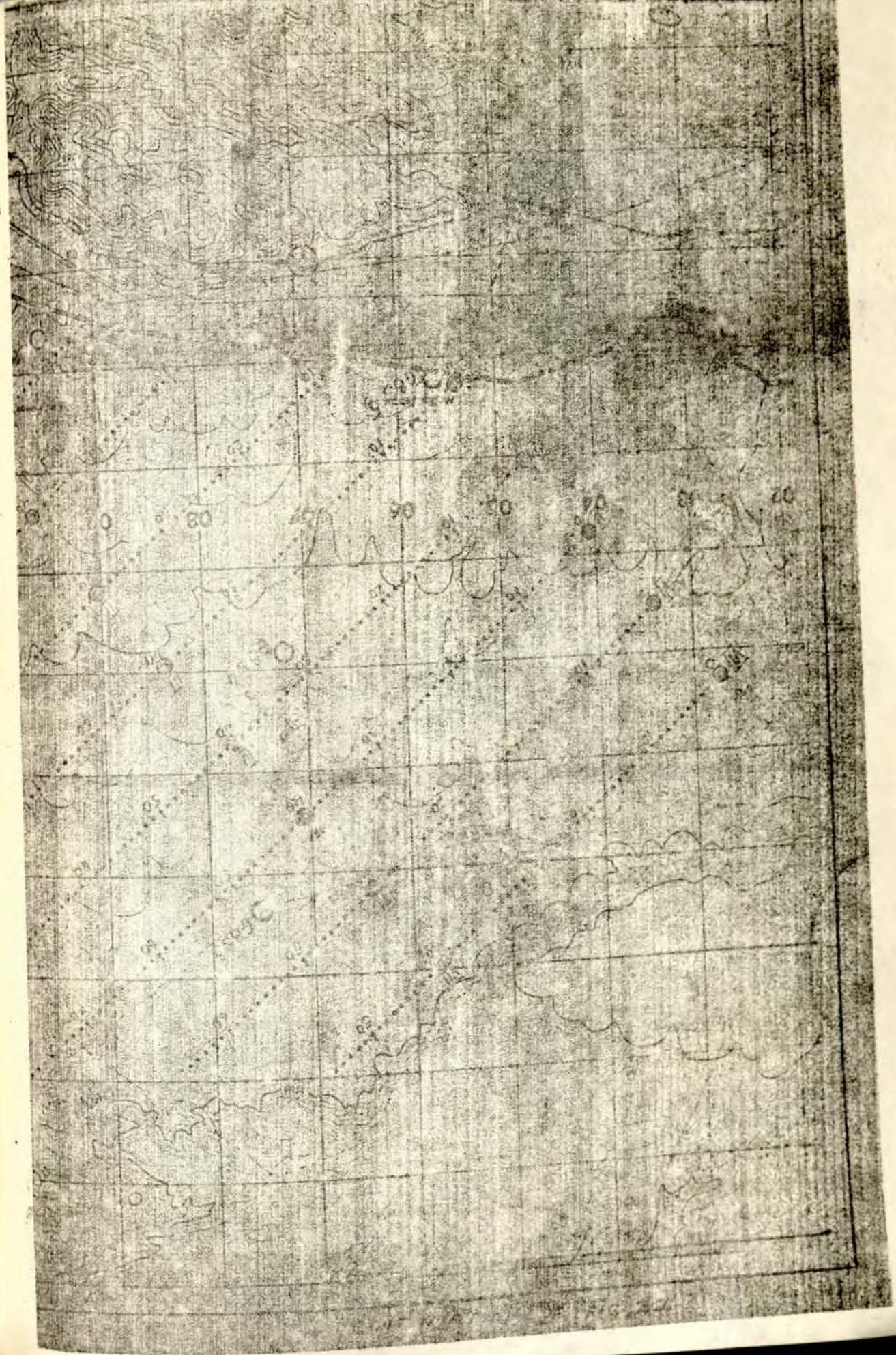

```
RDS-500 FORTRAN4 REV. H 24FEB 83
      PROGRAM APREME
      DIMENSION RADR11(12,10),RADR12(12,10),R2DR1(12),RDH(10)
      READ(2,1)R2DR1,RDH
    1 FORMAT(16F5.2)
      DO 4 J=1,10
      TDA=1/RDH(J)
      DO 4 I=1,12
      VK=(R2DR1(I)-1)/(R2DR1(I)+1)
      S1=0.
      S2=0.
      SVK=1.
      DO 5 K=1,50
      D=SQRT(1+(2*K*TDA)**2)
      D2=D**2
      D3=D2*D
      SVK=SVK*VK
      SVKD=SVK/D3
      S1=S1+SVKD
    5 S2=S2+SVKD/D2
      RADR11(I,J)=1+2*S1
    4 RADR12(I,J)=1-S1+3*S2
      WRITE(3,14)
   14 FORMAT(8(/))
      WRITE(3,2)
    2 FORMAT(//,50X,'APPARENT RESISTIVITY MEASURED')
      WRITE(3,3)
    3 FORMAT(47X,'WITH THE SCHLUMBERGER CONFIGURATION')
      WRITE(3,6)
    6 FORMAT(50X,'IN THE SINGLE OVERBURDED CASE')
      WRITE(3,7)
    7 FORMAT(129('*'))
      WRITE(3,8)RDH
    8 FORMAT(/,7X,10(' *',F10.3))
      WRITE(3,7)
      DO 10 I=1,12
   10 WRITE(3,9)R2DR1(I),(RADR11(I,J),J=1,10)
    9 FORMAT(F7.2,10(' *',F10.3))
      WRITE(3,2)
      WRITE(3,11)
   11 FORMAT(52X,'WITH A POLAR DIPOLE ARRAY')
      WRITE(3,12)
   12 FORMAT(52X,'OVER A SINGLE OVERBURDEN')
      WRITE(3,7)
      WRITE(3,8)RDH
      WRITE(3,7)
      DO 13 I=1,12
   13 WRITE(3,9)R2DR1(I),(RADR12(I,J),J=1,10)
      END
NO ERRORS
SYM3 REV.H
:GO
```

Fig. 23

APPARENT RESISTIVITY MEASURED
WITH THE SCHLUMBERGER CONFIGURATION
IN THE SINGLE OVERBURDED CASE

*	1.500 *	3.000 *	5.000 *	7.000 *	10.000 *	15.000 *	25.000 *	40.000 *	65.000 *	100.000
0.01 *	0.641 *	0.170 *	0.026 *	0.012 *	0.011 *	0.011 *	0.015 *	0.028 *	0.068 *	0.137
0.03 *	0.653 *	0.194 *	0.049 *	0.033 *	0.031 *	0.031 *	0.031 *	0.032 *	0.038 *	0.047
0.05 *	0.665 *	0.218 *	0.073 *	0.055 *	0.052 *	0.051 *	0.050 *	0.050 *	0.051 *	0.052
0.10 *	0.693 *	0.276 *	0.130 *	0.109 *	0.103 *	0.101 *	0.100 *	0.100 *	0.100 *	0.100
0.30 *	0.789 *	0.483 *	0.351 *	0.321 *	0.309 *	0.304 *	0.301 *	0.301 *	0.300 *	0.300
0.50 *	0.865 *	0.658 *	0.556 *	0.526 *	0.512 *	0.505 *	0.502 *	0.501 *	0.500 *	0.500
1.50 *	1.090 *	1.249 *	1.363 *	1.416 *	1.453 *	1.477 *	1.491 *	1.497 *	1.499 *	1.499
3.00 *	1.242 *	1.714 *	2.131 *	2.379 *	2.595 *	2.772 *	2.901 *	2.958 *	2.983 *	2.993
5.00 *	1.339 *	2.041 *	2.747 *	3.232 *	3.717 *	4.183 *	4.595 *	4.811 *	4.921 *	4.965
10.00 *	1.438 *	2.405 *	3.514 *	4.395 *	5.414 *	6.594 *	7.929 *	8.851 *	9.449 *	9.737
30.00 *	1.525 *	2.759 *	4.352 *	5.798 *	7.733 *	10.458 *	14.576 *	18.676 *	22.605 *	25.323
100.00 *	1.562 *	2.921 *	4.775 *	6.567 *	9.142 *	13.158 *	20.274 *	29.017 *	39.567 *	48.574

APPARENT RESISTIVITY MEASURED
WITH A POLAR DIPOLE ARRAY
OVER A SINGLE OVERBURDEN

*	1.500 *	3.000 *	5.000 *	7.000 *	10.000 *	15.000 *	25.000 *	40.000 *	65.000 *	100.000
0.01 *	0.964 *	0.427 *	0.073 *	0.018 *	0.011 *	0.010 *	0.008 *	0.005 *	0.006 *	0.041
0.03 *	0.966 *	0.448 *	0.100 *	0.041 *	0.032 *	0.031 *	0.030 *	0.029 *	0.030 *	0.034
0.05 *	0.968 *	0.468 *	0.126 *	0.065 *	0.054 *	0.051 *	0.050 *	0.050 *	0.050 *	0.051
0.10 *	0.972 *	0.516 *	0.189 *	0.123 *	0.107 *	0.103 *	0.101 *	0.100 *	0.100 *	0.100
0.30 *	0.984 *	0.675 *	0.421 *	0.348 *	0.319 *	0.308 *	0.303 *	0.301 *	0.300 *	0.300
0.50 *	0.992 *	0.796 *	0.618 *	0.555 *	0.525 *	0.510 *	0.504 *	0.501 *	0.501 *	0.500
1.50 *	1.002 *	1.124 *	1.270 *	1.351 *	1.413 *	1.456 *	1.483 *	1.493 *	1.497 *	1.499
3.00 *	1.000 *	1.307 *	1.738 *	2.039 *	2.332 *	2.599 *	2.815 *	2.919 *	2.967 *	2.986
5.00 *	0.994 *	1.401 *	2.025 *	2.522 *	3.077 *	3.680 *	4.288 *	4.648 *	4.847 *	4.932
10.00 *	0.985 *	1.472 *	2.286 *	3.015 *	3.951 *	5.173 *	6.771 *	8.054 *	9.000 *	9.501
30.00 *	0.973 *	1.508 *	2.456 *	3.385 *	4.716 *	6.766 *	10.280 *	14.353 *	18.952 *	22.705
100.00 *	0.966 *	1.512 *	2.496 *	3.485 *	4.958 *	7.378 *	12.074 *	18.717 *	28.511 *	39.087

Fig. 24

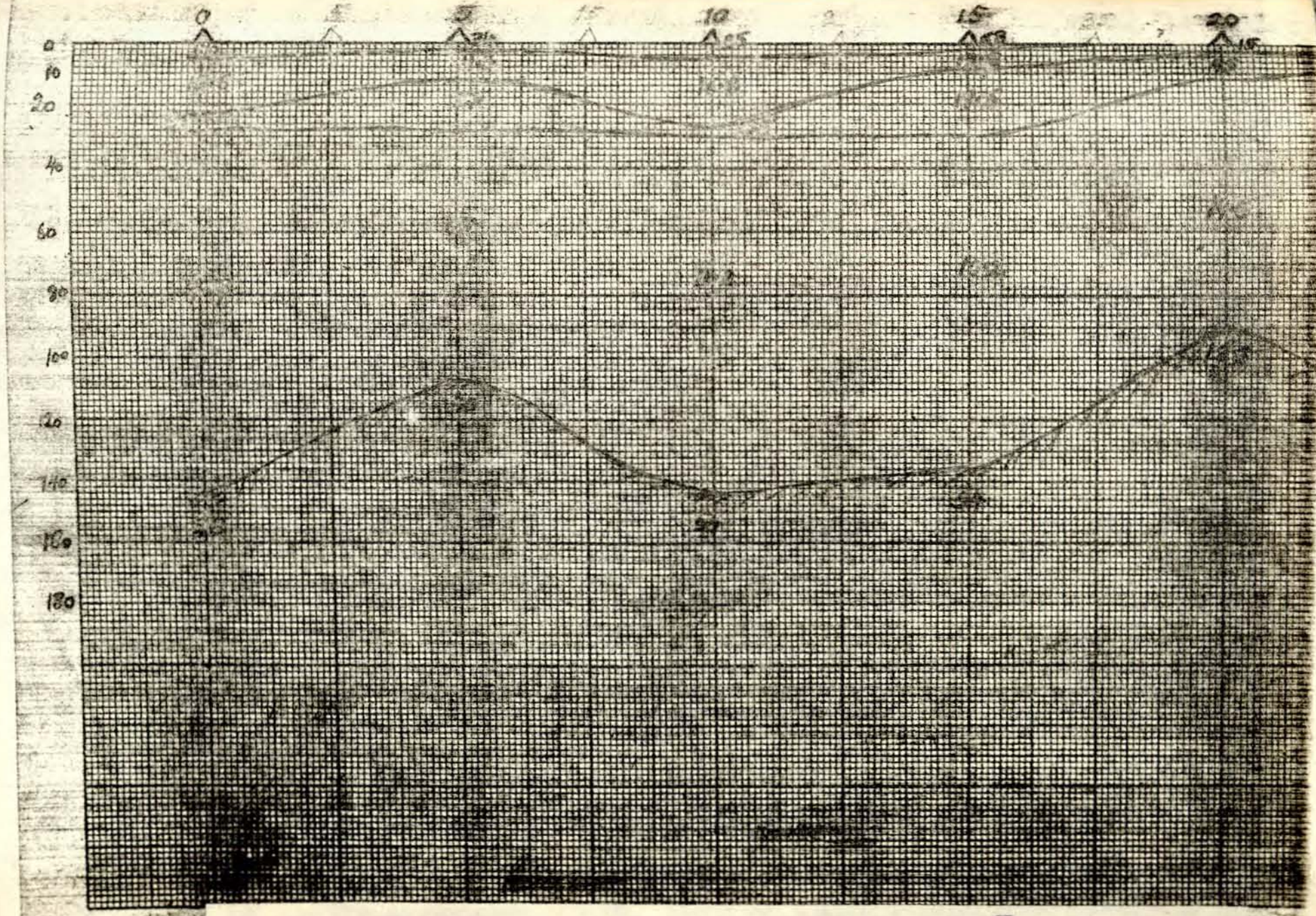

Fig. 25. Geo electrical section of profile W : Deredawa

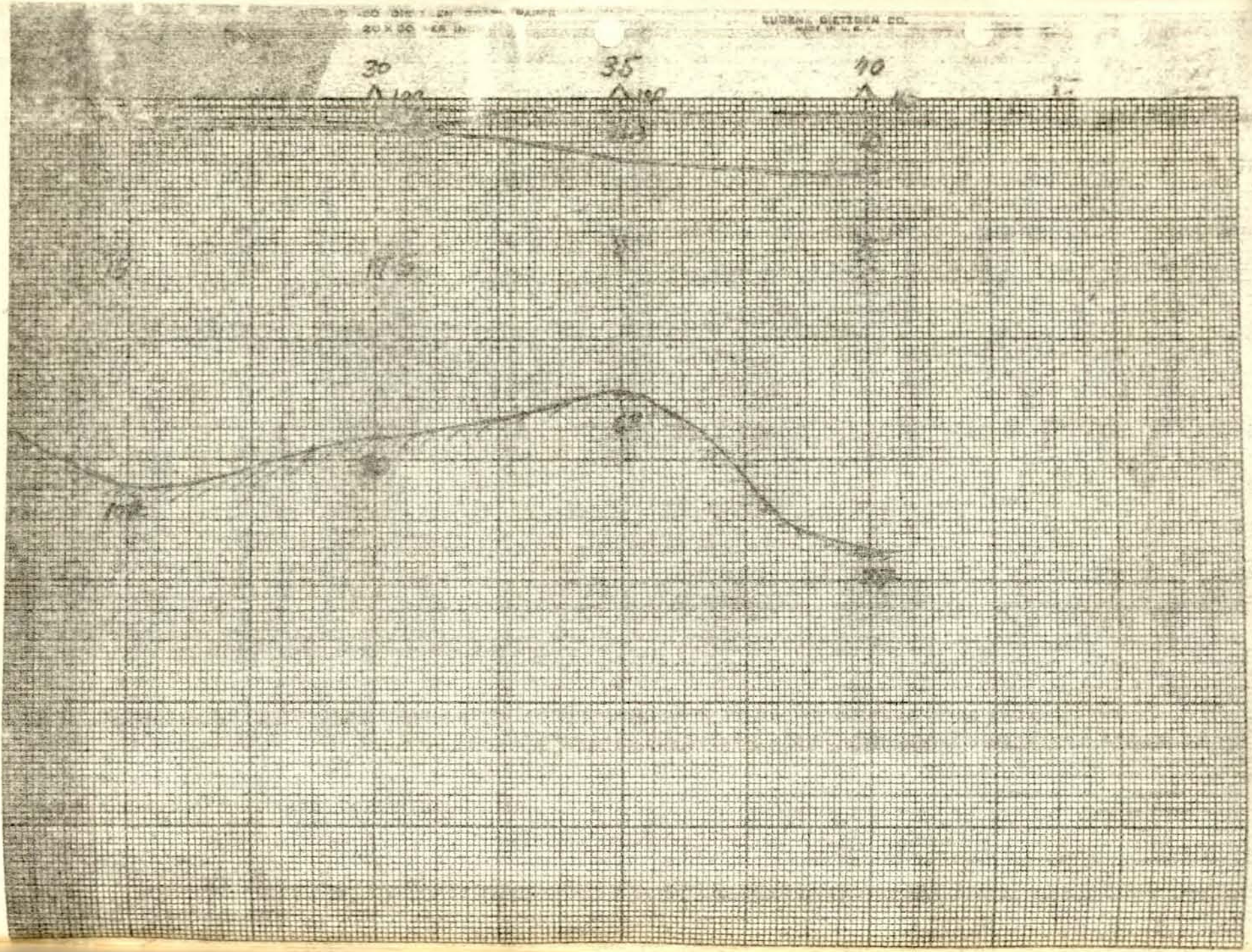
30
35
40
18
18
10

DECLARATION

I, the undersigned, declare that this thesis is my original work and that all the sources of material used for the thesis have been duly acknowledged.

GEBRECHRISTOS KASSA

PHYSICS DEPARTMENT

June, 1983

DECLARATION

This thesis has been submitted for examination with my approval as the University Advisor.

DR. BAIKEN E. ZHAKUPOV

June, 1983